UNIVERSITÀ DEGLI STUDI
DI GENOVA

Medical and Pharmaceutical School

Department of Health Sciences (DiSSal)

Research Doctorate in Health Sciences

Curriculum Prevention of Cancer and Chronic-Degenerative Diseases

Cycle XXXVIII

IRCCS Ospedale Policlinico San Martino

Neuro-oncology and Mutagenesis Unit

TARGETING THE p53/xCT/GSH AXIS WITH PRIMA-1^{Met} AND SULFASALAZINE AS A POTENTIAL STRATEGY TO PREVENT THERAPEUTIC RESISTANCE IN CHRONIC LYMPHOCYTIC LEUKEMIA

Supervisors:

Doctor Paola Menichini

Professor Alberto Izzotti

PhD Candidate:

Martina Pasino

Abstract

Chronic lymphocytic Leukemia (CLL) is a highly heterogeneous form of leukemia characterised by complex karyotype aberrations and by gene mutations at different genes including *TP53*. Mutations in this gene represent a significant hallmark of the disease, thus directing therapeutic decisions, as they can significantly impact the success of treatment protocols. PRIMA-1^{Met}/APR-246/Eprenetapopt is the most clinically advanced mutant p53-targeting agent, which has been shown to reactivate wild-type p53 apoptotic functions. Furthermore, PRIMA-1^{Met} can deplete the glutathione (GHS) reservoir, which levels can also be diminished by Sulfasalazine (SAS), an anti-inflammatory drug. This drug inhibits the xC^- transporter, which imports cystine for GSH synthesis. In this study, the association of PRIMA-1^{Met} and SAS was investigated as a strategy to impact on CLL cells by targeting both mutant p53 and GSH pathway.

A wild-type and a mutated p53 cell line (OSU-CLL and MEC-1, respectively) were treated with PRIMA-1^{Met} and SAS, alone or in combination, and the results obtained indicated that PRIMA-1^{Met} is unable to restore the wild-type functions in the mutant p53 protein. However, the combination of molecules synergistically decreased cell survival and strongly affected the antioxidant capacity in CLL cells, particularly in the p53-mutated cell line. The same studies have also been performed in CLL primary cells carrying wild-type or mutant p53 and confirmed previous results in CLL cell lines.

The association of PRIMA-1^{Met} and SAS represents, therefore, a valid strategy to target CLL cells and prevent the selection of resistant clones able to drive the development of a more aggressive disease.

Table of contents

1. Introduction

1.1. The Chronic Lymphocytic Leukemia

Chronic Lymphocytic Leukemia (CLL) is the most common form of leukemia among adults. The median age at diagnosis is 70 years, with an incidence of 4.6 per 100,000 inhabitants per year and men are generally more affected than women (1.9:1) (1). CLL begins as an indolent disease, characterised by long-term survival in many patients. However, the biological heterogeneity that distinguishes the disease results into an heterogeneous clinical course, with a subset of patients that undergo a very rapid progression (2-3 years of survival after diagnosis) (2).

For diagnosis of CLL the first parameter to consider is the amount of B lymphocytes in the peripheral blood, considered abnormal if ≥ 5000 B cells/μL for a minimum of three months. The clonality is confirmed by immunophenotyping of B cells at the flow cytometer. The morphology of circulating leukemic cells highlight small mature lymphocytes, characterised by a thin cytoplasm and a dense nucleus without visible nucleoli. Variable proportions of larger or atypical forms, such as cleaved cells or prolymphocytes, may accompany the typical morphology and can represent up to 55% of the lymphocytes (3).

1.1.1. Staging system

Two major clinical staging systems are employed for CLL, and both of them classify patients into three categories, associated with distinct clinical outcomes.

The Rai staging system stratifies CLL patients into three categories: low, intermediate, and high-risk groups. The first one represents the group defined "low risk" and includes patients with lymphocytosis and the presence of leukemic B cells in the peripheral blood or in the bone marrow (lymphoid infiltration > 30%) (Rai stage 0). The second one is the intermediate-risk group and classify patients characterised by lymphocytosis and lymphadenopathy or splenomegaly/hepatomegaly (Rai stages I–II). The third group includes patients with cytopenias and is divided in two different stages: anemia with hemoglobin < 11 g/dL (Rai stage III) or thrombocytopenia with a platelet count < 100×10^9/L (Rai stage IV) (4).

The Binet staging system stratifies CLL patients based on the number of areas which are involved in the disease and the presence of anemia or thrombocytopenia. Five anatomical regions are considered for this purpose: head and neck (including Waldeyer's ring), axillae, groins, palpable spleen, and hepatomegaly. Stage A includes patients with two regions involved in the disease, whereas stage B clusters patients with three or more implicated areas. Both stage A and B are defined by hemoglobin ≥ 10 g/dL and platelets ≥ 100×10^9/L Stage C is assigned in the presence of cytopenias, with hemoglobin < 10 g/dL or platelets < 100×10^9/L (5).

Conventional clinical staging systems have lost prognostic resolution with the recent progress in CLL therapy, therefore new scores have been developed to combine clinical, biological and genetic features. The most used system today is the CLL-International Prognostic Index (CLL-IPI), which incorporates a weighted scoring system based on five factors: *TP53* deletion or mutation, *IGHV* mutational status, levels of β_2-microglobulin in the serum, clinical stage, and patient age. This index stratifies patients into four risk categories, associated with different outcomes observed after 5 years from diagnosis (6).

1.1.2. Biological features of CLL

CLL is characterised by the proliferation and accumulation of clonal mature B-cells which are positive for CD5 and for the antigens normally expressed on the surface of B cells: CD19, CD20, CD23. With respect to normal B cells, the surface membrane immunoglobulin (smIg), CD20 and CD79b are expressed at lower levels (7,8). Each leukemic clone express only kappa or lambda immunoglobulin light-chain (9), and these clones generally accumulate in the blood, bone marrow, lymph nodes and spleen (10).The clonal behaviour is generally acquired at the hematopoietic stem cell (HSC) stage, thus indicating that the earliest leukemogenic event in CLL likely involves multipotent, self-renewing HSCs (11). The process is frequently induced by the loss or gain of chromosomal segments and is sustained by the accumulation of mutations leading to an increase in the aggressiveness of the leukemia (12).

The most frequent karyotype aberrations occurring in CLL are deletions at 13q14 (~55%), 11q23 (~15%), 17p13 (~8%) or trisomy of 12 (~15%) (13,14). Del(13q14) is associated with a less aggressive form of leukemia and involves miR-15a and 16-1 (15).These miRNA modulate the expression of anti-apoptotic proteins and drivers of cell cycle progression (16). Del(11q23) is associated with a more aggressive form of CLL since it causes the loss of *ATM*, a gene that encodes for the kinase ATM which participates in DNA damage repair (17). Del(17p13) includes the region where the gene *TP53* is coded and is associated with patients resistant to chemotherapies and, in general, a worse prognosis (18,19). Of note, del(17p) and del(11q) involve the *TP53* and *ATM* genes, which frequently harbour a mutation in the second allele and are often found mutated in patients resistant to conventional chemotherapy (20,21). Trisomy 12 is related to an intermediate prognosis and results in an increased copy number of *MDM2*, the main negative regulator of *TP53* (13).

In addition to the chromosomal aberrations described above, gene mutations and somatic copy number variations have been found in many genes, including *TP53*, *MYD88*, *SF3B1*, *BIRC3*, *NOTCH1*, *AMT*, *FBXW7*, *POT1*, *CHD2*, *RPS15*, *IKZF3*, *ZNF292*, *ZMYM3*, *ARID1A* and *PTPN11*(13,20–22).

An important biological feature of CLL to be considered is the mutational status of the immunoglobulin variable region heavy chain genes (IGHV).

During normal B-cell development, the V(D)J recombination generates the variable region of immunoglobulin heavy and light chain and this process, together with junctional nucleotide insertions and deletions, creates extensive antibody diversity. Antigen specificity is mainly defined by the complementarity-determining regions (CDRs) (23,24). Upon antigen stimulation, mature B cells may further diversify their immunoglobulin genes through somatic hypermutation, which introduces point mutations in V regions and drives affinity maturation by favouring cells with higher capacity to bind different antigens. Because germline IGHV sequences are well defined, analysis of somatic hypermutation allows determination of whether the malignant CLL clone has undergone this process, providing insight into its cellular origin and biological behaviour (25). Many studies have been conducted to identify the importance of somatic mutations in *IGHV* genes. In most cases, favourable cytogenetic abnormalities are associated with a mutated *IGHV* status, whereas unfavourable cytogenetic features are more frequently observed in cases with unmutated *IGHV* (26–28).

The most relevant gene involved in the karyotype aberrations and alterations occurring in CLL is *TP53*. Indeed, mutations affecting this gene constitute a major hallmark of CLL, since they influence therapeutic decisions and the clinical course of the disease. At initial diagnosis, only 5-7% of patients presents *TP53* mutations; however, this frequency increases to 40% in relapsed or refractory CLL, as a consequence of selective pressure exerted by prior treatments (19,29,30).

Alterations of *TP53* may vary from deletion of the short arm of chromosome 17 (del17p) to point mutations within the gene. Both events result in the impairment of p53 tumour-suppressive functions, such as the activation of DNA-damage response, apoptosis induction, and the maintenance of genomic stability. Importantly, *TP53* deletions and mutations commonly coexist and are defined as "*TP53* dysfunctions", which are associated with loss of cell death control and increased resistance to conventional chemoimmunotherapy. Because of its strong association with treatment failure and poor prognosis, *TP53* disruption is currently considered the most clinically relevant predictive biomarker in CLL (31,32). For this reason, international recommendations from the European Research Initiative on CLL (ERIC) group highlight the need for *TP53* status assessment at diagnosis and, in particular, before any therapeutic intervention, in order to select the appropriate treatment (33).

1.2. The p53 protein

The p53 protein was first described in 1979 by David Lane and Lionel Crawford as a 53 kDa non-viral protein that co-immunoprecipitated with the SV40 (Simian Virus 40) large T antigen, initially classified as tumour antigen (34). However, the term "p53" was officially adopted only few years later, during the first p53 Workshop in 1983 (35). Subsequent studies showed that p53 could also be isolated from tumour cells not infected with SV40, demonstrating that it is an endogenous cellular protein encoded by the host genome. At first, p53 was thought to act as an oncogene involved in cellular transformation; however, a decade after its discovery, it was definitively redefined as a tumour suppressor protein (36,37).

1.2.1. Protein structure

The p53 protein is a transcription factor that exerts a key role in the modulation of target genes that are critical for the maintenance of cellular homeostasis. For this reason, is widely known as "genome guardian". The *TP53* gene is situated on chromosome 17 (17p13.1) and codes for a protein with 393 amino acids. The p53 protein is organised in 11 exons, the first of which is non-coding, and is characterised by structural and functional domains (*Figure 1*): the N-terminal region, composed of a disordered transactivation domain (TAD) and a proline-rich domain (PD), the central region, which contains a DNA-binding core domain (DBD), and the C-terminal region, composed by the tetramerization domain (TD) and the regulatory domain (CTD) (38).

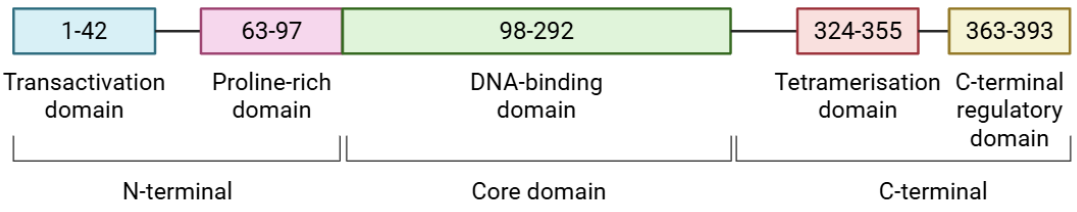

Figure 1. The p53 protein structure. Adapted from Tanaka al., Oncotarget, 2018 (39)

TAD (residues 1-42), divided into TAD1 and TAD2 (40), acts as a flexible interaction hub that binds numerous partners involved in transcriptional regulation, including p300/CBP and the negative regulators MDM2 and MDM4 (41,42).

PD (residues 63-97) links the TAD to the DBD and contributes to the structural rigidity of the protein. Its length appears to be important for the tumour suppressor activity, suggesting a modular spacer role between functional domains (43).

DBD (residues 98-292) adopts an immunoglobulin-like β-sandwich fold that provides the scaffold for DNA binding, which interaction involves a loop-sheet-helix motif (44). The human p53 core domain is not completely stable, and this intrinsic instability, partly due to inner unpaired polar residues, evolved to confer conformational flexibility and allow a tight regulation of p53 activity (45). p53 regulates transcription by binding specific DNA response elements (RE) composed of two decameric half-sites palindromes characterised by the general sequence 5′-RRRCWWGYYY-3′ (R = A, G; W = A, T; Y = C, T) (46). Variations in sequence symmetry and spacing influence whether target genes are activated or repressed (47). DNA binding occurs cooperatively through tetramerization of four p53 core domains, resulting in DNA bending and twisting (48).

TD allows the reversible tetramerization of full-length p53 forms (residues 324-355). Structural studies show that this domain is constituted by dimer of dimers; (49,50) the association of two dimers generates a four-helix bundle tetramer, stabilized mainly by hydrophobic interactions (51,52).

CTD (residues 363-393) is a region intrinsically disordered and displays pronounced structural plasticity. It serves as an interaction site for regulatory functions and is regulated by post-translational modifications (53). Modifications of lysine at the C-terminal region modulate p53 DNA binding and transcriptional activity in a context-dependent manner (54).

1.2.2. Protein regulation

The p53 protein expression is negatively regulated by MDM2, an E3 ubiquitin ligase that binds p53, inhibits its transcriptional activity and promotes its ubiquitination and proteasomal degradation. On the other hand, p53 induces MDM2 expression by binding to its promoter (55), thus generating a negative-feedback loop with an autoregulatory function. This mechanism provides a tight control of p53 activity under basal conditions, in order to prevent growth arrest or apoptosis mediated by p53 when not required (56,57). MDM2 represses p53 through different mechanisms: ubiquitination (58), nuclear export (59), inhibition of the interaction with transcriptional coactivators (60), and recruitment of transcriptional corepressors (61). For example, when MDM2 is expressed at low levels, its activity favours the monoubiquitination and nuclear export of p53, whereas a higher amount of MDM2 in the cell leads to polyubiquitination and degradation of p53 (61). Although initially thought to depend only on N-terminal interactions, the MDM2-p53 interaction is also influenced by modifications and structural features of the C-terminal region (62,63).

A wide variety of stimuli can activate p53, such as DNA damage, activation of oncogenes, dysfunctions in the mitotic apparatus, errors during DNA replications, hypoxia, oxidative stress, endoplasmic reticulum stress, telomere shortening, metabolic alterations, and others. In response to these stimuli, p53 regulates the transcription of genes involved in the pathways mentioned above in order to restore cellular homeostasis (64).

Cell cycle checkpoints mediate the arrest of cell cycle progression to preserve genomic stability when the cell undergo replication stress or DNA damage. In this manner, the accumulation of genomic alterations and the consequent induction of pro-oncogenic processes are avoided (65). The p53 protein is a central regulator of cellular checkpoints and induces cell cycle arrest through transcriptional activation of target genes, such as *CDKN1A* (p21), *GADD45A*, and the gene for the 14-3-3σ protein. P21 is responsible for the cell cycle arrest in the G1/S phase by inhibiting CDK/cyclin complexes and DNA synthesis. GADD45A and 14-3-3σ regulate the G2/M checkpoint by disrupting CDC2-cyclin B activity, preventing mitotic entry and promoting DNA repair (66–68).

All these mechanisms, regulated upstream by p53, coordinate cell cycle arrest at different levels, facilitating DNA repair and contributing to tumour suppression.

Tumour cells activate a metabolic reprogramming to sustain their high rate of proliferation, mainly by upregulating glycolysis and through the alteration of biosynthetic pathways (69). The p53 protein counteracts this shift by suppressing glycolysis, promoting oxidative phosphorylation, and reducing the uptake of nutrient, thus limiting tumour growth. The cellular metabolism is regulated by p53 via key effectors. The activation of AMPK and TSC2, for example, inhibits the anabolic signaling through the mTOR pathway (70,71), whereas PTEN suppresses PI3K/AKT signaling, causing a reduction of glucose and glutamine uptake, and stabilised p53 via inhibition of MDM2 (72). TIGAR further limits glycolytic flux and supports redox balance by the activation of the pentose phosphate pathway (73). Collectively, these metabolic programs regulated by p53 limited cancer cell growth and promote metabolic homeostasis under stress conditions.

The DNA repair pathways preserve genomic integrity and limit cancer risk. The role of p53 is related to the transcriptionally activation of genes involved in DNA repair and cellular stress responses. Among these targets, p53 induces DNA damage binding protein 2, essential for DNA damage recognition (74). The antioxidant proteins are also activated by p53 and mediate the reduction of oxidative stress, DNA repair and autophagy through AMPK-dependent pathways (75,76).

Apoptosis is critical for cellular homeostasis, and its dysregulation contributes to tumorigenesis. Both intrinsic and extrinsic apoptotic pathways are induced by p53 via transcriptional activation of pro-apoptotic genes. The mitochondrial apoptosis is driven by induction of Bax, NOXA, and PUMA, which promote mitochondrial permeabilization and caspase activation; p53 may also upregulate Fas ligand, that activate apoptosis binding the proper receptor on the cell surface (77–79). Collectively, these pathways enable p53 to eliminate damaged or transformed cells and are central to its tumour suppressor functions (80,81).

Many of the biological functions exerted by p53 through the transcriptional regulation of its target genes are essential for the cell to activate and maintain anti-cancer defences. On the other hand, these protective functions make p53 a frequent target of genetic alteration in cancer.

TP53 is the most mutated gene in human tumours, and its mutations occurs in more than 50% of all cancers (82). In addition to somatic mutations, *TP53* germline alterations are responsible for the Li-Fraumeni syndrome, a hereditary cancer predisposition disorder that is characterised by early onset and a development of a wide variety of cancers (83). The International Agency for Research on Cancer (IARC) has registered over 29,900 distinct *TP53* mutations which were firstly reported in the IARC database and are today maintained by the National Cancer Institute (NCI).

1.2.3. The role of p53 in cancer prevention

The importance of p53 and its mutations in tumorigenesis and cancer progression is well established. Understanding the consequences of *TP53* mutations is essential for the development of effective clinical strategies to limit tumour progression and improve patient outcomes. Mutant p53 has been shown to upregulate key mediators of invasion, angiogenesis, immune evasion, and therapy resistance. As previously described for CLL, increasing evidence indicates that distinct p53 mutations can influence therapeutic responses in different types of cancers; the study of these features allows the development of personalised approaches. Current knowledge of the role of p53 in tumour development and progression may help in the context of tertiary cancer prevention, which aims to prevent metastasis, recurrence, and therapy resistance in patients. This provides useful bases to develop proper strategies against mutant p53-driven tumors (84,85).

Together with the mutational status of *TP53*, downstream pathways and molecular targets regulated by mutant p53 represent promising alternative approaches for cancer prevention. Gain-of-function p53 mutations, for example, are frequently associated with aggressive tumour behaviour, metastatic potential, and resistance to therapy since they may reprogram cellular signaling pathways and promote tumour progression. (86,87).

The combination of *TP53* mutational status with the analysis of associated targets could provide a promising strategy to improve the prediction of metastasis development, associated with treatment resistance. Although the significant progress that has been made, many aspects of tumours evolution and therapy resistance driven by mutant p53 remain incompletely understood. Continued identification of novel mutant p53 targets and pathways will be crucial for the prediction of tumour behaviour, promote earlier intervention, and refine therapeutic strategies, thereby preventing the evolution of aggressive cancers and allow the development of highly targeted therapies.

1.3. CLL and oxidative stress

CLL cells are characterised by higher reactive oxygen species (ROS) levels than normal B lymphocytes, leading to oxidative stress which modulates the activity of transcription factors such as p53, NF-kB, hypoxia-inducible factor-1α and others (88,89). Moreover, when the concentration of ROS surpass antioxidant defence capacity, proteins and lipids become oxidised and lost their functions (90).

ROS, such as superoxide ($O_2^{\bullet -}$), hydrogen peroxide (H_2O_2), peroxynitrite ($ONOO^-$), and the hydroxyl radical (•OH), are generally regarded as unavoidable by-products of aerobic metabolism, generated through the incomplete reduction of molecular oxygen (91,92) (*Figure 2*). The mitochondrial electron transport chain is the primary mechanism of radical generation, although not the sole one (93). Indeed, the activity of various oxidases can also give rise to radical species, leading to an increase in oxidative stress. NADPH oxidase, for example, transfers electrons from NADPH to oxygen, resulting in superoxide radical production (94).

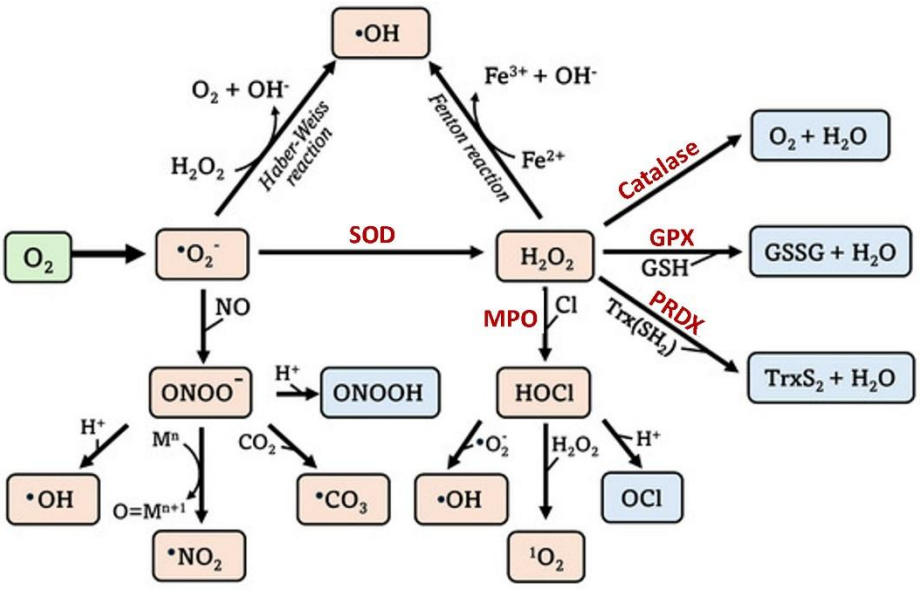

Figure 2. ROS generation pathways in the cell. Adapted from Kozlov et al., Antioxidant, 2024. (95)

Another endogenous source of free radicals is represented by lipid peroxidation, a process that is triggered when a free radical abstracts a hydrogen atom from a polyunsaturated fatty acid, thereby producing a lipid radical (L•). The lipid radical is then converted to a lipid peroxyl radical (LOO•) after the reaction with molecular oxygen. The lipid peroxyl radical can propagate the chain reaction to adjacent lipids (96). The main final products are malondialdehyde (MDA) and 4-hydroxynonenal (4-HNE), which can further extend the oxidative damage cascade (97).

Under physiological conditions, ROS function as key signaling mediators, modulating processes including cell proliferation, differentiation, and immune responses (98). When ROS production surpasses the antioxidant defences of non-malignant cells, the excess accumulates and results in oxidative modifications of DNA, proteins, and lipids, inducing cell death (99). All these alterations may contribute to genomic instability and lead to tumour development (100).

ROS intracellular levels are regulated by an elaborate network of antioxidant systems and non-enzymatic scavengers (101). The first group includes the superoxide dismutases (SOD), which catalyse the dismutation of superoxide radicals into molecular oxygen and hydrogen peroxide. The latter is subsequently broken down by catalase and glutathione peroxidases (GPx) into water and oxygen (102) (*Figure 2*). Among non-enzymatic scavengers are glutathione, flavonoids, vitamin C, and E (103). Since high amounts of ROS make CLL cells more vulnerable to substances that increase oxidative stress (104), the study of this mechanism could provide more insights to counteract resistant CLL cells.

1.3.1. The glutathione pathway

Glutathione (GSH) is the predominant intracellular thiol antioxidant. It maintains cellular redox homeostasis and protects cells from damage induced by ROS (105). On the other side, GSH plays additional roles in cancer, contributing to tumorigenesis and therapy resistance. High intracellular GSH levels in tumour cells have been associated with increased tumour growth and reduced sensitivity to chemotherapy (106,107).

GSH is a tripeptide composed of glutamate, cysteine, and glycine. Among these, cysteine is the rate-limiting precursor for GSH biosynthesis and is also the residue that provides the molecule with its antioxidant activity (108). In most cell types, cysteine availability depends on extracellular uptake. This is largely achieved through the xC^- antiporter system, formed by the heavy chain subunit SLC3A2 and the light chain subunit SLC7A11, which exchanges intracellular glutamate for oxidized cystine, subsequently reduced to cysteine inside the cell (109). Glutamate for GSH synthesis can be supplied by glutamine metabolism: glutamine is transported into cells, then converted to glutamate through the action of glutaminases (GLS) (110). Meanwhile, glycine, the third constituent of GSH, is produced from serine, threonine, and other amino acids through various metabolic pathways (111).

GSH is synthesised in the cytosol through a two-step enzymatic process, which is dependent on ATP (112). The first reaction, which represents the rate-limiting step of the pathway, is mediated by the glutamate-cysteine ligase (GCL). This enzyme is a heterodimer composed of a catalytic subunit (GCLC) and a modifier subunit (GCLM) and catalyses the formation of an intermediate dipeptide, the γ-glutamylcysteine (γ-GCS), by linking glutamate and cysteine (113). The second reaction is carried out by glutathione synthetase (GSS), which incorporates glycine into the γ-GCS, thus completing GSH biosynthesis (*Figure 3*). In physiological conditions, the reduced form GSH is abundant and exceeds the oxidized form GSSG by a factor of 10-100 (114). In oxidative stress conditions, intracellular GSH levels increase (115). Indeed, GSH is the key cofactor for glutathione peroxidases (GPx) and glutathione S-transferases (GSTs), two enzymes that neutralise ROS and other radical species, thus limiting oxidative damage to cellular components (116).

In the reactions catalysed by GPx, the GSH acts as an electron donor and reduce H_2O_2 to water, producing GSSG during the process. The oxidized GSSG is then converted to GSH through NADPH-dependent reductions mediated by GR and thioredoxin reductase (TrxR), in order to ensure a continuous regeneration of the GSH pool (117) (*Figure 3*).

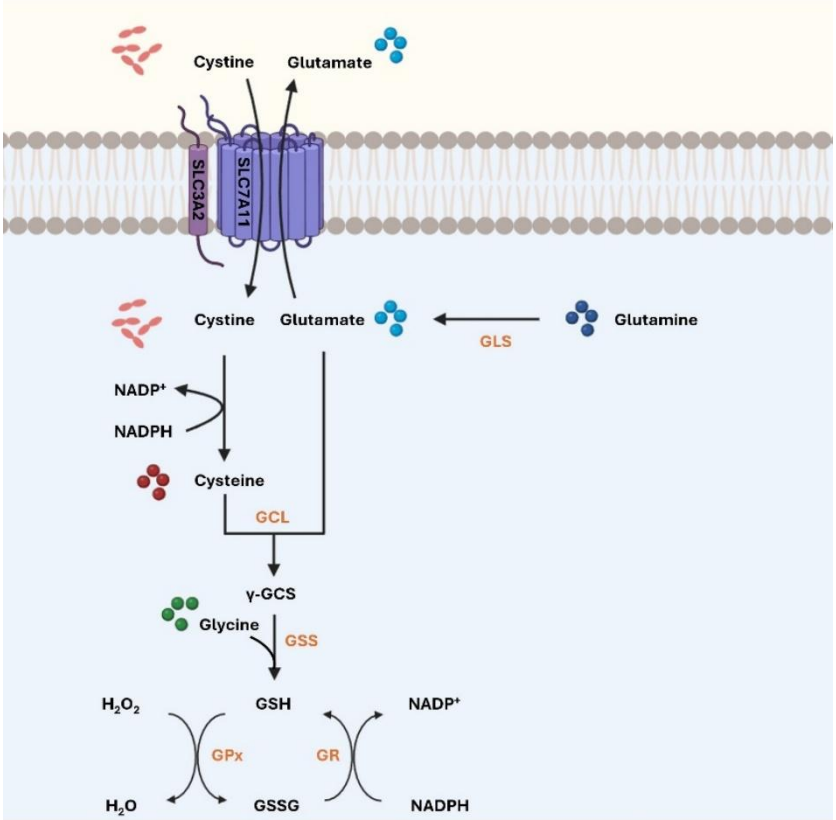

Figure 3. GSH synthesis pathway. Adapted from Velkova et al., J. Pers. Med., 2023 (118), Koppula et al., Protein Cell., 2020 (119).

The dual nature of ROS in cancer biology makes GSH and other antioxidants both protective and potentially pathogenic. On one side, GSH counteracts oxidative stress, which is a pro-tumorigenic factor, thereby limiting the genotoxic events that can mediate the neoplastic transformation. On the other hand, cancer cells highly depend on GSH functions as antioxidant agent that drives detoxification pathways and resistance to cytotoxic agents, thus making these defence systems essential for tumour growth.

Since oncogenic pathways regulate the transcription of genes that are involved in GSH uptake, biosynthesis, regeneration, and utilization, the altered GSH metabolism is considered a hallmark of cancer (120).

ROS can exert both pro- and anti-tumorigenic effects, and the influence of GSH on oxidative stress is complex: intermediate ROS concentrations can enhance cell survival and proliferation via the activation of signaling pathways, thereby promoting tumour expansion. Conversely, when ROS levels rise and the capacity of cellular detoxification systems is saturated, biomolecules undergo an extensive damage, which led to cell death (121).

1.3.2. Nrf2 regulation

Malignant cells preserve their viability through the interaction of ROS with key regulatory molecules, such as NF-E2-related factor 2 (Nrf2). This transcription factor activates signaling pathways that mediate a wide range of cellular processes (122). Under homeostatic conditions, Nrf2 is maintained at low levels through the continual ubiquitination and proteasomal degradation due to its association with the adaptor protein Kelch-like ECH-associated protein 1 (Keap1) (123). In cancer cells, Nrf2 promotes the upregulation of antioxidant proteins and Keap1 oxidizes reactive cysteine residues on Nrf2, preventing its degradation. This allows Nrf2 accumulation and nuclear translocation, where it activates the transcription of genes involved in the antioxidant response (124).

Mutant p53 has been shown to associate directly with Nrf2, and this association results in the transcription of genes related to a pro-survival oxidative stress response (125). Liu et al. reported that mutant p53 proteins suppress the expression of SLC7A11, a key Nrf2 target gene. The impairment of xCT/GSH pathway cause a reduction in the GSH biosynthesis, thus rendering tumours harbouring a mutant p53 more vulnerable to oxidative stress. Therefore, gain-of-function p53 variants can elevate ROS levels in cancer cells by interacting with transcription factors and remodulating the transcriptional profile of their downstream targets (126).

1.3.3. A ROS-dependent cell death: ferroptosis

Ferroptosis, a term coined in 2012, is a specific form of regulated cell death induced by the accumulation of lipid peroxides following iron and ROS overload (127). Ferroptosis is different from apoptosis, necrosis, and autophagy, since it is characterised by unique genetic, biochemical, and morphological features (118) and it represents an innate mechanism of tumour suppression. (128). Three different features define ferroptosis: the presence of polyunsaturated fatty acids (PUFAs) within the phospholipids that form the cell membrane, the availability of redox-active iron, and deficient mechanisms for the repair of lipid peroxidation. These three mechanisms collectively determine the susceptibility of tumour cells to this form of cell death (129,130) (*Figure 4*).

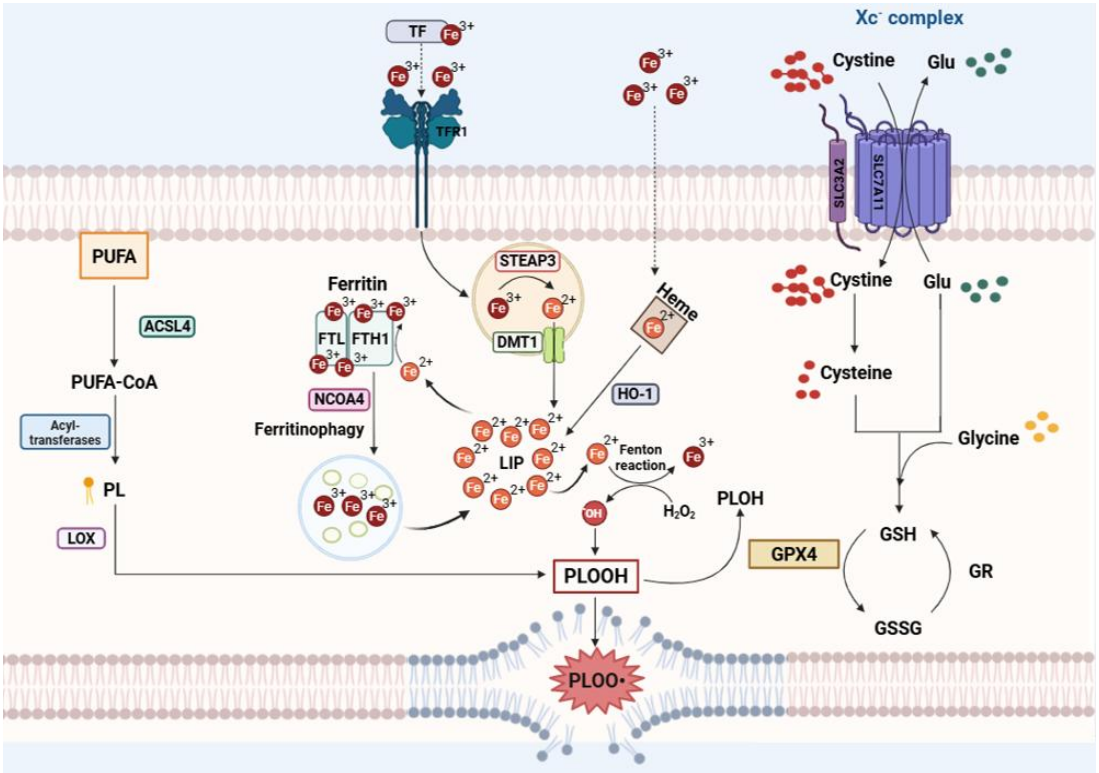

Figure 4. Interconnection of the three major pathways involved in ferroptosis. Adapted from Velkova et al., J. Pers. Med., 2023 (118).

Intracellular iron availability plays a key role in the regulation of ferroptosis. Iron in the blood is transported as Fe^{3+} bound to transferrin and enters cells through endocytosis mediated by transferrin receptor 1 (TFR1). Within endosomes, Fe^{3+} is reduced to Fe^{2+} by STEAP3 and released into the cytosol via DMT1, contributing to the labile iron pool (LIP) (131). Cytosolic Fe^{2+} is generally sequestered in ferritin (composed of ferritin light chain (FTL) and ferritin heavy chain (FTH1) subunits) or incorporated into heme(132). Iron is released from ferritin through ferritinophagy, a process driven by NCOA4, while iron export is mediated by ferroportin (133–135). Cellular iron balance is further controlled by IRP1 and IRP2 through iron-responsive elements on target mRNAs, whereas heme degradation by heme oxygenase-1 provides an additional source (136). When Fe^{2+} accumulates within the LIP, a high amount of ROS is generated by the Fenton reactions, thus promoting lipid peroxidation of membrane phospholipids and triggering the ferroptotic cell death program (137).

Lipid metabolism is a key driver of ferroptosis through lipid peroxidation. Oxidation of PUFA, particularly linoleic and arachidonic acids, generates toxic lipid peroxides and other products such as MDA, which affects the integrity of the cell membrane and promotes cell death. This process is facilitated by the incorporation of PUFA into membrane phospholipids by ACSL4 and by the action of an iron-dependent lipoxygenases that catalyse PUFA oxidation (138,139). Together with iron metabolism and impaired antioxidant defences, altered lipid metabolism orchestrates the molecular events that lead to ferroptosis.

More in general, ferroptosis is driven by the depletion of intracellular GSH, the reduction of glutathione peroxidase 4 (GPX_4) activity, and an inadequate detoxification of lipid peroxides via GSH pathway through a reaction mediated by GPX_4. All these mechanisms ultimately lead to the loss of cell membrane integrity, thus inducing ferroptosis (140). To counteract this process and maintain cell growth, malignant cells activate a set of anti-ferroptotic pathways. A key component of this protective network is GPX_4, which prevents the oxidative damage that would otherwise trigger ferroptosis (141,142). Oncogenic signaling can further enhance this protective machinery. First of all, inactivation of p53 augments the activity of the SLC7A11/GSH/GPX_4 axis, thereby enhancing redox defences, supporting tumour progression, and promoting resistance to therapy (119,143).

Recent studies indicate that the *TP53* gene is involved in the regulation of ferroptosis (144). The p53 protein is able to transcriptionally repress its direct target SLC7A11 (145). However, malignant cells harbouring a mutant p53 may also exhibit reduced SLC7A11 expression, together with an increased ferroptotic sensitivity, as a consequence of the inhibition exerted by the mutated protein on Nrf2 (146). Primary CLL cells display a low expression of xCT and, therefore, depend on cysteine supplied by stromal cells located in the bone marrow to control intracellular ROS levels. Indeed, stromal cells import cystine from the environment and convert it into cysteine. Cysteine is then released into the microenvironment and internalised by CLL cells. Since leukemic cells exhibit low levels of xCT, this process allows them to counteract oxidative stress by importing the cysteine in the reduced form, ready for the GSH synthesis. This mechanism protect CLL cells from the cytotoxic activity of chemotherapeutic agents (147). This highlights the importance of further elucidating the interplay among these mechanisms to exploit them to target CLL cells.

1.4. CLL and microenvironment

A permissive tumour microenvironment (TME) plays an important role to allow CLL cells survival (148,149). Tumour growth is supported by T cells, fibroblasts, macrophages and dendritic cells through the release of soluble mediators, such as chemokines, cytokines and angiogenic factors, that activate signaling pathways for survival and expansion (149,150).

An important role is mediated by interferons (IFNs), which may suppress tumour growth by inducing apoptosis and cell-cycle arrest and inhibiting angiogenesis (151–153). Moreover, they regulate anti-tumour immunity (154). On the other hand, IFN signaling may promote cell survival in cancer cells, mainly via Signal Transducer and Activators of Transcription proteins (STATs) (155) (*Figure 5*). Indeed, aberrant STAT3 expression and activation was observed in different solid and hematological tumours (156–158), where the phosphorylation of STAT3 allows the nuclear translocation and the following transcription of genes involved in the cell survival, proliferation and metastasis (159,160).

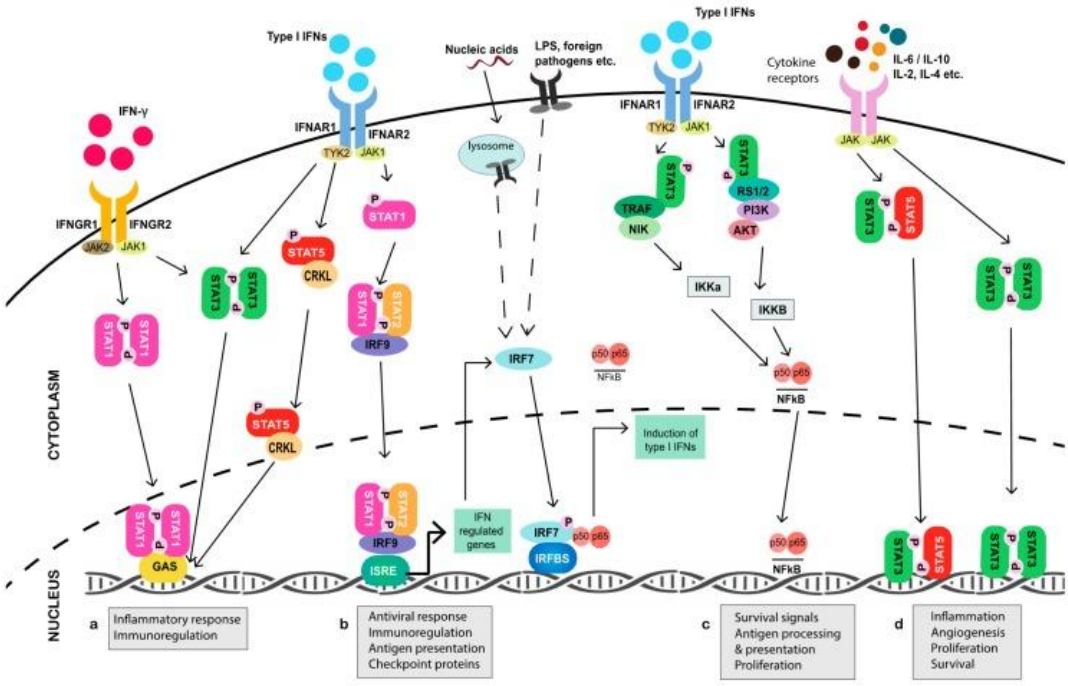

Figure 5. IFN signaling pathway. Adapted from Owen et al., Cancers, 2019 (160).

STAT3 was found to inhibit wild-type p53, and *vice versa*, in fibroblast cells (161,162), whereas mutant p53 induce a persistent phosphorylation of STAT3 following a strong increase of ROS species in pancreatic cancer cells (163).

The presence of a STAT-ROS cycle was studied in different solid tumours, where ROS were found to induce the phosphorylation of STAT1/3, thus enhancing the effect of IFNs on STAT activation (164). Higher amount of activated STAT3 has been found in CLL cells (165) and these cells exhibit receptors on the membrane with high affinity for type I and II IFNs (166), which transduce anti-apoptotic signals (167–169). Moreover, both STAT1 and STAT3 were found to be persistently activated in B lymphocytes from CLL patients, inducing cell survival and proliferation (170,171). Of note, STAT1 was found to inhibit MDM2, the main regulator of p53, in response to DNA damage, thus inducing wild-type p53 and the transcription of pro-apoptotic genes in mouse embryonic fibroblasts and in human fibrosarcoma cell lines (172). On the other hand, p53 was found to negative regulate STAT1 phosphorylation in non-small cell lung cancer (173).

Taken together, all this information highlights how complex is this system, which is probably regulated in a tumour-dependent manner. In addition, the role of mutant p53 in the modulation of IFN pathway has not yet been investigated in CLL. For this reason, the study of IFN/STAT/p53 axis could provide more details to better understand how CLL cells reacts to external stimuli, such as drug treatments, in order to exploit these features to target CLL cells.

1.5. Therapeutic strategies for CLL

A huge variety of options is available nowadays for the treatment of CLL. For several decades, the therapeutic gold standard has been the use of cytostatic agents, such as chlorambucil and fludarabine (174,175). Then monoclonal antibodies were developed, mainly anti-CD20; among these are rituximab, ofatumumab and obinutuzumab (176–179).

Agents targeting signaling pathways of CLL cells were also developed, for example PI3K inhibitors (i.e. idelalisib) (180), BTK degraders (181) and the well-known BTK inhibitors: ibrutinib, acalabrutinib, zanubrutinib, pirtobrutinib (182–185). Other therapeutic approaches include Bcl2 inhibitor venetoclax (186), the checkpoint inhibitor pembrolizumab (187) and the treatment with CAR-T cells (188).

Bruton's tyrosine kinase (BTK) is a kinase involved in the signal transduction pathway downstream of the B-cell receptor (BCR) (189,190). BCR is expressed on the surface of B cells and mediates specific recognition of antigens through hypervariable regions within the immunoglobulin heavy and light chains that together constitute the BCR (191). This pathway is essential for B cell development and proliferation and is abnormally activated in CLL (192). BTK is a composed by five functional domains: a pleckstrin homology (PH) domain, a TEC homology (TH) domain, SRC homology domains SH3 and SH2, and a catalytic kinase domain (193). These domains are involved in the recruitment of the BTK to the cell membrane (PH) (182,194), and its stability (TH) (182,194), mediate protein-protein interactions (SH2 and SH3) (195) and propagate the signal downstream in the cell (catalytic kinase domain) (196). Consistent with its crucial role in B cell differentiation, proliferation and survival, the inhibition of BTK has been studied, to prevent the BCR pathway activation and allow tumour reduction (192,197) (*Figure 6*).

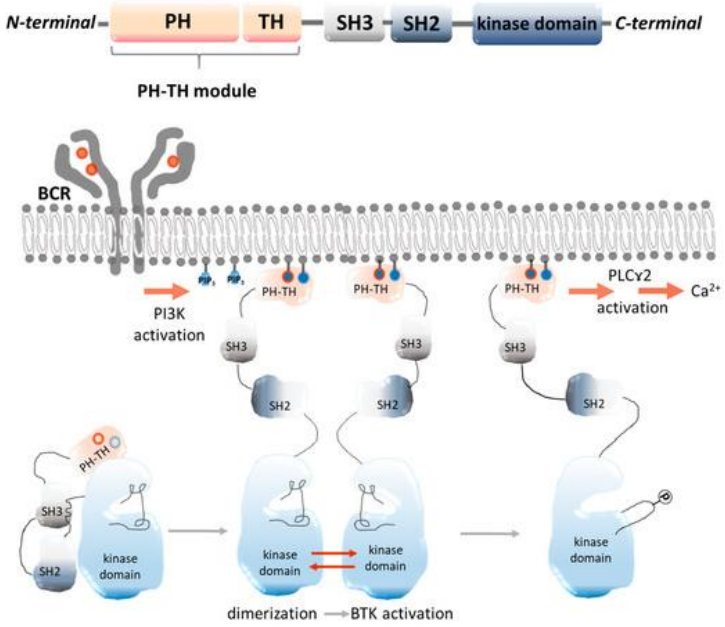

Figure 6. BTK structure and activation. Adapted from Rozkiewicz et al., Molecules, 2023 (198).

A central strategy in the development of more effective CLL therapies has been the combination of agents that induce a synergistic, or at minimum additive, therapeutic effects while minimizing overlapping toxicities. More recently, this concept has been extended to the use of targeted therapies, offering the potential for durable disease control through short treatment regimens with a fixed duration, employing highly potent inhibitors (199).

The chemotherapy combination fludarabine plus cyclophosphamide (FC) is the most studied and generated encouraging results (200): Chemoimmunotherapy with monoclonal antibodies anti-CD20 highly increased the response rates and long term remissions with the combination rituximab-fludarabine-cyclophosphamide (FCR) (201,202). Another promising treatment puts together BTK inhibitors or Bcl2 antagonists with anti-CD20, such as ibrutinib plus rituximab (203), acalabrutinib plus obinutuzumab (204) or venetoclax and rituximab (205).

Considering the high number of available choices for CLL treatment, different parameters need to be considered when selecting the optimal therapeutic option. The main indicators are the clinical stage of the disease, the symptoms of the patients, the fitness and concomitant diseases of the patients, the genetic risk of leukemia, and the treatment situation (206).

The first-line treatment is indicated for patients with advanced or symptomatic CLL. Current therapeutic options include fixed-duration venetoclax-obinutuzumab, second-generation BTK inhibitor monotherapy, or combinations of venetoclax with BTK inhibitors. The toxicity profile guide the therapeutic choice by considering the cardiovascular risk for the treatment with BTK inhibitors, and tumour lysis or renal complications with regimens that include venetoclax (206). Patients with del(17p) or *TP53* mutations represent a high-risk subgroup. Indeed, chemoimmunotherapy should be avoided for these patients, in favour of BTK inhibitors; in selected cases, allogeneic stem cell transplantation may be considered at relapse (207,208). When targeted therapies are unavailable, chemoimmunotherapy with FCR may still be an option for fit patients with mutated *IGHV* and intact *TP53* (209).

First-line therapy may be repeated when the remission lasts more than 3-4 years. In contrast, patients with early relapse, refractory disease, or del(17p) require a change in therapeutic strategy and the use of a second-line regimen highly effective. Patients that were initially treated with a BTK inhibitor receive as second treatment venetoclax combined with an anti-CD20 antibody or non-covalent BTK inhibitor. Patients who received venetoclax-obinutuzumab may repeat this regimen after a prolonged remission; in alternative are treated with a BTK inhibitor-based approach. Finally, patients previously administered chemoimmunotherapy should receive either a BTK inhibitor or venetoclax plus an anti-CD20 antibody (206).

Double-refractory CLL represents cases with very limited therapeutic options. Available strategies include PI3K inhibitor-based regimens, cellular approaches such as CAR-T therapy or allogeneic stem cell transplantation, and, less effectively, chemoimmunotherapy (208,210). Given the poor prognosis, these patients are good candidates for clinical trials evaluating novel agents. Furthermore, although a variety of molecules and treatments are available, p53-deficient CLL patients remain challenging to treat, and novel therapeutic approaches targeting the p53-pathway are needed.

1.6. PRIMA-1^{Met}

Despite the availability of many molecules and therapeutic approaches to treat CLL patients, carriers of *TP53* mutations are associated with treatment resistance and decreased progression-free survival, highlighting the importance of developing alternative targeted strategies to enhance therapeutic efficacy in these patients (211).

Over recent years, multiple compounds capable of restoring mutant p53 activity have been identified. Among these, PRIMA-1^{Met}, also called APR-246 or Eprenetapopt (hereafter referred to as PRIMA-1^{Met}), represents the most clinically advanced small molecule, as it has been shown to reactivate wild-type-like p53 pro-apoptotic functions in mutant p53 variants, exerting anti-tumour activity in preclinical models (212).

PRIMA-1^{Met} is the methylated form of PRIMA-1, a compound that was discovered in 2002 through a cell-based screening of a low-molecular-mass compound library from the U.S. National Cancer Institute (NCI), aimed at identifying agents that suppress tumour cell growth based on the p53-R273H mutation status (213,214). This compound was later shown to restore the proper folding of mutant p53 and to activate key p53 target genes, including *CDKN1A*, *BAX*, and *PUMA*, in cancer cells (215,216). PRIMA-1 and PRIMA-1^{Met} are prodrugs that are hydrolysed to the active metabolite methylene quinuclidinone (MQ). MQ acts as a highly reactive electrophile and Michael acceptor, and its covalent interaction with cysteine residues in p53 appears to be essential for the ability of PRIMA-1 and PRIMA-1^{Met} to trigger apoptosis (216). Among these residues, Cys124, 135, and 141 were identified as possible targets for MQ; however, Cys124 has been confirmed to be the key site for the reactivation of mutant p53 (217).

In addition to its effects on p53, MQ has been shown to inhibit thioredoxin reductase 1 (TXNRD1) (218) and to reduce intracellular GSH levels (219), mechanisms that likely contribute to the antitumor activity of PRIMA-1^{Met} and MQ (220). Of note, PRIMA-1^{Met} exhibits a distinctive ability to reduce GSH levels while concomitantly elevating ROS (216).

Consistent with this mechanism, PRIMA-1^{Met} showed pronounced cytotoxic activity in primary multiple myeloma (MM) samples harbouring *TP53* deletions, as well as in diverse cell lines carrying different p53 alterations, reflecting the molecular heterogeneity of MM (221).

The NRF2/SLC7A11 axis critically modulates the GSH/ROS balance and determines cellular sensitivity to PRIMA-1^{Met}. The active metabolite MQ depletes GSH, by direct binding its cysteines residues, thus increasing ROS levels. These effects are amplified in cells harbouring mutant p53 due to the repression of SLC7A11 mediated by Nrf2 and the consequent impaired cystine uptake. Conversely, cells with wild-type or absent p53 present higher SLC7A11 expression and GSH levels, resulting in higher resistance. Accordingly, SLC7A11 levels inversely correlates with PRIMA-1^{Met} sensitivity, identifying it as a potential predictive biomarker of response (146). Of note, pharmacological inhibition of SLC7A11 may induce a synthetic lethal interaction with mutant p53, which is often highly expressed in tumour cells, leading to excessive oxidative stress and cell death (222).

The cytotoxic activity of PRIMA-1^{Met} was recently evaluated in 62 primary CLL samples characterised for their *TP53* mutational status and the p53 protein expression. PRIMA-1^{Met} induced similar effects in cell viability, causing apoptosis in both *TP53*-mutated and *TP53* wild-type samples. However, in a subset of CLL cases presenting accumulation of mutant p53, the treatment with PRIMA-1^{Met} led to a decrease of mutant p53 protein levels, which was associated with increased apoptosis in comparison to cells with a stable mutant p53 expression. Thus, sensitivity to PRIMA-1^{Met} correlated with a reduction in mutant p53 protein abundance in responsive CLL cells (223).

1.7. Sulfasalazine

Sulfasalazine (SAS) is a sulfonamide-derived drug widely used in the treatment of chronic inflammatory bowel disease and rheumatoid arthritis. It functions as a prodrug that is metabolised in the gut into sulfapyridine and 5-aminosalicylic acid, both of which contribute to its anti-inflammatory effects.

Its primary mechanism of action is the inhibition of Nuclear Factor-kB (NF-kB). This transcription factor is a central mediator of the immune response (224) and its dimers are generally sequestered in the cytoplasm in an inactive state through their association with inhibitory IkB proteins. Following cellular stimulation, IkB become phosphorylated, a process that triggers its ubiquitination and subsequent proteasomal degradation. This sequence of events releases NF-kB, which translocate into the nucleus to bind to specific DNA motifs within promoter or enhancer regions of target genes (225). SAS exerts its anti-inflammatory effects via the inhibition of the phosphorylation of IkB and the subsequent translocation of NF-kB into the nucleus (226).

In addition to its anti-inflammatory activity, SAS has been shown to inhibit xC^- functions. The limitation of cystine import reduces the intracellular cysteine availability and GSH synthesis, thus impairing antioxidant defences and promoting ROS accumulation. These effects disrupt redox homeostasis and may sensitise tumour cells to cell death as a consequence of oxidative stress, particularly in cancer cells that rely on the xC^-/GSH axis for their survival. Together with the constitutive activation of the NF-kB signaling pathway observed in CLL patients (227), this provides a rationale for exploiting this molecule as a strategy to limit CLL cell proliferation.

2. Aim and Rationale

This research aimed to evaluate a strategy that may help to prevent relapse in Chronic Lymphocytic Leukemia (CLL) cases that are resistant to standard therapies, a condition that is frequently associated with *TP53* mutations. Considering the high percentage of *TP53* mutations in refractory CLL patients, a deep understanding of the mechanisms that involve p53 and its role in the resistance of CLL cells may contribute to develop specific strategies to prevent the proliferation of clones.

The project focused on the study of a specific vulnerability of CLL cells that could be exploited to counteract leukemic clones by targeting a parallel pathway: the cellular antioxidant defence.

For this purpose, PRIMA-1^{Met}, a molecule able to target the p53 and deplete glutathione (GSH), was associated to Sulfasalazine, which inhibits the activity of SLC7A11, the principal transporter used by cells for the uptake of cystine, a GSH precursor (*Figure 7*). The idea was to boost the oxidative stress, due to the strong reduction in the antioxidant response, in order to generate an unsustainable condition for CLL cell survival.

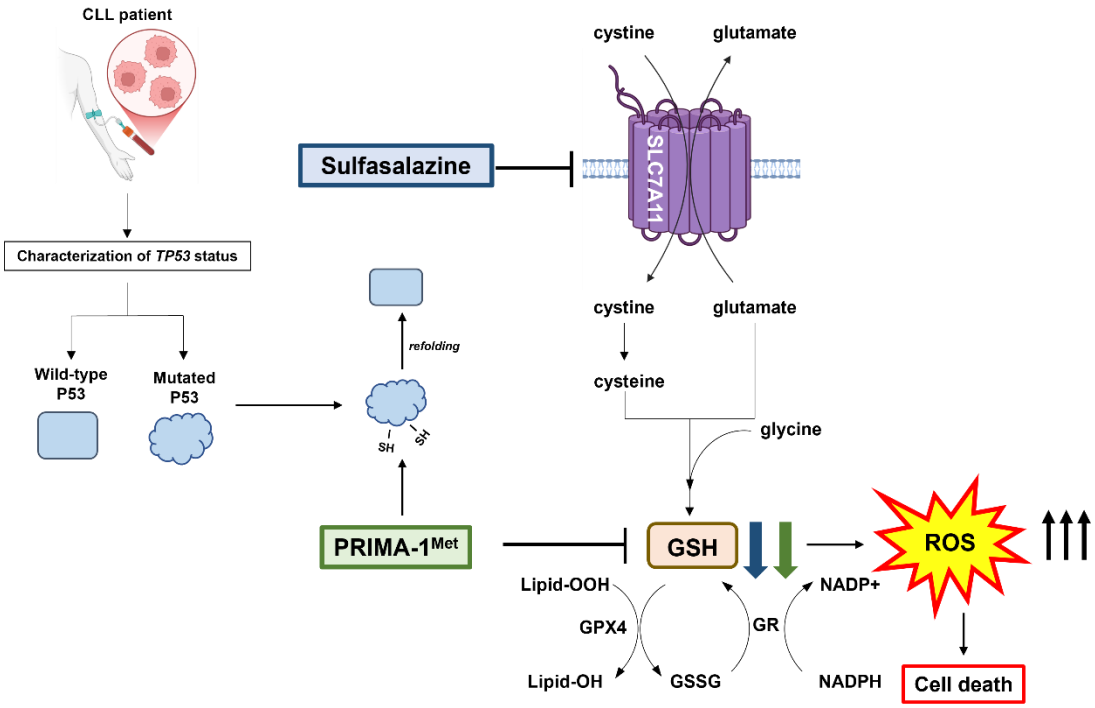

Figure 7. Graphical abstract.

3. Materials and Methods

3.1. CLL cell lines

OSU-CLL (OSU) cell line was used as a *TP53* wild-type model of CLL and was obtained by Hertlein et al. at the Ohio State University by EBV transformation of PBMC from CLL patients. This cell line is *IGHV* mutated and positive for CD19, CD20, CD23 and CD5 (228).

MEC-1 cell line was used as a *TP53* mutated model of CLL as it carries a double mutation involving this gene: p.Q317fs and del17p. The cell line was isolated from the PBMC of a CLL patient from Deutsche Sammlung von Mikroorganismen und Zellkulturen GmbH (DSMZ, Braunschweig, Germany). MEC-1 cells are positive for CD19, CD20, CD23, CD5 and *IGHV* unmutated (229).

Both cell lines were sequenced to confirm the *TP53* status. Cells were cultured in RPMI complete medium, added with 10% of fetal bovine serum (FBS), 1% L-glutamine and 1% of penicillin-streptomycin mixture (Euroclone, Milan, Italy) and maintained at 37 °C with 5% CO_2, at 100% humidity.

3.2. CLL primary cells

CLL primary cells were isolated from the PBMC of untreated CLL patients after informed consent according to the Declaration of Helsinki. CLL patients were recruited from the Vivo-CLL protocol, a prospective study conducted in the IRCCS Ospedale Policlinico San Martino and approved by the Regional Ethics Committee.

In *Table 1* the molecular features of the patients are summarised. Peripheral blood mononuclear cells (PBMC) were isolated by density gradient centrifugation using Ficoll-Hypaque (Lympholyte-H, Cedarlane Labs, distributed by Euroclone, Milan, Italy). Then CD19-positive CLL cells were purified by the B-CLL isolation Kit (Miltenyi Biotec Srl, Bologna, Italy) through negative selection. The percentage of purified B cells (CD19+) was verified to exceeded 95%.

Biological and molecular features of CLL patient's samples

Patient ID	*TP53* status	*TP53* mutation	*TP53* mutation (%)	Variant effect	FISH				*IgHV* status
					17p-	11q-	12	13q-	
#1	MUT	p.G245S	84	missense	yes (86%)	no	no	no	mut
		p.R213L	1.7	missense					
		p.R248W	1.5	missense					
		p.V197E	8.7	missense					
#2	MUT	p.143E	93.2	missense	yes (64%)	no	no	yes (86%)	unmut
#3	MUT	p.I195T	43.87	missense	no	no	yes (12%?)	yes (93%)	mut
#4	MUT	p.I195T	100	missense	yes (80%)	no	no	no	unmut
#5	MUT	p.P89fs	78	frame shift deletion	yes (73%)	no	no	yes (89%)	mut
		p.T211I	4	missense					
		p.K164E	6	missense					
		p.S215G	7.5	missense					
#6	MUT	p.F134V	Sanger	missense	yes (98%)	no	no	no	unmut
#7	MUT	p.V272M	100	missense	yes (98%)	no	no	no	mut
#8	MUT	p.Y234C	Sanger	missense	yes (60%)	yes (62%)	no	yes (50%)	mut
#9	MUT	p.I195T		missense	yes (25%)	no	no	no	unmut
#10	WT				no	no	no	yes (92%)	unmut
#11	WT				no	no	no	yes (71%)	mut
#12	WT				no	no	no	yes (90%)	mut
#13	WT				no	no	no	yes (22%)	unmut
#14	WT				no	no	yes (68%)	no	unmut
#15	WT				no	yes (57%)	no	no	unmut
#16	WT				no	no	yes (72%)	no	
#17	WT				no	no	no	no	mut

Table 1. Sample analysed were characterised for their molecular features and clustered following the *TP53* mutational status, in mutated and wild-type groups. FISH analysis was conducted to detect deletions at chromosomes 17p, 11q, 13q and the trisomy at chromosome 12. IGHV mutational status was also assayed. Adapted from Pasino et al., Int. J. Mol. Sci., 2025 (239).

3.3. Drug treatments

For the treatment of OSU and MEC-1 cells, the PRIMA-1^{Met} (ab145974, Abcam, Cambridge, UK) stock solution was dissolved in H_2O at a concentration of 50 mM. The Sulfasalazine (SAS, Cayman Chemical, Ann Arbor, MI, USA) stock solution was prepared by dissolving the powder in Dimethyl Sulfoxide (DMSO) at 50 mM concentration. Working solutions were diluted in RPMI added with L-glutamine and antibiotic mixture, without serum. Cells were plated at a concentration of 5 x 10^5 /mL in flasks or plates (depending on the experimental design) and treated 2 h later with the two molecules alone or in different combination.

H_2O_2 (Farmac-Zabban S.p.A., Bologna, Italy) was diluted in Dulbecco's Phosphate Buffered Saline 1X (PBS, Euroclone, Milan, Italy) from the stock solution (880 mM) at a final concentration of 50 mM and was added 2 h before PRIMA-1^{Met} and SAS.

Ferrostatin-1 (Sigma-Aldrich, St. Louis, MO, USA) stock solution was dissolved in DMSO at a concentration of 38.1 mM. Working solutions were then prepared in RPMI serum-free and added 1 h before the treatment with PRIMA-1^{Met} and SAS.

Primary cells were stimulated by CpG/ODN2006 (hTLR9 ligand) at a concentration of 5 μg/mL (Aurogene, Rome, Italy) in combination with IL-15 at 10 ng/mL (PeproTech, Rocky Hill, NJ, USA). Subsequently, PRIMA-1^{Met} and SAS, either alone or in combination, were added both in activated and non-activated cells.

3.4. Protein extraction and quantification

Cells were harvested and washed with 1X Dulbecco's Phosphate Buffered Saline (Euroclone, Milan, Italy) and cell lysis was performed adding 100 µL / 106 cells of buffer with the following composition: 50 mM Tris/HCl pH 7.5, 150 mM NaCl, 1% NP-40, 10% glycerol and 10 mM EDTA, added with 7X protease inhibitors cocktail (cOmpleteTM ULTRA Tablets, Mini, EASYpack, Roche, Manneheim, Germany) and 100X phosphatase inhibitors cocktail (Phosphatase InhibitorCocktail, Cell Signaling Technology, Danvers, MA, USA). Cell lysates were incubated for 30 min at 4°C and centrifuged at 13,200 rpm for 5 min at 4°C.

Protein concentration was determined using the BCA assay kit (Thermo Scientific, Rockford, Illinois, U.S.A.), following the manufacturer's protocol. The calibration curve was generated using Bovine Serum Albumin (BSA) by plotting its known concentrations (µg/mL) on the x-axis against the corresponding absorbance values on the y-axis. The protein concentration was compared to standard curve and calculated using the equation derived from the standard curve's linear relationship. The absorbance was measured at 570 nm (Mithras LB 940, Multilabel reader, Berthold Technologies, BadWildbad, Germany).

3.5. Western blotting analysis

A total amount of 10 to 20 μg of total proteins was prepared, for each sample, in a solution with Loading Buffer (SDS 9%, glycerol 50%, Bromophenol Blue 0.03%, Tris-HCl 375 mM pH 6.8, H2O), added with Dithiothreitol (DTT) with a final concentration of 1 mM. Samples were then denatured at 95 °C for 5 min and resolved on 4‑15% Mini Protean TGX precast gels (Bio-Rad, Milan, Italy), together with a molecular weight marker, for 5 min at 90 V followed by 35 min at 180 V. At this stage the gel was immersed in a Running Buffer (Tris 0.25 M, glycine 1.9 M, SDS 20%, H2O) to facilitate the migration.

The transfer of the proteins to nitrocellulose membranes was executed, at the end of the run, by Trans-Blot Turbo Blotting System (Bio-Rad, Milan, Italy). Subsequently, membranes were blocked with 2% non-fat dry milk in 0.1% Tween-20 in PBS 1X for 1 h. The incubation with appropriate primary antibodies, diluted in 1% non-fat dry milk in 0.1% Tween-20 in PBS, was conducted 1 h at room temperature or overnight at 4 °C.

The antibodies employed were used to evaluate the following targets: P53 (clone DO-1, Santa Cruz Biotechnology, Dallas, TX, USA), P21 Waf1/Cip1 (clone DCS60, #2946, Cell Signaling Technology, Danvers, MA, USA), MDM2 (clone SPM14, sc-965, Santa Cruz Biotechnology), Bcl-2 (sc-509, Santa Cruz Biotechnology), SLC7A11/xCT (clone D2M7A, #12691 Cells Signaling Technology, Danvers, MA, USA), p-STAT1 (clone 58D6, #9167, Cell Signaling Technology, Danvers, MA, USA), p-STAT2 (clone D3P2P, #88410, Cell Signaling Technology, Danvers, MA, USA), p-STAT3 (clone D3A7, #9172, Cell Signaling Technology, Danvers, MA, USA), CASP-3 (#9661, Cell Signaling Technology, Danvers, MA, USA), γH2A.X (clone 20E3, #9718, Cell Signaling Technology, Danvers, MA, USA), OAS2 (clone E2G4K, #24344, Cell Signaling Technology, Danvers, MA, USA), ISG20 (#73235, Cell Signaling Technology, Danvers, MA, USA), human β-Actin (clone AC-74, Sigma‑Aldrich, St. Louis, MO, USA).

Membranes were then incubated with IgG-horseradish peroxidase-conjugated secondary antibodies: anti-rabbit IgG HRP (A9169, Sigma-Aldrich, St. Louis, MO, USA) or anti-mouse IgG HRP (A9044, Sigma-Aldrich, St. Louis, MO, USA). Detection was then performed with ECL FAST PICO (ECL-1002, Immunological Sciences, Rome, Italy); the chemiluminescence was analysed by Alliance LD, UVITEC Cambridge (Cambridge, UK).

3.6. MTT assay

This colorimetric assay detects the cell viability based on the activity of mitochondrial enzymes: viable cells are able to reduce the Thiazol Blue Tetrazolium Blue (MTT) to MTT-formazan crystals, giving a purple shade to the cell suspension. The absorbance is then measured to calculate the cell viability of each sample (230).

Cells were seeded at a density of 5 x 104 cells per well in 100 µL of complete RPMI in 96-well plates and cultured for 24 h before treatment. PRIMA-1^{Met} and SAS were then added alone or in combination for 24 h and 48 h of treatment. Subsequently, 11 µL of MTT (Sigma-Aldrich, St. Louis, MO, USA) dissolved in PBS 1X at a stock concentration of 5 mg/mL were added to each well. Cells were kept in the incubator for the following 4 h and the reaction was stopped by adding 110 µL of a solubilising solution (10% sodium dodecyl sulfate (SDS) in 0.01M HCl) to solubilise the purple MTT-formazan crystals (231). After overnight incubation, the absorbance was measured by Mithras LB 940 (Multilabel reader, Berthold Technologies, BadWildbad, Germany) at 570 nm with a reference at 690 nm.

3.7. Apoptosis determination

The percentage of apoptotic cells was measured using the Annexin V-FITC/propidium iodide (PI) double staining method, which exploits the different phospholipid composition of the inner and outer layer of the cell membrane in viable vs apoptotic cells. In physiological conditions, the extracellular leaflet is enriched in phosphatidylcholine (PC) and sphingomyelin (SM), whereas the intracellular side is mainly composed of phosphatidylethanolamine (PE) and phosphatidylserine (PS).

During the early phase of apoptosis, PS is exposed on the outer layer. Since Annexin-V binds to negatively charged phospholipids, as PS, this principle is used to discriminate viable cells from those undergoing early apoptosis (232). To better distinguish the different stages of apoptosis, from cells with an intact membrane (early apoptosis) to those who have lost their cell membrane integrity (late apoptosis), PI is used as a dye exclusion test (233).

OSU and MEC-1 cells were harvested 24 h and 48 h after treatment, centrifugated for 5 min at 1,200 rpm, washed once with PBS 1X and resuspended in 100 µL binding buffer 1X at a concentration of 2 x 105 cells/mL (Annexin V-FITC Apoptosis detection kit, Invitrogen, Milan, Italy). Cells were then added with 2.5 µL Annexin V-FITC and 5 µL PI (20 µg/mL) and were stained 10 min at room temperature in the dark.

The percentages of cells in early and late apoptotic stages (FITC-positive/PI-negative and FITC-positive/PI-positive, respectively) were assessed by flow cytometry. Data were collected via dual-colour analysis conducted on 10,000 gated cells using a Cytoflex S flow cytometer (Beckman-Coulter, Brea, CA, USA). Annexin V-FITC was excited at 488 nm, and its fluorescence emission was detected at 520 nm, whereas the PI probe was excited at 535 nm and the emitted fluorescence was collected at 617 nm. For the apoptosis determination of CLL primary cells, cells were treated for 24 h, 48 h, and 72 h, then harvested and processed as described above. All the data were analysed with FlowJoTM version 10.8.1.

3.8. Synergy calculation

OSU and MEC-1 cell lines were treated with all the possible combination between PRIMA-1^{Met} and SAS at five different concentrations for each molecule. The isobole method (234) was used to assess the effects of the combined treatment based on the MTT assay. The combination index, indicated as "D" was calculated for each condition as described below (S = SAS, P = PRIMA-1^{Met}):

$$D = Sc/Se + Pc/Pe$$

Sc and Pc indicate the concentrations of SAS and PRIMA-1^{Met} used in combination, respectively, while Se and Pe represent the drug concentrations that gave, alone, the same magnitude of effect (235). For $D < 1$ the final effect of the combination was considered synergistic, when $D = 1$ the effect is considered additive and if $D > 1$ the combination is considered antagonistic. Since the dose-response curves were linear for both PRIMA-1^{Met} and SAS, the effect between the two drugs was calculated using the concept of "summation of doses" (234) as described below:

- $Ecomb = Ea + Eb$ for additive effect
- $Ecomb > Ea + Eb$ for synergistic effect
- $Ecomb < Ea + Eb$ for antagonistic effect

3.9. GSH intracellular levels determination

Intracellular levels of reduced glutathione (GSH) were quantified by high-performance liquid chromatography (HPLC) according to the method described by Fariss and Reed for total GSH (236).

After 24 h of treatment, cells were harvested, centrifuged 5 min at 1,200 rpm, washed once in PBS 1X and precipitated with 10% perchloric acid (PCA). Iodoacetic acid (pH 8) was then added to block the thiol groups for 10 min at room temperature in the dark. The samples were then incubated with 1% 1-Fluoro-2,4-dinitrobenzene (FDNB at 4 °C overnight in the dark) to convert analytes to 2,4-dinitrophenyl derivatives.

The analytes were quantified by HPLC equipped with an NH2 Spherisorb column and a UV detector set at 365 nm, with a flow rate of 1.25 mL/min. The mobile phase was composed by different percentages of solution A (80% methanol and 20% water) and B (0.5 M sodium acetate in 64% methanol in water). At the beginning of the analysis the ratio was 80:20 A:B for 5 min, followed by a linear gradient to 1% A and 99% B for 10 min. Chromatography was performed with gradient elution and the data were normalized to the intracellular amount of protein content, expressed as μEq/mg of protein.

3.10. ROS determination

For the determination of reactive oxygen species (ROS) levels in OSU and MEC-1 cells the 2′,7′- dichlorodihydrofluorescein diacetate non-fluorescent dye (H2DCF-DA, Thermo Fisher Scientific, Waltham, MA, USA) was employed. The intracellular H2DCF-DA is cleaved to 2′,7′-dichlorofluorescein (H2DCF) which is then converted into the highly fluorescent 2′,7′-dichlorofluorescein (DCF) in the presence of pro-oxidant species (237).

Cells were treated for 24 h, harvested and centrifugated for 5 min at 1200 rpm and washed once with PBS 1X. Samples were then resuspended in PBS 1X at a concentration of 5 x 105 cells/mL and incubated for 20 min at 37 °C with H2DCF-DA at a final concentration of 5 μM in serum-free RPMI (the stock solution was previously prepared in DMSO at 10 mM concentration).

Flow cytometric analysis was then performed on 10.000 viable cells per condition using the Cytoflex S flow cytometer (Beckman Coulter, Brea, CA, USA): the probe was excited at 488 nm, and fluorescence emission was collected at 520 nm. Data were then analysed with FlowJoTM version 10.8.1.

3.11. Antioxidant enzymatic activity evaluation

Glutathione peroxidase (GPx) activity was determined using a reaction mixture containing 100 mM Tris-HCl (pH 7.4), 5 mM H2O2, and 5 mM GSH following the decomposition of H2O2 at 240 nm. Since H2O2 is also a substrate for catalases, GPx activity was calculated by subtracting the catalase activity from the total decomposition activity of H2O2 (catalase was assayed spectrophotometrically following again the H2O2 decomposition at 240 nm) (238).

Glutathione reductase (GR) activity was measured by spectrophotometric analysis following the oxidation of NADPH at 340 nm. The assay solution was composed of Tris HCl at 100 mM, pH 7.4, EDTA 1 mM, GSSH 5 mM, and NADPH 0.2 mM (238).

3.12. NADPH oxidase activity evaluation

NADPH oxidase enzymatic activity was evaluated by spectrophotometric analysis of the cell homogenates by measuring the cytochrome c reduction at 550 nm. The assay was conducted in the presence or absence (blank) of superoxide dismutase (SOD) added at a concentration of 20 mg/mL using a solution composed of 60 mM cytochrome c, 1 mM CaCl2, 1 mM MgCl2. Samples were incubated for 5 min at 37 °C and subsequently centrifuged at 800 x g for 5 min. The absorbance of the supernatant was detected at 550 nm and normalised to the protein content of the samples, reported as mU/mg (239).

3.13. MDA content and antioxidant capacity evaluation

Malondialdehyde (MDA) levels, an indicator of lipid peroxidation, were evaluated using the thiobarbituric acid reactive substances (TBARS) assay. This assay is based on the reaction of MDA with TBA (240): a 50 µg amount of cell homogenate was dissolved in 300 µL of Milli-Q water and 600 µL of TBARS solution (15% TCA in 0.25 N HCl and 26 mM TBA) were then added. The mixture was incubated for 40 min at 100 °C, after which samples were centrifuged at 14,000 rpm for 2 min and the supernatant was analysed by spectrophotometer at 532 nm.

For primary CLL cells, the intracellular GSH content ratio and the antioxidant capacity (AO), expressed as Trolox equivalent, were measured using commercial assay kits (Abcam; Cat #ab65329, and Merck; Cat #MAK440, respectively).

3.14. Statistical analyses

Statistical significance among experimental groups was calculated using unpaired t-test, ordinary one-way Anova, and two-way Anova, followed by multiple comparisons test. All statistical analyses were performed using GraphPad Prism version 9.0. for Windows, GraphPad Software (San Diego, CA, USA), and $p < 0.05$ was considered statistically significant.

4. Results

4.1. PRIMA-1^{Met} is unable to rescue mutant p53 transcriptional function in CLL cells

Considering the high involvement of *TP53* dysfunction in the treatment failure in CLL (31,32), this study firstly focused on the restoration of p53 functions as a strategy to target CLL cells and induce leukemic cell death. PRIMA-1^{Met} was used to treat two CLL cell lines since it may reactivate the wild-type functions of mutant p53 in many tumour cells, such as osteosarcoma cells, non-small cell lung cancer cells, ovarian carcinoma cells, and others (213).

For this study, OSU-CLL (OSU) and MEC-1 cell lines were used, respectively as *TP53* wild-type and *TP53* mutated models of Chronic Lymphocytic Leukemia (CLL). In MEC-1 cells, the *TP53* gene presents a mutation at codon Q317, which gives rise to a frameshift mutation, generating a truncating form of the protein. In western blot analysis, this mutant p53 protein migrates as a faster migrating band, detectable at 45 kDa (*Figure 8*).

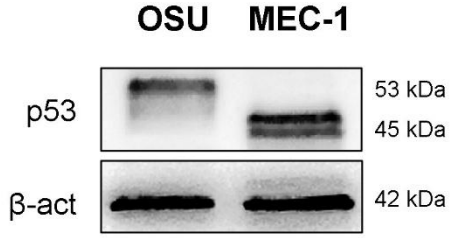

Figure 8. Levels of p53 protein in OSU and MEC-1 cells at basal conditions. Western blot is representative of three independent experiments, β-actin (β-act) was used for loading control. Adapted from Pasino et al., Int. J. Mol. Sci., 2025 (239).

To evaluate whether PRIMA-1^{Met} could reactivate the p53 protein in MEC-1 cells and modulate the wild-type p53 in OSU, CLL cells were treated with PRIMA-1^{Met}, and western blot analyses were performed to check the principal p53-target genes. After treatment at 5, 10, and 20 μM PRIMA-1^{Met}, p53, MDM2, and p21 levels were determined.

In OSU cells, after a partial reduction at 5 μM, the increase in the p53 levels was observed in a dose-dependent manner (*Figure 9A*). In MEC-1 cells, the opposite trend was observed: the treatment with PRIMA-1^{Met} induced a first rise in p53 levels at 5 μM, followed by a decrease at 10 and 20 μM (*Figure 9B*). The p21 and MDM2 proteins followed the same trend as p53, and a strong overall protein reduction was observed after treatment with PRIMA-1^{Met} at 20 μM.

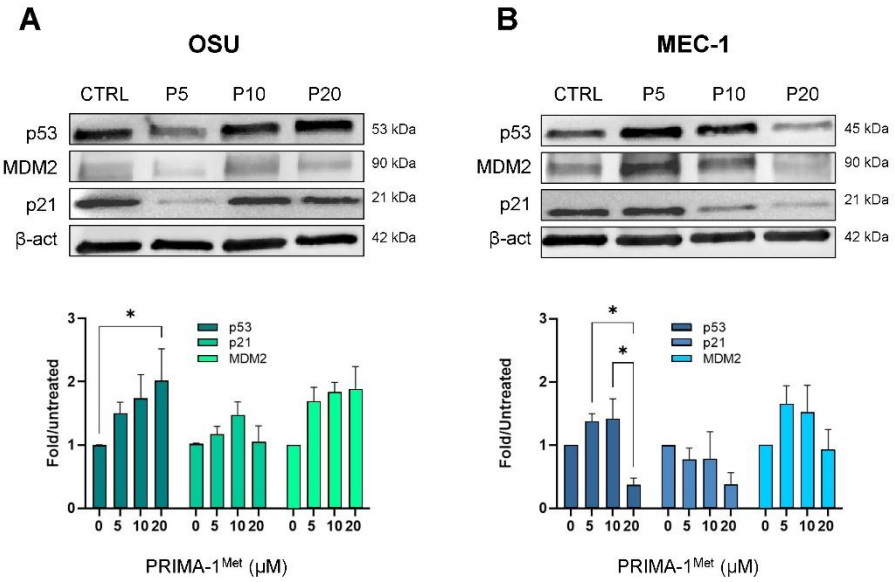

Figure 9. Modulation of p53, p21 and MDM2 expression in OSU and MEC-1 cells treated with PRIMA-1^{Met}. Western blots show how protein levels changed in p53, p21 and MDM2 after 24 h of treatment with PRIMA-1^{Met} at 5, 10 and 20 μM in OSU (**A**) and MEC-1 (**B**) cell lines. β-Actin (β-act) was used for loading control. Western blots are representative of four independent experiments. The relative histograms report the expression of p53, p21 and MDM2 proteins normalised for β-actin. Reported are the means ± SEM of chemiluminescence of four independent experiments calculated as fold over the levels of the same protein in untreated cells. * $p < 0.05$. Adapted from Pasino et al., Int. J. Mol. Sci., 2025 (239).

These data show that, in MEC-1 cells, PRIMA-1^{Met} did not reactivate the transactivation activity of the p53 mutated proteins; on the other hand, the molecule was able to induce p53 in OSU cells carrying a wild-type protein.

For the study of CLL only few cell lines are available as *in vitro* models of the disease. For this reason, the capacity of PRIMA-1^{Met} to reactivate wild-type functions of the p53 protein was also assayed in primary cells from CLL patients, to evaluate whether the two existing cell lines represent a good model for this study. The modulation of p53, MDM2 and p21 proteins was assayed both in wild-type and mutant p53 primary CLL samples.

In cells harbouring a wild-type protein, the increase in p53 levels was followed by an upregulation of MDM2 and p21 both in samples without (*Figure 10A*) and with (*Figure 10B*) pre-treatment with CpG-ODN/IL15. The 24 h stimulation boosted proteins expression; p21 and MDM2 modulation followed the trend observed in p53. A different behaviour was observed in samples carrying mutant p53, where p21 and MDM2 levels were undetectable in samples without pre-treatment with CpG-ODN/IL15 and p53 levels decreased following increasing concentrations of PRIMA-1^{Met} (*Figure 10C*). The 24 h of stimulation partially increased p53 and p21 expression after PRIMA-1^{Met} at 5µM (*Figure 10D*); yet, decreasing levels were detected following increasing PRIMA-1^{Met} concentrations and no MDM2 expression was observed at all.

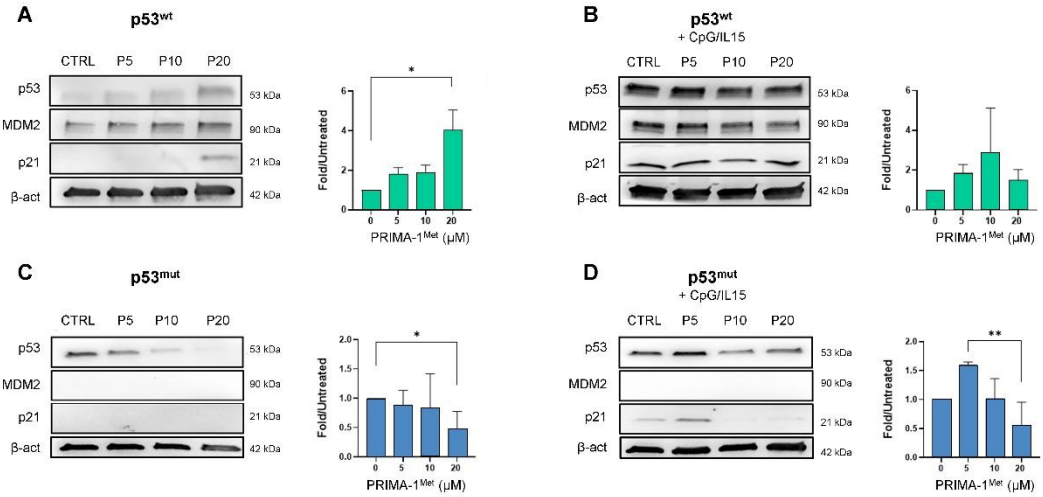

Figure 10. Modulation of p53, and its targets after treatment with PRIMA-1^{Met} in CLL primary cells. Samples were treated with PRIMA-1^{Met} at 5, 10 and 20 µM for 24 h. (**A**) Representative western blots of p53, MDM2 and p21 modulation after treatment in wild-type p53 samples without CpG-ODN/IL15 (Sample #16, *Table 1*). The relative histogram on the right reports data as means ± SEM from three independent samples (samples #10, #16, #17, *Table 1*). (**B**) Representative western blots of p53, MDM2 and p21 modulation after treatment in wild-type p53 samples pre-treated with CpG-ODN/IL15 (Sample #16, *Table 1*). The relative histogram on the right reports data as means ± SEM from two independent samples (samples #16, #17, *Table 1*). (**C**) Representative western blots of p53, MDM2 and p21 modulation after treatment in mutant p53 samples without CpG-ODN/IL15 (Sample #9, *Table 1*). The relative histogram on the right reports data as means ± SEM from three independent samples (samples #3, #4, #9 *Table 1*). (**D**) Representative western blots of p53, MDM2 and p21 modulation after treatment in mutant p53 samples pre-treated with CpG-ODN/IL15 (Sample #9, *Table 1*). The relative histogram on the right reports data as means ± SEM from two independent samples (samples #4, #9 *Table 1*). β-actin (β-act) was used for loading control and normalization. * $p < 0.05$, ** $p < 0.01$. Adapted from Pasino et al., Int. J. Mol. Sci., 2025 (239).

These data are in line with previous results on OSU and MEC-1 cells, confirming that PRIMA-1^{Met} in unable to restore p53 wild-type functions in p53 mutated CLL cells. Since the modulation of p53 and relative targets was similar in CLL cell lines and primary samples, OSU and MEC-1 cells represent good models for the study of the disease *in vitro*. For this reason, following experiments were conducted primarily on cell lines, then validated on CLL samples from patients.

4.2. Combined treatment with PRIMA-1^{Met} and SAS induces cell death in CLL cell lines

Besides the ability to reactivate wild-type functions in mutated p53 proteins in certain tumours (212), PRIMA-1^{Met} has been shown to induce glutathione (GSH) depletion (218,221), which may impact on cell viability. Since the p53 functions were not reactivated in p53 mutated CLL cells, as previously described in this study, this second effect on GSH was deeply investigated, in order to target CLL cells through different mechanisms. Based on this concept, Sulfasalazine (SAS), another molecule that targets the GSH pathway by acting on the xC^- transporter (241), was used in association with PRIMA-1^{Met} to potentiate the effect of the treatment.

CLL cell lines were treated for 24 h and 48 h with 5, 10 and 20 μM PRIMA-1^{Met} and 300 μM SAS alone or in combination. No statistically significant reduction in cell viability was observed for both OSU (*Figure 11A*) and MEC-1 (*Figure 11B*) cell lines after 24 h of treatment with the single molecules at low concentrations. On the other hand, there was a decrease in the cell survival after treatment with PRIMA-1^{Met} 20 μM at 48 h in OSU and 24 h and 48 h in MEC-1 cells.

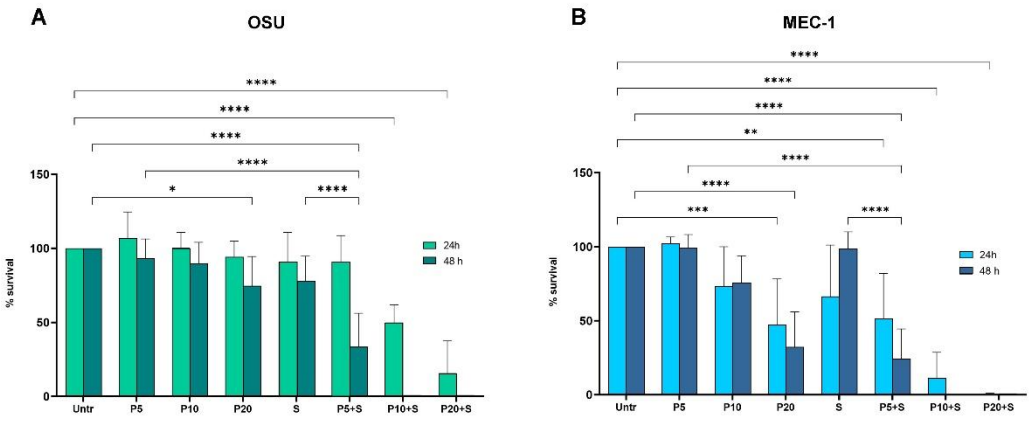

Figure 11. Cell viability of OSU (**A**) and MEC-1 (**B**) cell lines after treatment with PRIMA-1^{Met} (P) and SAS (S). MTT assay was performed after 24 h and 48 h of treatment with PRIMA-1^{Met} at 5, 10 and 20 μM alone or in combination with SAS at 300 μM. The histograms report the means ± SD of at least three independent experiments. Mean ± SD: 1.01 ± 0.32 (n = 36). * $p < 0.05$, ** $p < 0.01$, *** $p < 0.001$, **** $p < 0.0001$. Adapted from Pasino et al., Int. J. Mol. Sci., 2025 (239).

The co-treatment with PRIMA-1^{Met} 5 μM and SAS 300 μM reduced the percentage of viable cells to 51.2 % in MEC-1 at 24 h and to 33.7% in OSU and 24.2% in MEC-1 at 48 h, compared to the untreated control. Similar effects were observed after treatment with PRIMA-1^{Met} 10 μM together with SAS 300 μM at 24 h, while no surviving cells were detected at 48 h. The 20 μM concentration of PRIMA-1^{Met} was too high in combination with SAS; in fact, only 15,7% of surviving cells were detected in OSU at 24 h and no viable cells were observed at 24 h in MEC-1 and at 48 h in both cell lines.

All these data showed that the co-treatment affects both cell lines in a dose-dependent manner; however, MEC-1 cells seem to be more sensitive than OSU to the combined treatment.

4.3. PRIMA-1^{Met} and SAS combined treatment affects p53 mutated cell line more than the wild-type

To better elucidate previous results, apoptosis induction was evaluated by Annexin V/PI assay. OSU and MEC-1 cells were treated for 24 h with PRIMA-1^{Met} at 5 and 10 µM and SAS at 300 µM, and the apoptosis induction was determined. At basal conditions the percentage of apoptotic cells was 20% in OSU (*Figure 12A*) and 9% in MEC-1 (*Figure 12B*) and the treatment with PRIMA-1^{Met} at 5 or 10 µM and SAS at 300 µM alone did not increase the apoptotic population. The combination of 5 µM PRIMA-1^{Met} and 300 µM SAS caused a 30% of apoptosis in OSU and 17.7% in MEC-1. The concentration of 10 µM PRIMA-1^{Met} with 300 µM SAS further raised the percentage of apoptotic cells to 49% in OSU (*Figure 12A*) and 37% in MEC-1 (*Figure 12B*).

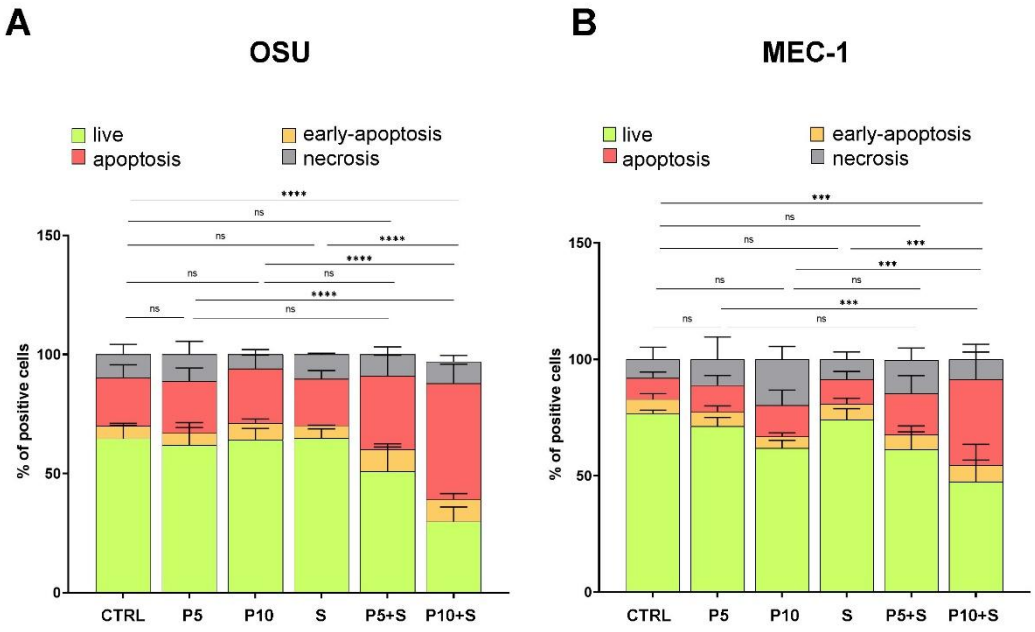

Figure 12. Apoptosis induction in OSU and MEC-1 cells after treatment. Annexin V-FITC/PI assay was performed in both cell lines treated with PRIMA-1^{Met} (P) at 5 and 10 µM alone or in combination with SAS (S) 300 µM. The histograms for OSU (**A**) and MEC-1 (**B**) cell lines show the means ± SD of the percentage of cells undergoing different conditions: live cells (Annexin -/PI -), cells in early apoptosis (Annexin +/PI -), apoptotic cells (Annexin +/PI +) and necrotic cells (Annexin -/PI +). These results were detected by cytofluorimetric assay of three independent experiments. * $p < 0.05$, ** $p < 0.01$, *** $p < 0.001$, **** $p < 0.0001$. Adapted from Pasino et al., Int. J. Mol. Sci., 2025 (239).

The percentage of apoptotic cells was higher in OSU cells than in MEC-1 both in single and combined treatment, suggesting an antiapoptotic behaviour in the p53 mutated cell line. These data were confirmed by Bcl-2 expression, which decreased in OSU (*Figure 13A*) and increased in MEC-1 (*Figure 13B*) following treatment. Of note, the overall apoptotic population after the combined treatment increased more in MEC-1 cells than in OSU (2- and 1.5- fold in the combination with PRIMA-1^{Met} 5 µM and SAS 300 µM, 4- and 2.5-fold with PRIMA-1^{Met} 10 µM and SAS 300 µM, respectively), thus indicating that the co-treatment may counteract the intrinsic antiapoptotic behaviour shown in the *TP53*-mutated cell line.

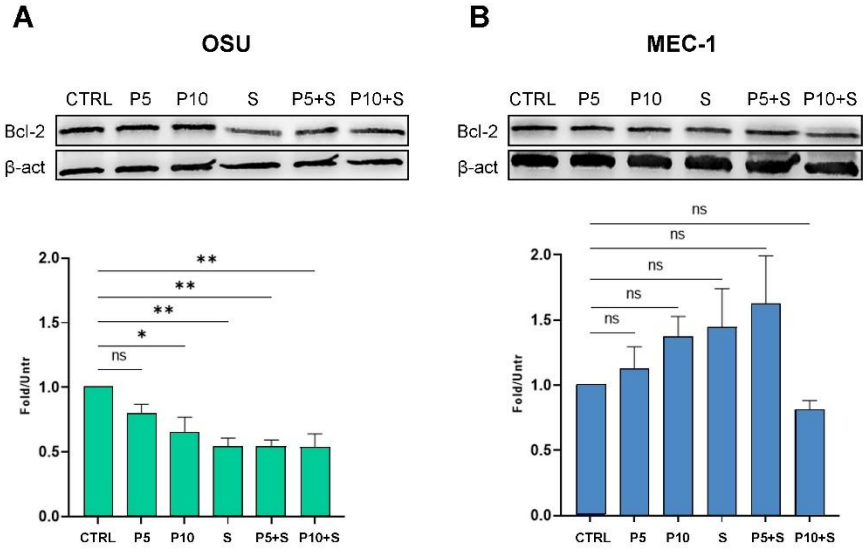

Figure 13. Representative western blots of Bcl-2 levels in OSU (**A**) and MEC-1 (**B**) cells treated with PRIMA-1^{Met} (P) at 5 and 10 µM alone or in combination with SAS (S) 300 µM for 24 h. The relative histograms report the means ± SEM, calculated as fold over the levels of untreated cells, of at least three independent experiments. β-actin (β-act) was used for loading control and normalization. ns = not significant, * $p < 0.05$, ** $p < 0.01$, *** $p < 0.001$, **** $p < 0.0001$. Adapted from Pasino et al., Int. J. Mol. Sci., 2025 (239).

4.4. Combined PRIMA-1^{Met} and SAS treatment synergistically decreases CLL cell survival

The results just described showed that the activity of the two molecules, when added together, seems to be potentiated. MTT experiments were conducted to define whether there was a synergistic effect between PRIMA-1^{Met} and SAS when added to OSU (*Figure 14A*) and MEC-1 (*Figure 14B*) cells as co-treatment. Cells were treated with PRIMA-1^{Met} at 5, 10, 20 and 40 μM, and SAS at 150, 300, 600, 1200 μM for 48 h, alone and in all the possible combinations of drug concentrations. Three different effects were observed: synergism, additivity, and antagonism.

When cells were treated with PRIMA-1^{Met} at 5 and 10 μM combined with SAS 150, 300 and 600 μM, a synergistic effect was observed (D value < 1) between the two molecules in both OSU and MEC-1 cell lines (up to 1200 μM SAS concentration in the *TP53* mutated cell line). The concentration of 20 μM PRIMA-1^{Met} was considered additive (D = 1) with all the concentrations of SAS, apart 150 μM, which was synergic. At PRIMA-1^{Met} 40 μM, an additive effect was observed for all the combinations, excluding the 1200 μM, which caused an antagonistic effect (D > 1) (*Figure 14*).

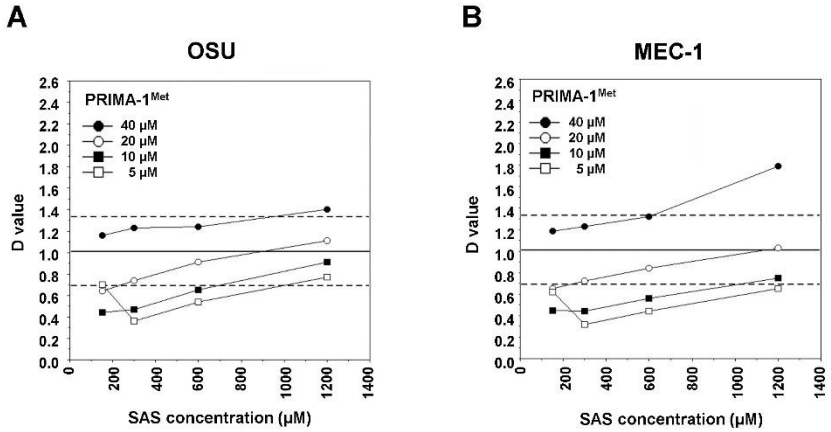

Figure 14. Synergism determination for OSU and MEC-1 cells treated with PRIMA-1^{Met} alone and in combination with SAS. D values for OSU (**A**) and MEC-1 (**B**) cells were calculated based on the absorbance data obtained from the MTT assay. Cells were treated for 48 h: PPRIMA-1^{Met} concentrations were 5 (□), 10 (■), 20 (○) and 40 μM (●); SAS concentrations were 150, 300, 600 and 1200 μM. The experimental D value for additivity was calculated using combinations of two serial dilutions of the tested compounds. Adapted from Pasino et al., Int. J. Mol. Sci., 2025 (239).

These data indicate that the combination of the two compounds can synergistically affect the cell survival of CLL cells. Since these effects are the same for both OSU and MEC-1 cell lines, the *TP53* status seems not to influence the behaviour of the co-treatment in terms of synergy.

4.5. PRIMA-1^{Met} and SAS promote SLC7A11/xCT induction in MEC-1 cells

Since the p53 protein functions are not reactivated by PRIMA-1^{Met} in MEC-1 cells (*Figure 9B*), the effect observed on cell viability was likely due to the potential impairment of the antioxidant defence related to the action of the molecules on the GSH pathway. Indeed, PRIMA-1^{Met} directly targets the GSH molecule, leading to a decrease in the antioxidant response (221). On the other hand, SAS targets the SLC7A11/xCT antiporter, inhibiting its activity (241). It has also been demonstrated that the level of SLC7A11/xCT may represent a determinant of PRIMA-1^{Met} response in a wide variety of tumour cells since low SLC7A11/xCT levels can contribute to decreasing the GSH level and promote cell death (242). Many studies have shown that SLC7A11/xCT protein levels increase after treatment with PRIMA-1^{Met} in different tumour types, such as breast cancer and acute myeloid leukemia (243,244).

Since SLC7A11/xCT is involved in the Glutathione (GSH) synthesis pathway (245), its levels was determined in OSU and MEC-1 cell lines, in order to determine whether the modulation of GSH could explain the increase of cell death observed after treatment of both cell lines (*Figure 11*).

OSU and MEC-1 cells were treated with PRIMA-1^{Met} at 5, 10 and 20 μM alone or in combination with 300 μM SAS and SLC7A11/xCT levels were measured through western blot analysis. At baseline, OSU presented a higher level of SLC7A11/xCT compared to MEC-1 cells, and its expression increased in both cell lines following PRIMA-1^{Met} increasing concentrations (*Figure 15A*). This was likely the consequence of the depletion of GSH triggered by PRIMA-1^{Met}, which induced an antioxidant response in the cells, resulting in the induction of SLC7A11/xCT synthesis.

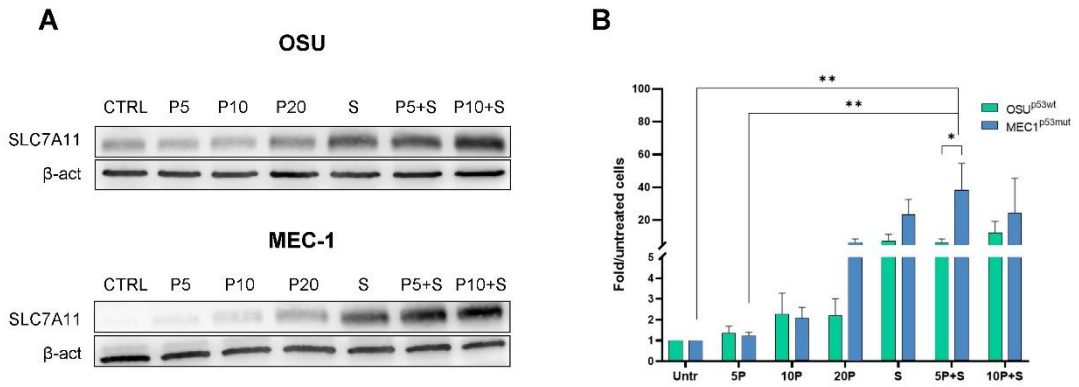

Figure 15. SLC7A11/xCT levels in OSU and MEC-1 cells. (**A**) Representative western blot showing the modulation of SLC7A11/xCT levels after 24 h of treatment with PRIMA-1^{Met} (P) at 5, 10 and 20 μM alone or in combination with SAS (S) 300 μM in OSU and MEC-1 CLL cells. β-actin (β-act) was used as a loading control. (**B**) Histograms showing the quantification of SLC7A11/xCT levels, based on western blots analysis, in OSU and MEC-1 cells. In the graph are reported the means ± SEM of chemiluminescence calculated as fold over the levels of the same proteins in untreated controls of at least three independent experiments. β-actin was used as internal control for normalization. * $p < 0.05$, ** $p < 0.01$. Adapted from Pasino et al., Int. J. Mol. Sci., 2025 (239).

Of particular relevance is the statistically significant increase of SLC7A11/xCT in MEC-1 cells after treatment with 5 μM PRIMA-1^{Met} in combination with SAS, compared to the control or 5 μM PRIMA-1^{Met} alone (*Figure 15B*). This could be due to the effect of SAS, which inhibits the transport of cystine inside the cells, limiting the synthesis of GSH. This inhibition probably increased the cellular oxidative stress that, in turn, triggers the synthesis of new SLC7A11/xCT as an attempt to revert the pro-oxidative environment.

4.6. Combined PRIMA-1^{Met} and SAS treatment depletes intracellular GSH and enhances ROS levels

The depletion of the antioxidant response leads to an increase of reactive oxygen species (ROS). The results showed in *Figure 15* indicated a relation between the targeting of GSH pathway and the induction of SLC7A11/xCT protein expression, probably mediated as compensatory mechanism. To better define these hypotheses and the consequences occurring in CLL cells after treatment with PRIMA-1^{Met} and SAS, both GSH and ROS amounts were measured.

In the control untreated cells, GSH levels were higher in OSU than in MEC-1 (*Figure 16A*), in line with the trend observed for SLC7A11/xCT in *Figure 15*. The treatment with 5 μM PRIMA-1^{Met} induced a reduction in GSH levels of 50% in OSU and 30% in MEC-1, and, after 10 μM of PRIMA-1^{Met}, the depletion was around 23% in OSU and 55% in MEC-1 compared to the controls. The major effect was observed after the addition of SAS: a depletion of GSH around 80% in OSU and 90% in MEC-1 was detected with SAS alone, and the co-treatment with PRIMA-1^{Met} completely exhausted the GSH reservoir. These results indicate that PRIMA-1^{Met} alone mainly affects the GSH content in MEC-1 cells, whereas the combination with SAS induces a strong decrease in GSH content in both cell lines.

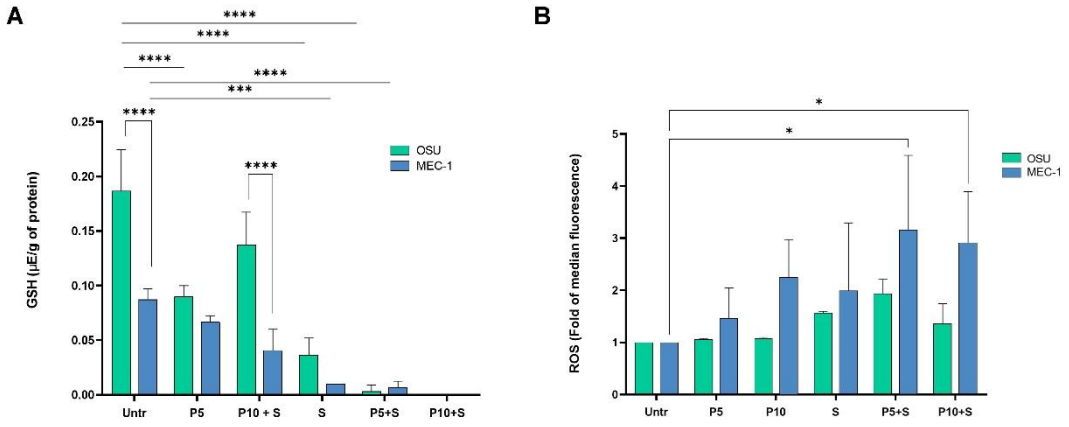

Figure 16. Levels of GSH and ROS in OSU and MEC-1 cells treated with PRIMA-1^{Met} at 5 and 10 μM alone or in combination with SAS 300 μM for 24 h. (**A**) GSH was assayed by HPLC analysis, and the histogram reports the mean ± SD of three independent experiments. GSH co concentrations were expressed as μE/g of total protein. (**B**) ROS levels were detected by flow cytometry analysis. Reported data are the mean ± SD calculated as fold over the levels of untreated cells of three independent experiments. ns not significant, * $p < 0.05$, *** $p < 0.001$, **** $p < 0.0001$. Adapted from Pasino et al., Int. J. Mol. Sci., 2025 (239).

Regarding ROS production, there was no statistically significant increase after treatment with PRIMA-1^{Met} or SAS alone, although a slight increase was observed in MEC-1 cells (*Figure 16B*). The combination of molecules induced a significant rise in ROS levels in MEC-1 compared to the untreated control, confirming that the p53-mutated cell line is more sensitive to GSH depletion compared to OSU.

These results confirmed the hypothesis related to the increase in oxidative stress in the cells after treatment and the consequent activation of adaptive responses, such as the induction of SLC7A11/xCT expression (*Figure 15*).

4.7. Combined treatment with PRIMA-1^{Met} and SAS alters the redox balance in OSU and MEC-1 cells

To evaluate whether the treatment with PRIMA-1^{Met} and SAS, alone or in combination, modulates the antioxidant machinery of OSU and MEC-1 cells, the activity of two enzymes involved in the GSH pathway: glutathione peroxidase (GPx), the key enzyme for the neutralisation of phospholipid peroxides on the cell membrane, and glutathione reductase (GR). To exert its effect, GPx consumes two molecules of GSH, then converted into its oxidized form (GSSG). GR is responsible for reducing the GSSG and thus restoring the GSH reduced molecule using NADPH (246).

Cells were pretreated with a pro-oxidant agent (H_2O_2) to boost the GSH pathway, then 5 and 10 μM PRIMA-1^{Met} and 300 μM SAS were added, alone or in combination. At baseline, the activity of the two enzymes was similar in both cell lines (*Figure 17A, B*) and a 25% increase was observed following the addition of H_2O_2. This confirmed the adaptive response capability of both OSU and MEC-1 cell lines. In OSU, the activity of the two enzymes was not affected by the increasing concentration of PRIMA-1^{Met}, alone or in combination with SAS. On the other hand, in MEC-1 cells the enzymatic function of GPx and GR decreased in a dose-dependent manner with PRIMA-1^{Met} alone and after the co-treatment. Of note, in both cell lines, the addition of SAS significantly reduced the activity of the two enzymes, either alone or in combination with PRIMA-1^{Met} (*Figure 17A, B*).

NADPH oxidase, a pro-oxidant enzyme involved in the formation of the superoxide anion radical from NADPH and oxygen (247), was also assayed. The activity of the enzyme increased after the addition of H_2O_2, even though the treatment with PRIMA-1^{Met} or SAS alone and, particularly, in combination, further increased the activity of NDAPH oxidase (*Figure 17C*).

Finally, intracellular levels of malondialdehyde (MDA), the main product of lipid peroxidation, were evaluated to confirm the actual oxidation of phospholipids in the membrane due to the pro-oxidant environment. As expected, both OSU and MEC-1 cells showed an increase in MDA, in particular after treatment with the highest concentration of PRIMA-1^{Met} in combination with SAS (*Figure 17D*).

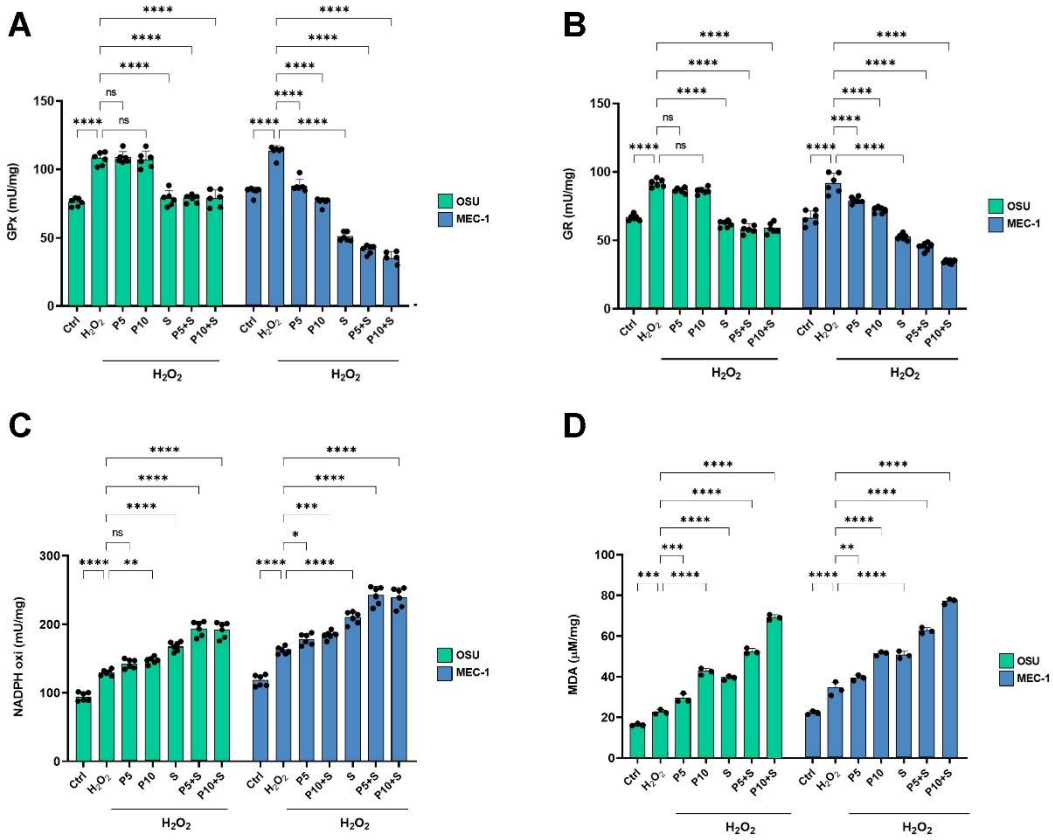

Figure 17. Evaluation of the activity of enzymes involved in redox balance and lipid peroxidation accumulation in OSU and MEC-1 cells pre-treated with H_2O_2. Activity determination of (**A**) glutathione peroxidase (GPx), (**B**) glutathione reductase (GR), (**C**) NADPH oxidase and (**D**) malondialdehyde (MDA) in H_2O_2 pre-treated CLL cells and treated subsequently with PRIMA-1^{Met} alone and in combination with SAS. Each histogram is representative of three independent experiments. Data reported are expressed as mean ± SD of three independent experiments. ns, not significant, * $p < 0.05$; ** $p < 0.01$, *** $p < 0.001$, **** $p < 0.0001$. Adapted from Pasino et al., Int. J. Mol. Sci., 2025 (239).

All these data indicated that MEC-1 cells are less effective than OSU in developing a proper antioxidant response and, consequently, are more affected by oxidative damage.

4.8. PRIMA-1^{Met} and SAS co-treatment induces ferroptosis in CLL cell lines

The SLC7A11/GSH axis has been shown to play a key role in the modulation of ferroptosis, and *TP53* was recently discovered to transcriptionally repress *SLC7A11* gene expression (144,145). Based on these considerations and on the results obtained on the oxidative stress induction and antioxidant defence in OSU and MEC-1 cells, ferroptosis induction was investigated in CLL cell lines.

For this purpose, cells were pre-treated with Ferrostatin-1, a ferroptosis inhibitor, at 2 μM concentration. PRIMA-1^{Met} 10 μM and SAS 300 μM were then added, alone or in combination, for 24 h. The pre-treatment with Ferrostatin-1 induced a rescue in the cell viability in both cell lines, with the highest statistically significance observed in MEC-1 cells (*Figure 18*). This suggest that the combined treatment, by reducing GSH levels and promoting a pro-oxidant environment, is able to induce ferroptosis, in addition to apoptosis, in CLL cell lines. Considering the highest rescue observed in p53-mutated cells, these data confirm that MEC-1 cell line is more sensitive to the redox changes than OSU.

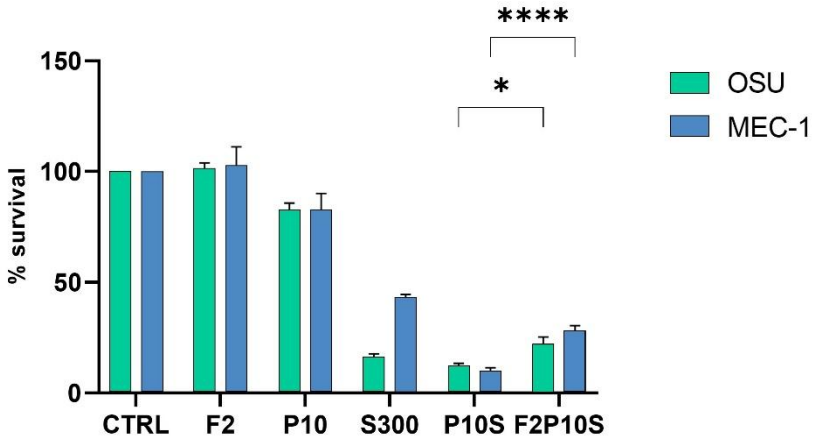

Figure 18. Ferroptosis induction in OSU and MEC-1 cell lines pre-treated with 2 μM Ferrostatin-1 (F). Cell viability was assayed by MTT assay 24 h after treatment with PRIMA-1^{Met} (P) at 10 μM alone or in combination with SAS (S) 300 μM. The histograms report the means ± SD of at least three independent experiments. * $p < 0.05$, **** $p < 0.0001$.

4.9. Primary CLL cell survival is affected by PRIMA-1^{Met} and SAS combined treatment regardless of the p53 status

Based on the results described above, some experiments were repeated on CLL primary cells, which reflect more accurately the heterogeneity of the disease. For this purpose, samples from CLL patients were collected, stratified according to the *TP53* mutational status, and then analysed (see M&M for their description).

First of all, the cell viability was assayed in p53 wild-type and p53 mutant groups of patients previously activated with CpG-ODN/IL-15 to mimic the microenvironment stimuli (248). After 24 h of activation, cells were treated with PRIMA-1^{Met} at 1, 2.5 and 5 μM alone or in combination with 300 μM SAS, and cell viability was determined at 24 and 48 h of treatment by flow cytometry analysis. In both wild-type (*Figure 19A*) and mutant (*Figure 19B*) CLL samples, PRIMA-1^{Met} induced a decrease in cell viability in a dose-dependent manner, either alone or in combination with SAS, with a stronger effect observed after 48 h. The addition of SAS alone did not affect the overall survival.

Considering the general trend, no statistically significant differences were observed between the wild-type and mutant groups of CLL samples for the same conditions of treatment, indicating that PRIMA-1^{Met} affected the cell viability regardless of the *TP53* mutational status.

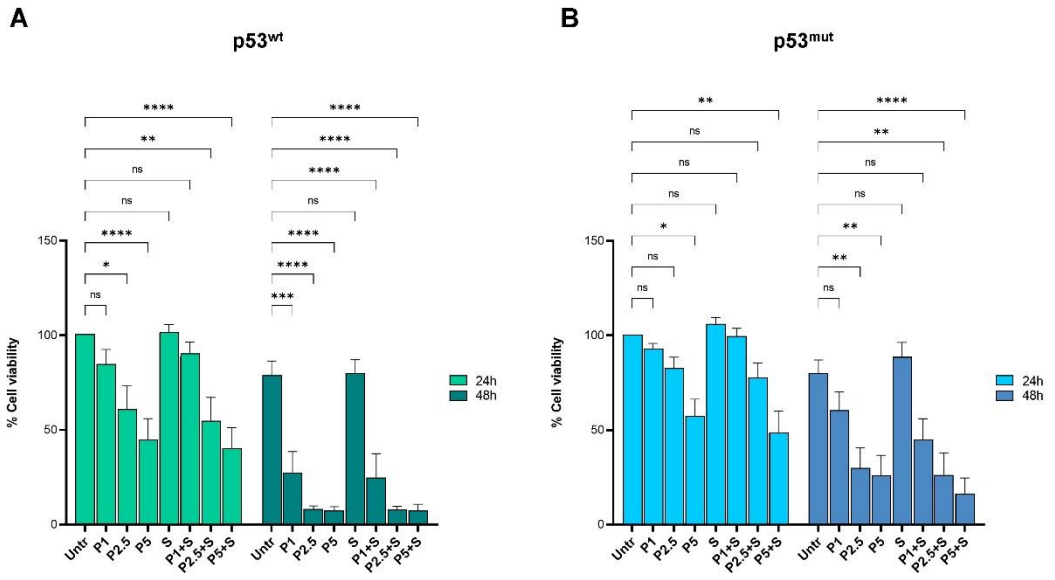

Figure 19. Cell viability determination of CLL primary cells activated with CpG-ODN/IL15 and treated with PRIMA-1^{Met} (P) and SAS (S). CLL cells from 6 CLL patients carrying wild-type p53 (**A**) and 8 patients with a mutant p53 (**B**) were stimulated 24h with CpG-ODN/IL15, then treated for 24 and 48 h with PRIMA-1^{Met} at 1, 2.5 and 10 μM alone or in combination with SAS 300 μM. Flow cytometric analysis was subsequently performed, and the percentage of viable cells was calculated as the percentage of double Annexin V and PI negative cells. For each treatment condition, the percentage of viable cells was normalised for the corresponding untreated sample. The histograms report the means ± SEM from 6 CLL patients carrying a wild-type p53 and from 8 patients with a mutant p53. ns not significant; * $p < 0.05$, ** $p< 0.01$, *** $p < 0.001$, **** $p < 0.0001$. Adapted from Pasino et al., Int. J. Mol. Sci., 2025 (239).

4.10. PRIMA-1^{Met} and SAS treatment modulates the cellular redox status, especially in *TP53*-mutated CLL primary cells

The variations in antioxidant defence and the accumulation of oxidative damage, in relation to the *TP53* mutational status, were also assessed in primary CLL cells. To this end, cells were stimulated for 24 h with CpG-ODN/IL-15, then treated with PRIMA-1^{Met} 1 μM alone or in combination with 300 μM SAS. In this case, no pre-treatment with H_2O_2 was carried out to avoid excessive stress to the cells since they are physiologically less resistant in culture than CLL cell lines (246).

Cells with a wild-type p53 exhibit a higher GSH content compared to those with a mutant p53 at baseline, and the trend was maintained after treatment with PRIMA-1^{Met} or SAS alone and in combination (*Figure 20A*). A statistically significant reduction of GSH levels was observed in comparison to the untreated cells, already after the addition of PRIMA-1^{Met}, and became increasingly evident after the addition of SAS.

No differences in total glutathione content (GSH + GSSG) were detected in control cells between the two groups of samples, whereas the treatment with PRIMA-1^{Met} or SAS alone and, especially, in combination, induced a significant reduction of total glutathione amount (GSH + GSSG) (*Figure 20B*). In any condition, this depletion was always more pronounced in primary cells carrying a mutant p53. The behaviour already described was perfectly reflected by the global antioxidant capacity, which followed the same trend as total glutathione content for any condition of treatment (*Figure 20C*).

Finally, MDA levels were measured to assess whether the reduction of the antioxidant response affected membrane lipid peroxidation levels. In untreated controls, the p53-mutated group showed the highest amount of MDA (*Figure 20D*), in line with the lower GSH content (*Figure 20A*), and this difference was maintained after treatment with PRIMA-1^{Met} and SAS alone. The highest increase of MDA was observed in the p53-mutated group after the co-treatment (*Figure 20D*), confirming once again the correlation between the depletion of antioxidant defence and the induction of phospholipids oxidation.

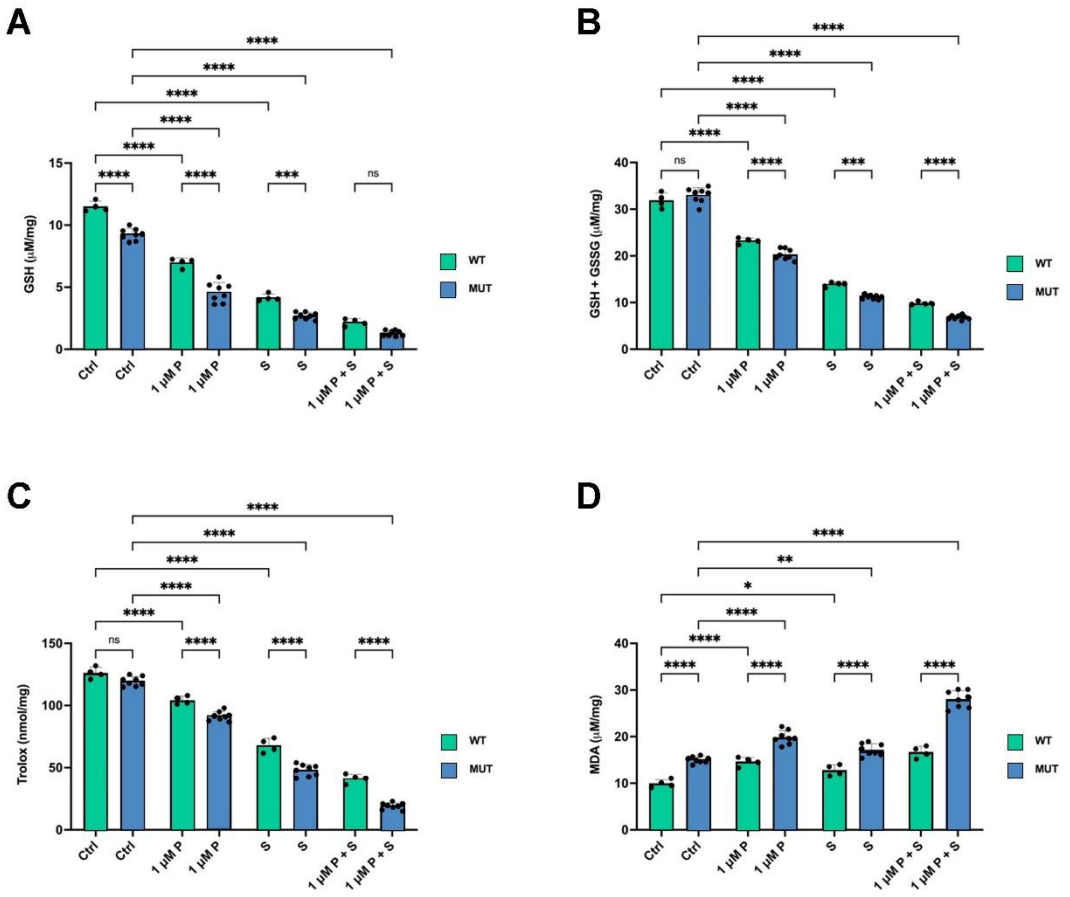

Figure 20. Metabolic markers in CLL primary cells. Evaluation of (**A**) GSH levels, (**B**) GSH + GSSG content, (**C**) cellular antioxidant capacity and (**D**) MDA intracellular levels in CLL primary cells after treatment with PRIMA-1^{Met} 1 μM (P) and SAS 300 μM (S) alone or in combination. Each histogram is representative of three independent experiments; data are expressed as means ± SD. ns, not significant, * $p < 0.05$; ** $p < 0.01$, *** $p < 0.001$, **** $p < 0.0001$. Adapted from Pasino et al., Int. J. Mol. Sci., 2025 (239).

The results collected from primary CLL cells are highly consistent with the data obtained from OSU and MEC-1 CLL cell lines, corroborating the idea that CLL cells expressing a mutant p53 are more sensitive to oxidative stress and less prone to developing an effective antioxidant response.

4.11. IFN pathway is differently modulated in p53 wild-type and p53 mutated CLL cell lines

The Interferon (IFN) pathway was also assayed, although studies are still ongoing, to better characterise the modulation of this axis in relation to the treatment. Cells were treated 16 h with PRIMA-1^{Met} 10 μM and SAS 300 μM, alone or in combination, and western blot analysis was performed to evaluate the expression of the main players of the pathway. All the phosphorylated STAT proteins were expressed at higher levels in MEC-1 cells than OSU (*Figure 21*) and the modulation of interferon stimulated genes OAS2 and ISG20 followed the trend of STATs.

Since the IFN pathway could be activated when DNA damage occurs in the cell, the proteins related to DNA damage were also assayed. CASP-3 and p-H2A.X, strongly increased after the co-treatment with PRIMA-1^{Met} and SAS, whereas p53 levels increased after the combined treatment in OSU cells and the opposite behaviour was observed in MEC-1 at the same conditions.

Altogether these data suggest that STATs are more induced in the p53-mutated cell line, even though the trend after treatment was the same both in OSU and MEC-1 cells. The combined treatment caused a strong DNA damage, particularly in MEC-1 cells, and apoptosis, with higher induction in OSU. Although preliminary, these data suggest that p53 may play a different role in according to its wild-type or mutant status in the regulation of STATs phosphorylation and IFNs induction.

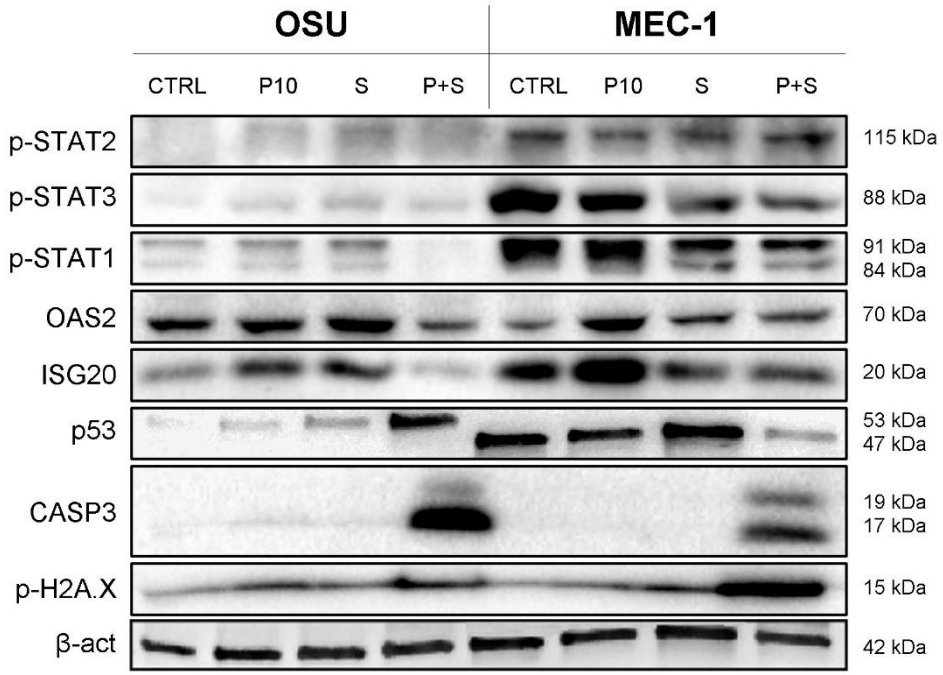

Figure 21. Modulation of p53 and proteins involved in the IFN pathway (p-STATs, OAS2, ISG20), DNA damage (p-H2A.X), apoptosis induction (CASP-3). OSU and MEC-1 cells were treated for 16 h with PRIMA-1^{Met} 10 μM (P) and SAS 300 μM (S), alone or in combination. Western blot is representative of three independent experiments. β-Actin (β-act) was used for loading control.

5. Discussion

TP53 gene mutations occur with a low incidence in CLL at diagnosis, while the percentage of p53-mutated leukemic B cells rises in refractory patients. For this reason, the disruption of the *TP53* gene represents the most relevant biomarker in CLL and is considered an indicator to drive the therapeutic decisions, since it may affect the success of the treatment (31). These features render the p53 protein a promising target for the development of new anticancer therapies.

To date, a lot of molecules have been studied and tested in different kind of tumours to specifically target mutant p53 proteins, in order to reactivate or definitively eliminate the protein (249). PRIMA-1^{Met} represents the most promising molecule, tested in many clinical trials on haematological malignancies as Acute Myeloid Leukemia and Multiple Myeloma (250). Besides the ability to reactivate wild-type functions in mutant p53 proteins, PRIMA-1^{Met} has been shown to induce Glutathione (GSH) depletion and NADPH oxidase induction, which results in ROS overproduction (218,221). Based on these observations, the combination of PRIMA-1^{Met} with molecules able to affect the intracellular antioxidant response may effectively impact the tumour cell viability (222). The cytotoxic capability of PRIMA-1^{Met} in CLL has been studied by Jaskova et al. in 62 clinical CLL samples, which have been characterised for *TP53* mutations and p53 protein levels. The results obtained showed a similar decrease in the cell viability and apoptosis induction both in wild-type and mutant p53 samples (223). Apart from this study, nothing else has been published regarding neither the activity of PRIMA-1^{Met} in CLL, nor the effect of a combined treatment with drugs able to modulate the antioxidant response.

In this study PRIMA-1^{Met} was tested in combination with Sulfasalazine (SAS), a drug that inhibits the functionality of the SLC7A11/xCT complex, the key transporter of cystine (precursor of GSH) inside the cell (241). The effects of the co-treatment were evaluated in two CLL cell lines (OSU, carrying a wild-type p53, and MEC-1, with a mutant form of the protein) and on primary cells from CLL patients.

First of all, the effect of PRIMA-1^{Met} was assessed in both CLL cell lines, with particular focus on MEC-1, to determine whether the compound was able to restore wild-type functions of the mutant p53 protein. For this purpose, the expression of the main p53 target genes (MDM2 and p21) was evaluated. In OSU cells the expression of these genes followed p53 levels proportionally, as expected, whereas in MEC-1 cells, increasing concentrations of PRIMA-1^{Met} did not result in a corresponding rise in p53 expression, and the same behaviour was followed by MDM2 and p21 (*Figure 9*). These results were not unexpected since the mutation carried by MEC-1 generates a truncated form of the protein (251), which is likely unable to regain the wild-type-like conformation after treatment with PRIMA-1^{Met}. Moreover, the mutation is located close to the tetramerization domain of p53 (codon Q317), thereby impairing the formation of the transcriptionally active tetramer. However, the activity of PRIMA-1^{Met} on CLL primary cells resembled the behaviour observed in CLL cell lines, with a lack of mutant p53 reactivation (*Figure 10*).

Given that PRIMA-1^{Met} is also capable of depleting GSH, this mechanism was deeply studied in association with the effect of SAS in CLL cells. The co-treatment with PRIMA-1^{Met} and SAS induced a general significant decrease in cell survival when compared to the effects observed when the molecules were added alone. This was evident in both OSU and MEC-1 CLL cells (*Figure 11*), and in primary CLL cells (*Figure 19*), where the concentrations applied for PRIMA-1^{Met} were even lower than those used with cell lines (up to 5 μM). In CLL primary cells the viability in the p53-mutated group appeared higher than the p53 wild-type after the co-treatment, in contrast with the effects shown in cell lines, where MEC-1 resulted more sensitive. However, this can be related to the intrinsic diversity of samples derived from different patients, as, for instance, different levels of SLC7A11.

The two drugs induced a synergistic effect in OSU and MEC-1 cells. This was observed already at 5 and 10 μM PRIMA-1^{Met} concentrations combined with 300 μM SAS (*Figure 14*). Considering the low doses of drugs used, the results obtained suggest that it is possible to induce a cytotoxic effect on cancer cells already with very low concentrations of PRIMA-1^{Met}, thus reducing side effects. Given that the decrease in cell viability was detected in p53 wild-type as well as in p53-mutated cells, these data indicate that the efficacy of PRIMA-1^{Met} was not strictly dependent on the restoration of the p53 transcriptional activity.

Considering that the p53 wild-type functions were not restored in the mutant p53 proteins by the effect of PRIMA-1^{Met} (*Figure 9, Figure 10*), the reduction in cell viability was probably due to the action on the GSH pathway, mechanisms that were enhanced by SAS. The expression of SLC7A11/xCT, which was proposed as a predictive biomarker of PRIMA-1^{Met} sensitivity (146,242), may influence the response to the treatment. In this regard, SAS could lead to synthetic lethality by inhibiting the SLC7A11/xCT transporter in cells with a mutant p53, resulting in high induction of oxidative stress and, consequently, in cell death (222). These concepts, together with the lower expression of SLC7A11/xCT observed in MEC-1 than in OSU (*Figure 15*), may explain why the mutant p53 cell line was more affected by the co-treatment. For this reason, the co-treatment with PRIMA-1^{Met} and SAS may be a promising strategy to sensitise CLL cells, regardless of the *TP53* mutational status. In light of this, it is reasonable to assume that a stratification of CLL patients based on SLC7A11/xCT levels could provide a clearer overview of the sensitivity to PRIMA-1^{Met} in combination with SAS, facilitating the customisation of therapeutic approaches.

The ability to manage oxidative stress was also impaired in CLL cells after treatment. Cells with a mutant p53 accumulated more reactive oxygen species (ROS) than those with a wild-type p53 after the addition of PRIMA-1^{Met} and SAS (*Figure 16B*). This is primarily attributable to PRIMA-1^{Met}, which reduces the cells' ability to cope with pro-oxidant stimuli as a result of the depletion of GSH (*Figure 16A*). The decrease of GSH and the accumulation of ROS were more evident in MEC-1 cells than in OSU, in particular when the two molecules were added together. These results, along with the previous observations on SLC7A11/xCT expression, support the concept that cells harbouring a mutant p53 are more sensitive to oxidative stress and exhibit a reduced capacity to manage an oxidative environment.

The p53 protein modulates the GSH metabolism through different mechanisms, as the regulation of genes involved in GSH synthesis and recycling, and the redox cofactor homeostasis, thus modulating cellular antioxidant capacity and oxidative stress responses (252). However, the GSH levels may be reduced as a consequence of several processes, including a diminished capacity of GR to convert oxidised glutathione (GSSG) to the reduced form, an increase of GSH consumption to counteract oxidative stress and a limited supply of GSH precursors.

Considering the substrates availability, previous data indicated that the treatment with PRIMA-1^{Met} and SAS alone or in combination induced an upregulation of SLC7A11/xCT, with a stronger effect observed in MEC-1 cells compared to OSU (*Figure 15*). The induction of SLC7A11/xCT has been already described and related to the inability of mutant p53 to interact with Nrf2, thereby failing to repress SLC7A11/xCT transcription (146,253). Furthermore, the results obtained regarding GPx activity (*Figure 17A*) did not completely align with the hypothesis of the decrease of GSH as a consequence of its high consumption in response to oxidative stress. Indeed, a reduction in GPx activity was observed after treatment with PRIMA-1^{Met} or SAS in MEC-1 cells, whereas in OSU cells, no differences were detected after the addition of increasing concentrations of PRIMA-1^{Met}.

The depletion of GSH could be explained, on the other hand, by the decreased activity of GR (the enzyme responsible for reducing the GSSG to GSH) detected after treatment, which followed the same trend observed for GPx (*Figure 17B*). Moreover, NADPH oxidase could play an indirect role in the reduction of GSH: this enzyme, with a pro-oxidant capacity, uses NADPH as a cofactor, as GR does. Since the treatment with PRIMA-1^{Met} and SAS alone or in combination led to an increase in NADPH oxidase activity (*Figure 17C*), GR functions may have been reduced due to the limited availability of the common cofactor NADPH. The alterations described above regarding GPx, GR and NADPH oxidase together resulted in an increase in membrane phospholipid peroxidation (*Figure 17D*) as consequence of a pro-oxidant environment, corroborating the idea that the combination of PRIMA-1^{Met} and SAS can disrupt the redox balance in CLL cell lines, especially those expressing a mutant p53. This was also confirmed by ferroptosis induction, the outcome of the cell when a strong oxidative stress occurs, which was detected in both CLL cell lines, with the highest rate in MEC-1 cells (*Figure 18*).

Similar findings were obtained in primary CLL samples (*Figure 20*) where a defective antioxidant defence was detected already at basal conditions in p53-mutated cells. Of note, the treatment with the molecules, both alone and in combination, led to a strong reduction in GSH levels, even though total glutathione amount (GSH+GSSG) remained unchanged. This indicates that glutathione availability was not the limiting factor, but rather its conversion to the reduced form after oxidation.

Beyond GSH itself, a reduction in overall antioxidant capacity was observed in both wild-type and mutant p53 cells. This further contributed to the accumulation of oxidative damage following treatment, an effect that, similar to what was observed in CLL cell lines, predominantly affected cells harbouring mutant p53.

Altogether, these results show that CLL cell survival is highly dependent on the redox homeostasis. PRIMA-1^{Met} strongly influences antioxidant response and ROS induction, and the combination with SAS deeply affects this delicate balance, leading to an increase in oxidative stress and cell death. Even though these effects were detectable both in p53 wild-type and mutated CLL cells, the major damage was observed in p53-mutated samples.

In p53-mutated cell line the IFN pathway is also more induced than in the p53 wild-type CLL cells. Results obtained for the STATs phosphorylation highlighted a major activation of these proteins in the MEC-1 cells, and a partial decrease after the treatment with PRIMA-1^{Met} and SAS in combination was detected (*Figure 21*). A similar trend was observed for interferon-stimulated genes OAS15 and ISG20, likely indicating an activation of the downstream pathway. These results are in line with the concept that STAT1 and STAT3 are generally persistently activated in CLL cells (170,171), as shown in MEC-1 cells, whereas the low phosphorylation observed in OSU could be related to the presence of a wild-type p53, as described in fibroblast cells (161,162). The presence of DNA damage and apoptosis induction is stronger after the combined treatment, as expected. Of note, MEC-1 cells exhibited lower levels of cleaved CASP-3 than OSU after the combined treatment (*Figure 21*). Although apparently in contrast with the highest rate of cell death detected in MEC-1 cells (*Figure 11*), this behaviour may be explained by the highest ferroptosis induction (*Figure 18*), confirming that MEC-1 cells are more sensitive to oxidative stress.

Considering the impaired metabolic pathway in CLL cells, the next step will be to exploit this vulnerability to target clones resistant to other therapies, paying attention to the potential impact of basal levels of glutathione-related proteins, such as SLC7A11/xCT, which may influence the response to treatment. Thus, the combination of PRIMA-1^{Met} and SAS represents a promising strategy to prevent and overcome the resistance to first-line treatment in CLL patients, in particular for those carrying a mutant p53 protein.

6. Bibliography

1. Chronic Lymphocytic Leukemia — Cancer Stat Facts [Internet]. [cited 2025 Dec 6]. Available from: https://seer.cancer.gov/statfacts/html/clyl.html

2. Chiorazzi N, Chen SS, Rai KR. Chronic Lymphocytic Leukemia. Cold Spring Harb Perspect Med. 2021 Feb 1;11(2):a035220. doi:10.1101/cshperspect.a035220 PubMed PMID: 32229611; PubMed Central PMCID: PMC7849345.

3. Melo JV, Catovsky D, Gregory WM, Galton DA. The relationship between chronic lymphocytic leukaemia and prolymphocytic leukaemia. IV. Analysis of survival and prognostic features. Br J Haematol. 1987 Jan;65(1):23–9. doi:10.1111/j.1365-2141.1987.tb06130.x PubMed PMID: 3468997.

4. Rai KR, Sawitsky A, Cronkite EP, Chanana AD, Levy RN, Pasternack BS. Clinical staging of chronic lymphocytic leukemia. Blood. 1975 Aug;46(2):219–34. PubMed PMID: 1139039.

5. Binet JL, Auquier A, Dighiero G, Chastang C, Piguet H, Goasguen J, et al. A new prognostic classification of chronic lymphocytic leukemia derived from a multivariate survival analysis. Cancer. 1981 Jul 1;48(1):198–206. doi:10.1002/1097-0142(19810701)48:1%3C198::aid-cncr2820480131%3E3.0.co;2-v PubMed PMID: 7237385.

6. International CLL-IPI working group. An international prognostic index for patients with chronic lymphocytic leukaemia (CLL-IPI): a meta-analysis of individual patient data. Lancet Oncol. 2016 Jun;17(6):779–90. doi:10.1016/S1470-2045(16)30029-8 PubMed PMID: 27185642.

7. Ginaldi L, De Martinis M, Matutes E, Farahat N, Morilla R, Catovsky D. Levels of expression of CD19 and CD20 in chronic B cell leukaemias. J Clin Pathol. 1998 May;51(5):364–9. doi:10.1136/jcp.51.5.364 PubMed PMID: 9708202; PubMed Central PMCID: PMC500695.

8. Matutes E, Owusu-Ankomah K, Morilla R, Garcia Marco J, Houlihan A, Que TH, et al. The immunological profile of B-cell disorders and proposal of a scoring system for the diagnosis of CLL. Leukemia. 1994 Oct;8(10):1640–5. PubMed PMID: 7523797.

9. Moreau EJ, Matutes E, A'Hern RP, Morilla AM, Morilla RM, Owusu-Ankomah KA, et al. Improvement of the chronic lymphocytic leukemia scoring system with the monoclonal antibody SN8 (CD79b). Am J Clin Pathol. 1997 Oct;108(4):378–82. doi:10.1093/ajcp/108.4.378 PubMed PMID: 9322589.

10. Hallek M, Cheson BD, Catovsky D, Caligaris-Cappio F, Dighiero G, Döhner H, et al. iwCLL guidelines for diagnosis, indications for treatment, response assessment, and supportive management of CLL. Blood. 2018 Jun 21;131(25):2745–60. doi:10.1182/blood-2017-09-806398 PubMed PMID: 29540348.

11. Kikushige Y, Ishikawa F, Miyamoto T, Shima T, Urata S, Yoshimoto G, et al. Self-renewing hematopoietic stem cell is the primary target in pathogenesis of human chronic lymphocytic leukemia. Cancer Cell. 2011 Aug 16;20(2):246–59. doi:10.1016/j.ccr.2011.06.029 PubMed PMID: 21840488.

12. Landau DA, Tausch E, Taylor-Weiner AN, Stewart C, Reiter JG, Bahlo J, et al. Mutations driving CLL and their evolution in progression and relapse. Nature. 2015 Oct 22;526(7574):525–30. doi:10.1038/nature15395 PubMed PMID: 26466571; PubMed Central PMCID: PMC4815041.

13. Döhner H, Stilgenbauer S, Benner A, Leupolt E, Kröber A, Bullinger L, et al. Genomic aberrations and survival in chronic lymphocytic leukemia. N Engl J Med. 2000 Dec 28;343(26):1910–6. doi:10.1056/NEJM200012283432602 PubMed PMID: 11136261.

14. Nadeu F, Delgado J, Royo C, Baumann T, Stankovic T, Pinyol M, et al. Clinical impact of clonal and subclonal TP53, SF3B1, BIRC3, NOTCH1, and ATM mutations in chronic lymphocytic leukemia. Blood. 2016 Apr 28;127(17):2122–30. doi:10.1182/blood-2015-07-659144 PubMed PMID: 26837699; PubMed Central PMCID: PMC4912011.

15. Calin GA, Dumitru CD, Shimizu M, Bichi R, Zupo S, Noch E, et al. Frequent deletions and down-regulation of micro- RNA genes miR15 and miR16 at 13q14 in chronic lymphocytic leukemia. Proc Natl Acad Sci U S A. 2002 Nov 26;99(24):15524–9. doi:10.1073/pnas.242606799 PubMed PMID: 12434020; PubMed Central PMCID: PMC137750.

16. Klein U, Lia M, Crespo M, Siegel R, Shen Q, Mo T, et al. The DLEU2/miR-15a/16-1 cluster controls B cell proliferation and its deletion leads to chronic lymphocytic leukemia. Cancer Cell. 2010 Jan 19;17(1):28–40. doi:10.1016/j.ccr.2009.11.019 PubMed PMID: 20060366.

17. Döhner H, Stilgenbauer S, James MR, Benner A, Weilguni T, Bentz M, et al. 11q deletions identify a new subset of B-cell chronic lymphocytic leukemia characterized by extensive nodal involvement and inferior prognosis. Blood. 1997 Apr 1;89(7):2516–22. PubMed PMID: 9116297.

18. Hallek M, Fischer K, Fingerle-Rowson G, Fink AM, Busch R, Mayer J, et al. Addition of rituximab to fludarabine and cyclophosphamide in patients with chronic lymphocytic leukaemia: a randomised, open-label, phase 3 trial. Lancet. 2010 Oct 2;376(9747):1164–74. doi:10.1016/S0140-6736(10)61381-5 PubMed PMID: 20888994.

19. Zenz T, Vollmer D, Trbusek M, Smardova J, Benner A, Soussi T, et al. TP53 mutation profile in chronic lymphocytic leukemia: evidence for a disease specific profile from a comprehensive analysis of 268 mutations. Leukemia. 2010 Dec;24(12):2072–9. doi:10.1038/leu.2010.208 PubMed PMID: 20861914.

20. Quesada V, Conde L, Villamor N, Ordóñez GR, Jares P, Bassaganyas L, et al. Exome sequencing identifies recurrent mutations of the splicing factor SF3B1

gene in chronic lymphocytic leukemia. Nat Genet. 2011 Dec 11;44(1):47–52. doi:10.1038/ng.1032 PubMed PMID: 22158541.

21. Puente XS, Pinyol M, Quesada V, Conde L, Ordóñez GR, Villamor N, et al. Whole-genome sequencing identifies recurrent mutations in chronic lymphocytic leukaemia. Nature. 2011 Jun 5;475(7354):101–5. doi:10.1038/nature10113 PubMed PMID: 21642962; PubMed Central PMCID: PMC3322590.

22. Puente XS, Beà S, Valdés-Mas R, Villamor N, Gutiérrez-Abril J, Martín-Subero JI, et al. Non-coding recurrent mutations in chronic lymphocytic leukaemia. Nature. 2015 Oct 22;526(7574):519–24. doi:10.1038/nature14666 PubMed PMID: 26200345.

23. Calis JJA, Rosenberg BR. Characterizing immune repertoires by high throughput sequencing: strategies and applications. Trends Immunol. 2014 Dec;35(12):581–90. doi:10.1016/j.it.2014.09.004 PubMed PMID: 25306219; PubMed Central PMCID: PMC4390416.

24. Sahota SS, Babbage G, Zojer N, Ottensmeier CH, Stevenson FK. Determining mutational status of immunoglobulin v genes in chronic lymphocytic leukemia: a useful prognostic indicator. Methods Mol Med. 2005;115:129–44. doi:10.1385/1-59259-936-2:129 PubMed PMID: 15998966.

25. Crombie J, Davids MS. IGHV mutational status testing in chronic lymphocytic leukemia. Am J Hematol. 2017 Dec;92(12):1393–7. doi:10.1002/ajh.24808 PubMed PMID: 28589701; PubMed Central PMCID: PMC5675754.

26. Hamblin TJ, Davis Z, Gardiner A, Oscier DG, Stevenson FK. Unmutated Ig V(H) genes are associated with a more aggressive form of chronic lymphocytic leukemia. Blood. 1999 Sep 15;94(6):1848–54. PubMed PMID: 10477713.

27. Damle RN, Wasil T, Fais F, Ghiotto F, Valetto A, Allen SL, et al. Ig V gene mutation status and CD38 expression as novel prognostic indicators in chronic lymphocytic leukemia. Blood. 1999 Sep 15;94(6):1840–7. PubMed PMID: 10477712.

28. Parikh SA, Strati P, Tsang M, West CP, Shanafelt TD. Should IGHV status and FISH testing be performed in all CLL patients at diagnosis? A systematic review and meta-analysis. Blood. 2016 Apr 7;127(14):1752–60. doi:10.1182/blood-2015-10-620864 PubMed PMID: 26841802.

29. Buccheri V, Barreto WG, Fogliatto LM, Capra M, Marchiani M, Rocha V. Prognostic and therapeutic stratification in CLL: focus on 17p deletion and p53 mutation. Ann Hematol. 2018 Dec;97(12):2269–78. doi:10.1007/s00277-018-3503-6 PubMed PMID: 30315344.

30. Rossi D, Cerri M, Deambrogi C, Sozzi E, Cresta S, Rasi S, et al. The prognostic value of TP53 mutations in chronic lymphocytic leukemia is independent of Del17p13: implications for overall survival and chemorefractoriness. Clin Cancer Res. 2009 Feb 1;15(3):995–1004. doi:10.1158/1078-0432.CCR-08-1630 PubMed PMID: 19188171.

31. Bomben R, Rossi FM, Vit F, Bittolo T, D'Agaro T, Zucchetto A, et al. TP53 Mutations with Low Variant Allele Frequency Predict Short Survival in Chronic Lymphocytic Leukemia. Clin Cancer Res. 2021 Oct 15;27(20):5566–75. doi:10.1158/1078-0432.CCR-21-0701 PubMed PMID: 34285062.

32. Morabito F, Del Poeta G, Mauro FR, Reda G, Sportoletti P, Laurenti L, et al. TP53 disruption as a risk factor in the era of targeted therapies: A multicenter retrospective study of 525 chronic lymphocytic leukemia cases. Am J Hematol. 2021 Aug 1;96(8):E306–10. doi:10.1002/ajh.26235 PubMed PMID: 33989438.

33. Malcikova J, Tausch E, Rossi D, Sutton LA, Soussi T, Zenz T, et al. ERIC recommendations for TP53 mutation analysis in chronic lymphocytic leukemia-update on methodological approaches and results interpretation. Leukemia. 2018 May;32(5):1070–80. doi:10.1038/s41375-017-0007-7 PubMed PMID: 29467486; PubMed Central PMCID: PMC5940638.

34. Lane DP, Crawford LV. T antigen is bound to a host protein in SY40-transformed cells. Nature. 1979 Mar;278(5701):261–3. doi:10.1038/278261a0

35. Levine AJ, Oren M. The first 30 years of p53: growing ever more complex. Nat Rev Cancer. 2009 Oct;9(10):749–58. doi:10.1038/nrc2723 PubMed PMID: 19776744; PubMed Central PMCID: PMC2771725.

36. Baker SJ, Fearon ER, Nigro JM, Hamilton SR, Preisinger AC, Jessup JM, et al. Chromosome 17 deletions and p53 gene mutations in colorectal carcinomas. Science. 1989 Apr 14;244(4901):217–21. doi:10.1126/science.2649981 PubMed PMID: 2649981.

37. Lane DP. Cancer. p53, guardian of the genome. Nature. 1992 Jul 2;358(6381):15–6. doi:10.1038/358015a0 PubMed PMID: 1614522.

38. Joerger AC, Fersht AR. Structural biology of the tumor suppressor p53. Annu Rev Biochem. 2008;77:557–82. doi:10.1146/annurev.biochem.77.060806.091238 PubMed PMID: 18410249.

39. Tanaka T, Watanabe M, Yamashita K. Potential therapeutic targets of TP53 gene in the context of its classically canonical functions and its latest non-canonical functions in human cancer. Oncotarget. 2018 Mar 23;9(22):16234–47. doi:10.18632/oncotarget.24611 PubMed PMID: 29662640; PubMed Central PMCID: PMC5882331.

40. Walker KK, Levine AJ. Identification of a novel p53 functional domain that is necessary for efficient growth suppression. Proc Natl Acad Sci U S A. 1996 Dec 24;93(26):15335–40. doi:10.1073/pnas.93.26.15335 PubMed PMID: 8986812; PubMed Central PMCID: PMC26405.

41. Gu W, Shi XL, Roeder RG. Synergistic activation of transcription by CBP and p53. Nature. 1997 Jun 19;387(6635):819–23. doi:10.1038/42972 PubMed PMID: 9194564.

42. Kussie PH, Gorina S, Marechal V, Elenbaas B, Moreau J, Levine AJ, et al. Structure of the MDM2 oncoprotein bound to the p53 tumor suppressor

transactivation domain. Science. 1996 Nov 8;274(5289):948–53. doi:10.1126/science.274.5289.948 PubMed PMID: 8875929.

43. Kay BK, Williamson MP, Sudol M. The importance of being proline: the interaction of proline-rich motifs in signaling proteins with their cognate domains. FASEB J. 2000 Feb;14(2):231–41. PubMed PMID: 10657980.

44. Duan J, Nilsson L. Effect of Zn2+ on DNA recognition and stability of the p53 DNA-binding domain. Biochemistry. 2006 Jun 20;45(24):7483–92. doi:10.1021/bi0603165 PubMed PMID: 16768444.

45. Klein C, Georges G, Künkele KP, Huber R, Engh RA, Hansen S. High thermostability and lack of cooperative DNA binding distinguish the p63 core domain from the homologous tumor suppressor p53. J Biol Chem. 2001 Oct 5;276(40):37390–401. doi:10.1074/jbc.M103801200 PubMed PMID: 11477076.

46. el-Deiry WS, Kern SE, Pietenpol JA, Kinzler KW, Vogelstein B. Definition of a consensus binding site for p53. Nat Genet. 1992 Apr;1(1):45–9. doi:10.1038/ng0492-45 PubMed PMID: 1301998.

47. Ma B, Pan Y, Zheng J, Levine AJ, Nussinov R. Sequence analysis of p53 response-elements suggests multiple binding modes of the p53 tetramer to DNA targets. Nucleic Acids Res. 2007;35(9):2986–3001. doi:10.1093/nar/gkm192 PubMed PMID: 17439973; PubMed Central PMCID: PMC1888811.

48. Nagaich AK, Zhurkin VB, Durell SR, Jernigan RL, Appella E, Harrington RE. p53-induced DNA bending and twisting: p53 tetramer binds on the outer side of a DNA loop and increases DNA twisting. Proc Natl Acad Sci U S A. 1999 Mar 2;96(5):1875–80. doi:10.1073/pnas.96.5.1875 PubMed PMID: 10051562; PubMed Central PMCID: PMC26704.

49. Veprintsev DB, Freund SMV, Andreeva A, Rutledge SE, Tidow H, Cañadillas JMP, et al. Core domain interactions in full-length p53 in solution. Proc Natl Acad Sci U S A. 2006 Feb 14;103(7):2115–9. doi:10.1073/pnas.0511130103 PubMed PMID: 16461914; PubMed Central PMCID: PMC1413758.

50. Sakaguchi K, Sakamoto H, Xie D, Erickson JW, Lewis MS, Anderson CW, et al. Effect of phosphorylation on tetramerization of the tumor suppressor protein p53. J Protein Chem. 1997 Jul;16(5):553–6. doi:10.1023/a:1026334116189 PubMed PMID: 9246643.

51. Mateu MG, Fersht AR. Mutually compensatory mutations during evolution of the tetramerization domain of tumor suppressor p53 lead to impaired hetero-oligomerization. Proc Natl Acad Sci U S A. 1999 Mar 30;96(7):3595–9. doi:10.1073/pnas.96.7.3595 PubMed PMID: 10097082; PubMed Central PMCID: PMC22339.

52. Brokx RD, Bolewska-Pedyczak E, Gariépy J. A stable human p53 heterotetramer based on constructive charge interactions within the tetramerization domain. J

Biol Chem. 2003 Jan 24;278(4):2327–32. doi:10.1074/jbc.M208528200 PubMed PMID: 12433927.

53. Hu M, Gu L, Li M, Jeffrey PD, Gu W, Shi Y. Structural basis of competitive recognition of p53 and MDM2 by HAUSP/USP7: implications for the regulation of the p53-MDM2 pathway. PLoS Biol. 2006 Feb;4(2):e27. doi:10.1371/journal.pbio.0040027 PubMed PMID: 16402859; PubMed Central PMCID: PMC1334386.

54. Luo J, Li M, Tang Y, Laszkowska M, Roeder RG, Gu W. Acetylation of p53 augments its site-specific DNA binding both in vitro and in vivo. Proc Natl Acad Sci U S A. 2004 Feb 24;101(8):2259–64. doi:10.1073/pnas.0308762101 PubMed PMID: 14982997; PubMed Central PMCID: PMC356938.

55. Vousden KH, Prives C. Blinded by the Light: The Growing Complexity of p53. Cell. 2009 May;137(3):413–31. doi:10.1016/j.cell.2009.04.037

56. Kussie PH, Gorina S, Marechal V, Elenbaas B, Moreau J, Levine AJ, et al. Structure of the MDM2 oncoprotein bound to the p53 tumor suppressor transactivation domain. Science. 1996 Nov 8;274(5289):948–53. doi:10.1126/science.274.5289.948 PubMed PMID: 8875929.

57. Moll UM, Petrenko O. The MDM2-p53 interaction. Mol Cancer Res. 2003 Dec;1(14):1001–8. PubMed PMID: 14707283.

58. Kubbutat MHG, Jones SN, Vousden KH. Regulation of p53 stability by Mdm2. Nature. 1997 May;387(6630):299–303. doi:10.1038/387299a0

59. Haupt Y, Maya R, Kazaz A, Oren M. Mdm2 promotes the rapid degradation of p53. Nature. 1997 May 15;387(6630):296–9. doi:10.1038/387296a0 PubMed PMID: 9153395.

60. Oliner JD, Pietenpol JA, Thiagalingam S, Gyuris J, Kinzler KW, Vogelstein B. Oncoprotein MDM2 conceals the activation domain of tumour suppressor p53. Nature. 1993 Apr 29;362(6423):857–60. doi:10.1038/362857a0 PubMed PMID: 8479525.

61. Wu X, Bayle JH, Olson D, Levine AJ. The p53-mdm-2 autoregulatory feedback loop. Genes & Development. 1993 Jul 1;7(7a):1126–32. doi:10.1101/gad.7.7a.1126

62. Chi SW, Lee SH, Kim DH, Ahn MJ, Kim JS, Woo JY, et al. Structural details on mdm2-p53 interaction. J Biol Chem. 2005 Nov 18;280(46):38795–802. doi:10.1074/jbc.M508578200 PubMed PMID: 16159876.

63. Poyurovsky MV, Katz C, Laptenko O, Beckerman R, Lokshin M, Ahn J, et al. The C terminus of p53 binds the N-terminal domain of MDM2. Nat Struct Mol Biol. 2010 Aug;17(8):982–9. doi:10.1038/nsmb.1872 PubMed PMID: 20639885; PubMed Central PMCID: PMC2922928.

64. Pflaum J, Schlosser S, MÃ¼ller M. p53 Family and Cellular Stress Responses in Cancer. Front Oncol. 2014 Oct 21;4. doi:10.3389/fonc.2014.00285

65. Fan X, Wang K, Lu Q, Lu Y, Sun J. Cell-Based Drug Delivery Systems Participate in the Cancer Immunity Cycle for Improved Cancer Immunotherapy. Small. 2023 Jan;19(4):e2205166. doi:10.1002/smll.202205166 PubMed PMID: 36437050.

66. Abbas T, Dutta A. p21 in cancer: intricate networks and multiple activities. Nat Rev Cancer. 2009 Jun;9(6):400–14. doi:10.1038/nrc2657 PubMed PMID: 19440234; PubMed Central PMCID: PMC2722839.

67. Sultan FA, Sweatt JD. The role of the Gadd45 family in the nervous system: a focus on neurodevelopment, neuronal injury, and cognitive neuroepigenetics. Adv Exp Med Biol. 2013;793:81–119. doi:10.1007/978-1-4614-8289-5_6 PubMed PMID: 24104475.

68. Aljabal G, Yap BK. 14-3-3σ and Its Modulators in Cancer. Pharmaceuticals (Basel). 2020 Dec 3;13(12):441. doi:10.3390/ph13120441 PubMed PMID: 33287252; PubMed Central PMCID: PMC7761676.

69. Parlani M, Jorgez C, Friedl P. Plasticity of cancer invasion and energy metabolism. Trends Cell Biol. 2023 May;33(5):388–402. doi:10.1016/j.tcb.2022.09.009 PubMed PMID: 36328835; PubMed Central PMCID: PMC10368441.

70. Drakos E, Atsaves V, Li J, Leventaki V, Andreeff M, Medeiros LJ, et al. Stabilization and activation of p53 downregulates mTOR signaling through AMPK in mantle cell lymphoma. Leukemia. 2009 Apr;23(4):784–90. doi:10.1038/leu.2008.348 PubMed PMID: 19225536.

71. Li C, Lin L, Zhang L, Xu R, Chen X, Ji J, et al. Long noncoding RNA p21 enhances autophagy to alleviate endothelial progenitor cells damage and promote endothelial repair in hypertension through SESN2/AMPK/TSC2 pathway. Pharmacol Res. 2021 Nov;173:105920. doi:10.1016/j.phrs.2021.105920 PubMed PMID: 34601081.

72. Matsuda S, Nakagawa Y, Kitagishi Y, Nakanishi A, Murai T. Reactive Oxygen Species, Superoxide Dimutases, and PTEN-p53-AKT-MDM2 Signaling Loop Network in Mesenchymal Stem/Stromal Cells Regulation. Cells. 2018 May 1;7(5):36. doi:10.3390/cells7050036 PubMed PMID: 29723979; PubMed Central PMCID: PMC5981260.

73. Bensaad K, Cheung EC, Vousden KH. Modulation of intracellular ROS levels by TIGAR controls autophagy. EMBO J. 2009 Oct 7;28(19):3015–26. doi:10.1038/emboj.2009.242 PubMed PMID: 19713938; PubMed Central PMCID: PMC2736014.

74. Tseng C, Han Y, Lv Z, Song Q, Wang K, Shen H, et al. The CRL4DCAF6 E3 ligase ubiquitinates CtBP1/2 to induce apoptotic signalling and promote intervertebral disc degeneration. J Mol Med (Berl). 2023 Feb;101(1–2):171–81. doi:10.1007/s00109-022-02277-1 PubMed PMID: 36688959.

75. Ding B, Haidurov A, Chawla A, Parmigiani A, van de Kamp G, Dalina A, et al. p53-inducible SESTRINs might play opposite roles in the regulation of early and late stages of lung carcinogenesis. Oncotarget. 2019 Dec 10;10(65):6997–7009. doi:10.18632/oncotarget.27367 PubMed PMID: 31857853; PubMed Central PMCID: PMC6916756.

76. Yu C, Liu S, Niu Y, Fu L. Exercise protects intestinal epithelial barrier from high fat diet- induced permeabilization through SESN2/AMPKα1/HIF-1α signaling. J Nutr Biochem. 2022 Sep;107:109059. doi:10.1016/j.jnutbio.2022.109059 PubMed PMID: 35643285.

77. Hao Q, Chen J, Lu H, Zhou X. The ARTS of p53-dependent mitochondrial apoptosis. J Mol Cell Biol. 2023 Mar 29;14(10):mjac074. doi:10.1093/jmcb/mjac074 PubMed PMID: 36565718; PubMed Central PMCID: PMC10053023.

78. Riccio M, Carnevale G, Cardinale V, Gibellini L, De Biasi S, Pisciotta A, et al. The Fas/Fas ligand apoptosis pathway underlies immunomodulatory properties of human biliary tree stem/progenitor cells. J Hepatol. 2014 Nov;61(5):1097–105. doi:10.1016/j.jhep.2014.06.016 PubMed PMID: 24953023.

79. Sobol RW. WRN suppresses p53/PUMA-induced apoptosis in colorectal cancer with microsatellite instability/mismatch repair deficiency. Proc Natl Acad Sci U S A. 2023 Jan 10;120(2):e2219963120. doi:10.1073/pnas.2219963120 PubMed PMID: 36598947; PubMed Central PMCID: PMC9926267.

80. Lin Z, Wan AH, Sun L, Liang H, Niu Y, Deng Y, et al. N6-methyladenosine demethylase FTO enhances chemo-resistance in colorectal cancer through SIVA1-mediated apoptosis. Mol Ther. 2023 Feb 1;31(2):517–34. doi:10.1016/j.ymthe.2022.10.012 PubMed PMID: 36307991; PubMed Central PMCID: PMC9931553.

81. Luedeke M, Coinac I, Linnert CM, Bogdanova N, Rinckleb AE, Schrader M, et al. Prostate cancer risk is not altered by TP53AIP1 germline mutations in a German case-control series. PLoS One. 2012;7(3):e34128. doi:10.1371/journal.pone.0034128 PubMed PMID: 22457820; PubMed Central PMCID: PMC3311578.

82. Giacomelli AO, Yang X, Lintner RE, McFarland JM, Duby M, Kim J, et al. Mutational processes shape the landscape of TP53 mutations in human cancer. Nat Genet. 2018 Oct;50(10):1381–7. doi:10.1038/s41588-018-0204-y

83. Li FP, Fraumeni JF. Soft-Tissue Sarcomas, Breast Cancer, and Other Neoplasms: A Familial Syndrome? Ann Intern Med. 1969 Oct 1;71(4):747–52. doi:10.7326/0003-4819-71-4-747

84. Mahon SM. Tertiary Prevention: Implications for Improving the Quality of Life of Long-Term Survivors of Cancer. Seminars in Oncology Nursing. 2005 Nov;21(4):260–70. doi:10.1016/j.soncn.2005.06.006

85. Gu KJ, Li G. An Overview of Cancer Prevention: Chemoprevention and Immunoprevention. J Cancer Prev. 2020 Sep 30;25(3):127–35. doi:10.15430/JCP.2020.25.3.127

86. Alexandrova EM, Yallowitz AR, Li D, Xu S, Schulz R, Proia DA, et al. Improving survival by exploiting tumour dependence on stabilized mutant p53 for treatment. Nature. 2015 Jul 16;523(7560):352–6. doi:10.1038/nature14430

87. Zhang C, Liu J, Xu D, Zhang T, Hu W, Feng Z. Gain-of-function mutant p53 in cancer progression and therapy. Lu H, editor. Journal of Molecular Cell Biology. 2020 Sep 1;12(9):674–87. doi:10.1093/jmcb/mjaa040

88. Chapman CM, Sun X, Roschewski M, Aue G, Farooqui M, Stennett L, et al. ON 01910.Na is selectively cytotoxic for chronic lymphocytic leukemia cells through a dual mechanism of action involving PI3K/AKT inhibition and induction of oxidative stress. Clin Cancer Res. 2012 Apr 1;18(7):1979–91. doi:10.1158/1078-0432.CCR-11-2113 PubMed PMID: 22351695; PubMed Central PMCID: PMC3321371.

89. Trachootham D, Alexandre J, Huang P. Targeting cancer cells by ROS-mediated mechanisms: a radical therapeutic approach? Nat Rev Drug Discov. 2009 Jul;8(7):579–91. doi:10.1038/nrd2803 PubMed PMID: 19478820.

90. Sciaccotta R, Gangemi S, Penna G, Giordano L, Pioggia G, Allegra A. Potential New Therapies “ROS-Based” in CLL: An Innovative Paradigm in the Induction of Tumor Cell Apoptosis. Antioxidants. 2024 Apr 17;13(4):475. doi:10.3390/antiox13040475

91. Sies H, Jones DP. Reactive oxygen species (ROS) as pleiotropic physiological signalling agents. Nat Rev Mol Cell Biol. 2020 Jul;21(7):363–83. doi:10.1038/s41580-020-0230-3 PubMed PMID: 32231263.

92. Zorov DB, Juhaszova M, Sollott SJ. Mitochondrial reactive oxygen species (ROS) and ROS-induced ROS release. Physiol Rev. 2014 Jul;94(3):909–50. doi:10.1152/physrev.00026.2013 PubMed PMID: 24987008; PubMed Central PMCID: PMC4101632.

93. Phaniendra A, Jestadi DB, Periyasamy L. Free radicals: properties, sources, targets, and their implication in various diseases. Indian J Clin Biochem. 2015 Jan;30(1):11–26. doi:10.1007/s12291-014-0446-0 PubMed PMID: 25646037; PubMed Central PMCID: PMC4310837.

94. Panday A, Sahoo MK, Osorio D, Batra S. NADPH oxidases: an overview from structure to innate immunity-associated pathologies. Cell Mol Immunol. 2015 Jan;12(1):5–23. doi:10.1038/cmi.2014.89 PubMed PMID: 25263488; PubMed Central PMCID: PMC4654378.

95. Kozlov AV, Javadov S, Sommer N. Cellular ROS and Antioxidants: Physiological and Pathological Role. Antioxidants. 2024 May 14;13(5):602. doi:10.3390/antiox13050602

96. Ayala A, Muñoz MF, Argüelles S. Lipid peroxidation: production, metabolism, and signaling mechanisms of malondialdehyde and 4-hydroxy-2-nonenal. Oxid Med Cell Longev. 2014;2014:360438. doi:10.1155/2014/360438 PubMed PMID: 24999379; PubMed Central PMCID: PMC4066722.

97. Barrera G, Pizzimenti S, Daga M, Dianzani C, Arcaro A, Cetrangolo GP, et al. Lipid Peroxidation-Derived Aldehydes, 4-Hydroxynonenal and Malondialdehyde in Aging-Related Disorders. Antioxidants (Basel). 2018 Jul 30;7(8):102. doi:10.3390/antiox7080102 PubMed PMID: 30061536; PubMed Central PMCID: PMC6115986.

98. Cui Q, Wang JQ, Assaraf YG, Ren L, Gupta P, Wei L, et al. Modulating ROS to overcome multidrug resistance in cancer. Drug Resist Updat. 2018 Nov;41:1–25. doi:10.1016/j.drup.2018.11.001 PubMed PMID: 30471641.

99. Hegedűs C, Kovács K, Polgár Z, Regdon Z, Szabó É, Robaszkiewicz A, et al. Redox control of cancer cell destruction. Redox Biol. 2018 Jun;16:59–74. doi:10.1016/j.redox.2018.01.015 PubMed PMID: 29477046; PubMed Central PMCID: PMC5842284.

100. Zhao Y, Ye X, Xiong Z, Ihsan A, Ares I, Martínez M, et al. Cancer Metabolism: The Role of ROS in DNA Damage and Induction of Apoptosis in Cancer Cells. Metabolites. 2023 Jun 27;13(7):796. doi:10.3390/metabo13070796 PubMed PMID: 37512503; PubMed Central PMCID: PMC10383295.

101. Bhattacharyya A, Chattopadhyay R, Mitra S, Crowe SE. Oxidative stress: an essential factor in the pathogenesis of gastrointestinal mucosal diseases. Physiol Rev. 2014 Apr;94(2):329–54. doi:10.1152/physrev.00040.2012 PubMed PMID: 24692350; PubMed Central PMCID: PMC4044300.

102. Wang Y, Branicky R, Noë A, Hekimi S. Superoxide dismutases: Dual roles in controlling ROS damage and regulating ROS signaling. J Cell Biol. 2018 Jun 4;217(6):1915–28. doi:10.1083/jcb.201708007 PubMed PMID: 29669742; PubMed Central PMCID: PMC5987716.

103. Kurutas EB. The importance of antioxidants which play the role in cellular response against oxidative/nitrosative stress: current state. Nutr J. 2016 Jul 25;15(1):71. doi:10.1186/s12937-016-0186-5 PubMed PMID: 27456681; PubMed Central PMCID: PMC4960740.

104. Trachootham D, Zhang H, Zhang W, Feng L, Du M, Zhou Y, et al. Effective elimination of fludarabine-resistant CLL cells by PEITC through a redox-mediated mechanism. Blood. 2008 Sep 1;112(5):1912–22. doi:10.1182/blood-2008-04-149815 PubMed PMID: 18574029; PubMed Central PMCID: PMC2518893.

105. Lapenna D. Glutathione and glutathione-dependent enzymes: From biochemistry to gerontology and successful aging. Ageing Res Rev. 2023 Dec;92:102066. doi:10.1016/j.arr.2023.102066 PubMed PMID: 37683986.

106. Liu J, Zhang Y, Yang B, Jia Y, Liu RT, Ding L, et al. Synergistic Glutathione Depletion and STING Activation to Potentiate Dendritic Cell Maturation and Cancer Vaccine Efficacy. Angew Chem Int Ed Engl. 2024 Mar 4;63(10):e202318530. doi:10.1002/anie.202318530 PubMed PMID: 38196070.

107. Ling X, Tu J, Wang J, Shajii A, Kong N, Feng C, et al. Glutathione-Responsive Prodrug Nanoparticles for Effective Drug Delivery and Cancer Therapy. ACS Nano. 2019 Jan 22;13(1):357–70. doi:10.1021/acsnano.8b06400 PubMed PMID: 30485068; PubMed Central PMCID: PMC7049173.

108. Espinosa-Diez C, Miguel V, Mennerich D, Kietzmann T, Sánchez-Pérez P, Cadenas S, et al. Antioxidant responses and cellular adjustments to oxidative stress. Redox Biol. 2015 Dec;6:183–97. doi:10.1016/j.redox.2015.07.008 PubMed PMID: 26233704; PubMed Central PMCID: PMC4534574.

109. Hu K, Li K, Lv J, Feng J, Chen J, Wu H, et al. Suppression of the SLC7A11/glutathione axis causes synthetic lethality in KRAS-mutant lung adenocarcinoma. J Clin Invest. 2020 Apr 1;130(4):1752–66. doi:10.1172/JCI124049 PubMed PMID: 31874110; PubMed Central PMCID: PMC7108883.

110. Yoo HC, Yu YC, Sung Y, Han JM. Glutamine reliance in cell metabolism. Exp Mol Med. 2020 Sep;52(9):1496–516. doi:10.1038/s12276-020-00504-8 PubMed PMID: 32943735; PubMed Central PMCID: PMC8080614.

111. Tajan M, Hennequart M, Cheung EC, Zani F, Hock AK, Legrave N, et al. Serine synthesis pathway inhibition cooperates with dietary serine and glycine limitation for cancer therapy. Nat Commun. 2021 Jan 14;12(1):366. doi:10.1038/s41467-020-20223-y PubMed PMID: 33446657; PubMed Central PMCID: PMC7809039.

112. Wu G, Fang YZ, Yang S, Lupton JR, Turner ND. Glutathione metabolism and its implications for health. J Nutr. 2004 Mar;134(3):489–92. doi:10.1093/jn/134.3.489 PubMed PMID: 14988435.

113. Espinosa-Díez C, Miguel V, Vallejo S, Sánchez FJ, Sandoval E, Blanco E, et al. Role of glutathione biosynthesis in endothelial dysfunction and fibrosis. Redox Biol. 2018 Apr;14:88–99. doi:10.1016/j.redox.2017.08.019 PubMed PMID: 28888203; PubMed Central PMCID: PMC5596265.

114. Giustarini D, Colombo G, Garavaglia ML, Astori E, Portinaro NM, Reggiani F, et al. Assessment of glutathione/glutathione disulphide ratio and S-glutathionylated proteins in human blood, solid tissues, and cultured cells. Free Radic Biol Med. 2017 Nov;112:360–75. doi:10.1016/j.freeradbiomed.2017.08.008 PubMed PMID: 28807817.

115. Forman HJ, Zhang H, Rinna A. Glutathione: overview of its protective roles, measurement, and biosynthesis. Mol Aspects Med. 2009;30(1–2):1–12. doi:10.1016/j.mam.2008.08.006 PubMed PMID: 18796312; PubMed Central PMCID: PMC2696075.

116. Georgiou-Siafis SK, Tsiftsoglou AS. The Key Role of GSH in Keeping the Redox Balance in Mammalian Cells: Mechanisms and Significance of GSH in Detoxification via Formation of Conjugates. Antioxidants (Basel). 2023 Nov 1;12(11):1953. doi:10.3390/antiox12111953 PubMed PMID: 38001806; PubMed Central PMCID: PMC10669396.

117. Kennedy L, Sandhu JK, Harper ME, Cuperlovic-Culf M. Role of Glutathione in Cancer: From Mechanisms to Therapies. Biomolecules. 2020 Oct 9;10(10):1429. doi:10.3390/biom10101429 PubMed PMID: 33050144; PubMed Central PMCID: PMC7600400.

118. Velkova I, Pasino M, Khalid Z, Menichini P, Martorana E, Izzotti A, et al. Modulation of Ferroptosis by microRNAs in Human Cancer. J Pers Med. 2023 Apr 24;13(5):719. doi:10.3390/jpm13050719 PubMed PMID: 37240889; PubMed Central PMCID: PMC10221902.

119. Koppula P, Zhuang L, Gan B. Cystine transporter SLC7A11/xCT in cancer: ferroptosis, nutrient dependency, and cancer therapy. Protein Cell. 2021 Aug;12(8):599–620. doi:10.1007/s13238-020-00789-5 PubMed PMID: 33000412; PubMed Central PMCID: PMC8310547.

120. Desideri E, Ciccarone F, Ciriolo MR. Targeting Glutathione Metabolism: Partner in Crime in Anticancer Therapy. Nutrients. 2019 Aug 16;11(8):1926. doi:10.3390/nu11081926 PubMed PMID: 31426306; PubMed Central PMCID: PMC6724225.

121. Bansal A, Simon MC. Glutathione metabolism in cancer progression and treatment resistance. J Cell Biol. 2018 Jul 2;217(7):2291–8. doi:10.1083/jcb.201804161 PubMed PMID: 29915025; PubMed Central PMCID: PMC6028537.

122. Cordani M, Butera G, Pacchiana R, Masetto F, Mullappilly N, Riganti C, et al. Mutant p53-Associated Molecular Mechanisms of ROS Regulation in Cancer Cells. Biomolecules. 2020 Feb 26;10(3):361. doi:10.3390/biom10030361

123. Lo SC, Li X, Henzl MT, Beamer LJ, Hannink M. Structure of the Keap1:Nrf2 interface provides mechanistic insight into Nrf2 signaling. EMBO J. 2006 Aug 9;25(15):3605–17. doi:10.1038/sj.emboj.7601243 PubMed PMID: 16888629; PubMed Central PMCID: PMC1538563.

124. Moloney JN, Cotter TG. ROS signalling in the biology of cancer. Seminars in Cell & Developmental Biology. 2018 Aug;80:50–64. doi:10.1016/j.semcdb.2017.05.023

125. Kalo E, Kogan-Sakin I, Solomon H, Bar-Nathan E, Shay M, Shetzer Y, et al. Mutant p53R273H attenuates the expression of phase 2 detoxifying enzymes and promotes the survival of cells with high levels of reactive oxygen species. J Cell Sci. 2012 Nov 15;125(Pt 22):5578–86. doi:10.1242/jcs.106815 PubMed PMID: 22899716.

126. Liu DS, Duong CP, Haupt S, Montgomery KG, House CM, Azar WJ, et al. Inhibiting the system xC−/glutathione axis selectively targets cancers with mutant-p53 accumulation. Nat Commun. 2017 Mar 28;8(1):14844. doi:10.1038/ncomms14844

127. Dixon SJ, Lemberg KM, Lamprecht MR, Skouta R, Zaitsev EM, Gleason CE, et al. Ferroptosis: an iron-dependent form of nonapoptotic cell death. Cell. 2012 May 25;149(5):1060–72. doi:10.1016/j.cell.2012.03.042 PubMed PMID: 22632970; PubMed Central PMCID: PMC3367386.

128. Stockwell BR, Friedmann Angeli JP, Bayir H, Bush AI, Conrad M, Dixon SJ, et al. Ferroptosis: A Regulated Cell Death Nexus Linking Metabolism, Redox Biology, and Disease. Cell. 2017 Oct 5;171(2):273–85. doi:10.1016/j.cell.2017.09.021 PubMed PMID: 28985560; PubMed Central PMCID: PMC5685180.

129. Cao JY, Dixon SJ. Mechanisms of ferroptosis. Cell Mol Life Sci. 2016 Jun;73(11–12):2195–209. doi:10.1007/s00018-016-2194-1

130. Mou Y, Wang J, Wu J, He D, Zhang C, Duan C, et al. Ferroptosis, a new form of cell death: opportunities and challenges in cancer. J Hematol Oncol. 2019 Dec;12(1):34. doi:10.1186/s13045-019-0720-y

131. Feng H, Schorpp K, Jin J, Yozwiak CE, Hoffstrom BG, Decker AM, et al. Transferrin Receptor Is a Specific Ferroptosis Marker. Cell Rep. 2020 Mar 10;30(10):3411-3423.e7. doi:10.1016/j.celrep.2020.02.049 PubMed PMID: 32160546; PubMed Central PMCID: PMC7172030.

132. Arosio P, Elia L, Poli M. Ferritin, cellular iron storage and regulation. IUBMB Life. 2017 Jun;69(6):414–22. doi:10.1002/iub.1621

133. Bradley JM, Le Brun NE, Moore GR. Ferritins: furnishing proteins with iron. J Biol Inorg Chem. 2016 Mar;21(1):13–28. doi:10.1007/s00775-016-1336-0 PubMed PMID: 26825805; PubMed Central PMCID: PMC4771812.

134. Hu W, Zhou C, Jing Q, Li Y, Yang J, Yang C, et al. FTH promotes the proliferation and renders the HCC cells specifically resist to ferroptosis by maintaining iron homeostasis. Cancer Cell Int. 2021 Dec 29;21(1):709. doi:10.1186/s12935-021-02420-x PubMed PMID: 34965856; PubMed Central PMCID: PMC8717654.

135. Mancias JD, Wang X, Gygi SP, Harper JW, Kimmelman AC. Quantitative proteomics identifies NCOA4 as the cargo receptor mediating ferritinophagy. Nature. 2014 May;509(7498):105–9. doi:10.1038/nature13148

136. Hentze MW, Muckenthaler MU, Galy B, Camaschella C. Two to tango: regulation of Mammalian iron metabolism. Cell. 2010 Jul 9;142(1):24–38. doi:10.1016/j.cell.2010.06.028 PubMed PMID: 20603012.

137. Kwon MY, Park E, Lee SJ, Chung SW. Heme oxygenase-1 accelerates erastin-induced ferroptotic cell death. Oncotarget. 2015 Sep 15;6(27):24393–403. doi:10.18632/oncotarget.5162

138. Brigelius-Flohé R, Maiorino M. Glutathione peroxidases. Biochim Biophys Acta. 2013 May;1830(5):3289–303. doi:10.1016/j.bbagen.2012.11.020 PubMed PMID: 23201771.

139. Doll S, Proneth B, Tyurina YY, Panzilius E, Kobayashi S, Ingold I, et al. ACSL4 dictates ferroptosis sensitivity by shaping cellular lipid composition. Nat Chem Biol. 2017 Jan;13(1):91–8. doi:10.1038/nchembio.2239 PubMed PMID: 27842070; PubMed Central PMCID: PMC5610546.

140. Dixon SJ. Ferroptosis: bug or feature? Immunological Reviews. 2017 May;277(1):150–7. doi:10.1111/imr.12533

141. Yang WS, SriRamaratnam R, Welsch ME, Shimada K, Skouta R, Viswanathan VS, et al. Regulation of ferroptotic cancer cell death by GPX4. Cell. 2014 Jan 16;156(1–2):317–31. doi:10.1016/j.cell.2013.12.010 PubMed PMID: 24439385; PubMed Central PMCID: PMC4076414.

142. Ingold I, Berndt C, Schmitt S, Doll S, Poschmann G, Buday K, et al. Selenium Utilization by GPX4 Is Required to Prevent Hydroperoxide-Induced Ferroptosis. Cell. 2018 Jan 25;172(3):409-422.e21. doi:10.1016/j.cell.2017.11.048 PubMed PMID: 29290465.

143. Badgley MA, Kremer DM, Maurer HC, DelGiorno KE, Lee HJ, Purohit V, et al. Cysteine depletion induces pancreatic tumor ferroptosis in mice. Science. 2020 Apr 3;368(6486):85–9. doi:10.1126/science.aaw9872 PubMed PMID: 32241947; PubMed Central PMCID: PMC7681911.

144. Zhao L, Zhou X, Xie F, Zhang L, Yan H, Huang J, et al. Ferroptosis in cancer and cancer immunotherapy. Cancer Commun (Lond). 2022 Feb;42(2):88–116. doi:10.1002/cac2.12250 PubMed PMID: 35133083; PubMed Central PMCID: PMC8822596.

145. Kang R, Kroemer G, Tang D. The tumor suppressor protein p53 and the ferroptosis network. Free Radical Biology and Medicine. 2019 Mar;133:162–8. doi:10.1016/j.freeradbiomed.2018.05.074

146. Liu DS, Duong CP, Haupt S, Montgomery KG, House CM, Azar WJ, et al. Inhibiting the system xC-/glutathione axis selectively targets cancers with mutant-p53 accumulation. Nat Commun. 2017 Mar 28;8:14844. doi:10.1038/ncomms14844 PubMed PMID: 28348409; PubMed Central PMCID: PMC5379068.

147. Zhang W, Trachootham D, Liu J, Chen G, Pelicano H, Garcia-Prieto C, et al. Stromal control of cystine metabolism promotes cancer cell survival in chronic lymphocytic leukaemia. Nat Cell Biol. 2012 Mar;14(3):276–86. doi:10.1038/ncb2432

148. Tsukada N, Burger JA, Zvaifler NJ, Kipps TJ. Distinctive features of ‘nurselike’ cells that differentiate in the context of chronic lymphocytic leukemia. Blood. 2002 Feb 1;99(3):1030–7. doi:10.1182/blood.v99.3.1030 PubMed PMID: 11807009.

149. Burger JA, Ghia P, Rosenwald A, Caligaris-Cappio F. The microenvironment in mature B-cell malignancies: a target for new treatment strategies. Blood. 2009 Oct 15;114(16):3367–75. doi:10.1182/blood-2009-06-225326 PubMed PMID: 19636060; PubMed Central PMCID: PMC4969052.

150. Chiorazzi N, Rai KR, Ferrarini M. Chronic lymphocytic leukemia. N Engl J Med. 2005 Feb 24;352(8):804–15. doi:10.1056/NEJMra041720 PubMed PMID: 15728813.

151. Kotredes KP, Gamero AM. Interferons as inducers of apoptosis in malignant cells. J Interferon Cytokine Res. 2013 Apr;33(4):162–70. doi:10.1089/jir.2012.0110 PubMed PMID: 23570382; PubMed Central PMCID: PMC3624694.

152. Sangfelt O, Erickson S, Grander D. Mechanisms of interferon-induced cell cycle arrest. Front Biosci. 2000 Apr 1;5:D479-487. doi:10.2741/sangfelt PubMed PMID: 10762599.

153. Sun T, Yang Y, Luo X, Cheng Y, Zhang M, Wang K, et al. Inhibition of tumor angiogenesis by interferon-γ by suppression of tumor-associated macrophage differentiation. Oncol Res. 2014;21(5):227–35. doi:10.3727/096504014X13890370410285 PubMed PMID: 24854099.

154. Martin-Hijano L, Sainz B. The Interactions Between Cancer Stem Cells and the Innate Interferon Signaling Pathway. Front Immunol. 2020;11:526. doi:10.3389/fimmu.2020.00526 PubMed PMID: 32296435; PubMed Central PMCID: PMC7136464.

155. Puthier D, Thabard W, Rapp M, Etrillard M, Harousseau J, Bataille R, et al. Interferon alpha extends the survival of human myeloma cells through an upregulation of the Mcl-1 anti-apoptotic molecule. Br J Haematol. 2001 Feb;112(2):358–63. doi:10.1046/j.1365-2141.2001.02575.x PubMed PMID: 11167829.

156. Banerjee K, Resat H. Constitutive activation of STAT3 in breast cancer cells: A review. Int J Cancer. 2016 Jun 1;138(11):2570–8. doi:10.1002/ijc.29923 PubMed PMID: 26559373; PubMed Central PMCID: PMC4801660.

157. Arora L, Kumar AP, Arfuso F, Chng WJ, Sethi G. The Role of Signal Transducer and Activator of Transcription 3 (STAT3) and Its Targeted Inhibition in Hematological Malignancies. Cancers (Basel). 2018 Sep 13;10(9):327. doi:10.3390/cancers10090327 PubMed PMID: 30217007; PubMed Central PMCID: PMC6162647.

158. Boudny M, Trbusek M. The Important Role of STAT3 in Chronic Lymphocytic Leukaemia Biology. Klin Onkol. 2020;33(1):32–8. doi:10.14735/amko202032 PubMed PMID: 32075387.

159. Hammarén HM, Virtanen AT, Raivola J, Silvennoinen O. The regulation of JAKs in cytokine signaling and its breakdown in disease. Cytokine. 2019 Jun;118:48–63. doi:10.1016/j.cyto.2018.03.041 PubMed PMID: 29685781.

160. Owen KL, Brockwell NK, Parker BS. JAK-STAT Signaling: A Double-Edged Sword of Immune Regulation and Cancer Progression. Cancers (Basel). 2019 Dec 12;11(12):2002. doi:10.3390/cancers11122002 PubMed PMID: 31842362; PubMed Central PMCID: PMC6966445.

161. Niu G, Wright KL, Ma Y, Wright GM, Huang M, Irby R, et al. Role of Stat3 in regulating p53 expression and function. Mol Cell Biol. 2005 Sep;25(17):7432–40. doi:10.1128/MCB.25.17.7432-7440.2005 PubMed PMID: 16107692; PubMed Central PMCID: PMC1190305.

162. Pham TH, Park HM, Kim J, Hong JT, Yoon DY. STAT3 and p53: Dual Target for Cancer Therapy. Biomedicines. 2020 Dec 21;8(12):637. doi:10.3390/biomedicines8120637 PubMed PMID: 33371351; PubMed Central PMCID: PMC7767392.

163. Wörmann SM, Song L, Ai J, Diakopoulos KN, Kurkowski MU, Görgülü K, et al. Loss of P53 Function Activates JAK2-STAT3 Signaling to Promote Pancreatic Tumor Growth, Stroma Modification, and Gemcitabine Resistance in Mice and Is Associated With Patient Survival. Gastroenterology. 2016 Jul;151(1):180-193.e12. doi:10.1053/j.gastro.2016.03.010 PubMed PMID: 27003603.

164. Wang Y, Yu X, Song H, Feng D, Jiang Y, Wu S, et al. The STAT-ROS cycle extends IFN-induced cancer cell apoptosis. Int J Oncol. 2017 Nov 8. doi:10.3892/ijo.2017.4196

165. Tomic J, Lichty B, Spaner DE. Aberrant interferon-signaling is associated with aggressive chronic lymphocytic leukemia. Blood. 2011 Mar 3;117(9):2668–80. doi:10.1182/blood-2010-05-285999 PubMed PMID: 21205928.

166. Ostlund L, Grandér D, Juliusson G, Robèrt KH, Lundgren E, Einhorn S. Alpha-interferon receptors in malignant B-cells from patients with chronic lymphocytic leukemia: relation to induction of 2'-5'-oligoadenylate synthetase and blast transformation. Cancer Res. 1989 Jun 15;49(12):3425–30. PubMed PMID: 2524252.

167. Jewell AP. Interferon-alpha, Bcl-2 expression and apoptosis in B-cell chronic lymphocytic leukemia. Leuk Lymphoma. 1996 Mar;21(1–2):43–7. doi:10.3109/10428199609067578 PubMed PMID: 8907268.

168. Rojas R, Roman J, Torres A, Ramirez R, Carracedo J, Lopez R, et al. Inhibition of apoptotic cell death in B-CLL by interferon gamma correlates with clinical stage. Leukemia. 1996 Nov;10(11):1782–8. PubMed PMID: 8892682.

169. Bauvois B, Pramil E, Jondreville L, Quiney C, Nguyen-Khac F, Susin SA. Activation of Interferon Signaling in Chronic Lymphocytic Leukemia Cells Contributes to Apoptosis Resistance via a JAK-Src/STAT3/Mcl-1 Signaling Pathway. Biomedicines. 2021 Feb 13;9(2):188. doi:10.3390/biomedicines9020188 PubMed PMID: 33668421; PubMed Central PMCID: PMC7918075.

170. Frank DA, Mahajan S, Ritz J. B lymphocytes from patients with chronic lymphocytic leukemia contain signal transducer and activator of transcription (STAT) 1 and STAT3 constitutively phosphorylated on serine residues. J Clin Invest. 1997 Dec 15;100(12):3140–8. doi:10.1172/JCI119869 PubMed PMID: 9399961; PubMed Central PMCID: PMC508527.

171. Hazan-Halevy I, Harris D, Liu Z, Liu J, Li P, Chen X, et al. STAT3 is constitutively phosphorylated on serine 727 residues, binds DNA, and activates transcription in CLL cells. Blood. 2010 Apr 8;115(14):2852–63. doi:10.1182/blood-2009-10-230060 PubMed PMID: 20154216; PubMed Central PMCID: PMC2918366.

172. Townsend PA, Scarabelli TM, Davidson SM, Knight RA, Latchman DS, Stephanou A. STAT-1 Interacts with p53 to Enhance DNA Damage-induced Apoptosis. Journal of Biological Chemistry. 2004 Feb;279(7):5811–20. doi:10.1074/jbc.M302637200

173. Będzińska A, Łasut-Szyszka B, Krześniak M, Gdowicz-Kłosok A, Rusin M. The puzzling regulation of the interferon signaling system by the p53 tumor suppressor protein. Cell Mol Life Sci. 2025 Jun 13;82(1):233. doi:10.1007/s00018-025-05763-0 PubMed PMID: 40512405; PubMed Central PMCID: PMC12165926.

174. Chemotherapeutic options in chronic lymphocytic leukemia: a meta-analysis of the randomized trials. CLL Trialists' Collaborative Group. J Natl Cancer Inst. 1999 May 19;91(10):861–8. doi:10.1093/jnci/91.10.861 PubMed PMID: 10340906.

175. Steurer M, Pall G, Richards S, Schwarzer G, Bohlius J, Greil R. Purine antagonists for chronic lymphocytic leukaemia. Cochrane Database Syst Rev. 2006 Jul 19;2006(3):CD004270. doi:10.1002/14651858.CD004270.pub2 PubMed PMID: 16856041; PubMed Central PMCID: PMC8407449.

176. Hagemeister F. Rituximab for the treatment of non-Hodgkin's lymphoma and chronic lymphocytic leukaemia. Drugs. 2010 Feb 12;70(3):261–72. doi:10.2165/11532180-000000000-00000 PubMed PMID: 20166765.

177. Huhn D, von Schilling C, Wilhelm M, Ho AD, Hallek M, Kuse R, et al. Rituximab therapy of patients with B-cell chronic lymphocytic leukemia. Blood. 2001 Sep 1;98(5):1326–31. doi:10.1182/blood.v98.5.1326 PubMed PMID: 11520778.

178. Wierda WG, Kipps TJ, Mayer J, Stilgenbauer S, Williams CD, Hellmann A, et al. Ofatumumab as single-agent CD20 immunotherapy in fludarabine-refractory chronic lymphocytic leukemia. J Clin Oncol. 2010 Apr 1;28(10):1749–55. doi:10.1200/JCO.2009.25.3187 PubMed PMID: 20194866; PubMed Central PMCID: PMC4979101.

179. Patz M, Isaeva P, Forcob N, Müller B, Frenzel LP, Wendtner CM, et al. Comparison of the in vitro effects of the anti-CD20 antibodies rituximab and GA101 on chronic lymphocytic leukaemia cells. Br J Haematol. 2011

Feb;152(3):295–306. doi:10.1111/j.1365-2141.2010.08428.x PubMed PMID: 21155758.

180. Brown JR, Byrd JC, Coutre SE, Benson DM, Flinn IW, Wagner-Johnston ND, et al. Idelalisib, an inhibitor of phosphatidylinositol 3-kinase p110δ, for relapsed/refractory chronic lymphocytic leukemia. Blood. 2014 May 29;123(22):3390–7. doi:10.1182/blood-2013-11-535047 PubMed PMID: 24615777; PubMed Central PMCID: PMC4123414.

181. Anwar Z, Ali MS, Galvano A, Perez A, La Mantia M, Bukhari I, et al. PROTACs: The Future of Leukemia Therapeutics. Front Cell Dev Biol. 2022;10:851087. doi:10.3389/fcell.2022.851087 PubMed PMID: 36120561; PubMed Central PMCID: PMC9479449.

182. Wen T, Wang J, Shi Y, Qian H, Liu P. Inhibitors targeting Bruton's tyrosine kinase in cancers: drug development advances. Leukemia. 2021 Feb;35(2):312–32. doi:10.1038/s41375-020-01072-6 PubMed PMID: 33122850; PubMed Central PMCID: PMC7862069.

183. Mato AR, Shah NN, Jurczak W, Cheah CY, Pagel JM, Woyach JA, et al. Pirtobrutinib in relapsed or refractory B-cell malignancies (BRUIN): a phase 1/2 study. Lancet. 2021 Mar 6;397(10277):892–901. doi:10.1016/S0140-6736(21)00224-5 PubMed PMID: 33676628; PubMed Central PMCID: PMC11758240.

184. Byrd JC, Harrington B, O'Brien S, Jones JA, Schuh A, Devereux S, et al. Acalabrutinib (ACP-196) in Relapsed Chronic Lymphocytic Leukemia. N Engl J Med. 2016 Jan 28;374(4):323–32. doi:10.1056/NEJMoa1509981 PubMed PMID: 26641137; PubMed Central PMCID: PMC4862586.

185. Tam CS, Trotman J, Opat S, Burger JA, Cull G, Gottlieb D, et al. Phase 1 study of the selective BTK inhibitor zanubrutinib in B-cell malignancies and safety and efficacy evaluation in CLL. Blood. 2019 Sep 12;134(11):851–9. doi:10.1182/blood.2019001160 PubMed PMID: 31340982; PubMed Central PMCID: PMC6742923.

186. Souers AJ, Leverson JD, Boghaert ER, Ackler SL, Catron ND, Chen J, et al. ABT-199, a potent and selective BCL-2 inhibitor, achieves antitumor activity while sparing platelets. Nat Med. 2013 Feb;19(2):202–8. doi:10.1038/nm.3048 PubMed PMID: 23291630.

187. Rogers KA, Huang Y, Dotson E, Lundberg J, Andritsos LA, Awan FT, et al. Use of PD-1 (PDCD1) inhibitors for the treatment of Richter syndrome: experience at a single academic centre. Br J Haematol. 2019 Apr;185(2):363–6. doi:10.1111/bjh.15508 PubMed PMID: 30028000.

188. Porter DL, Levine BL, Kalos M, Bagg A, June CH. Chimeric antigen receptor-modified T cells in chronic lymphoid leukemia. N Engl J Med. 2011 Aug 25;365(8):725–33. doi:10.1056/NEJMoa1103849 PubMed PMID: 21830940; PubMed Central PMCID: PMC3387277.

189. Koehrer S, Burger JA. B-cell receptor signaling in chronic lymphocytic leukemia and other B-cell malignancies. Clin Adv Hematol Oncol. 2016 Jan;14(1):55–65. PubMed PMID: 27057669.

190. Pal Singh S, Dammeijer F, Hendriks RW. Role of Bruton's tyrosine kinase in B cells and malignancies. Mol Cancer. 2018 Feb 19;17(1):57. doi:10.1186/s12943-018-0779-z PubMed PMID: 29455639; PubMed Central PMCID: PMC5817726.

191. Hendriks RW, Yuvaraj S, Kil LP. Targeting Bruton's tyrosine kinase in B cell malignancies. Nat Rev Cancer. 2014 Apr;14(4):219–32. doi:10.1038/nrc3702 PubMed PMID: 24658273.

192. Woyach JA, Bojnik E, Ruppert AS, Stefanovski MR, Goettl VM, Smucker KA, et al. Bruton's tyrosine kinase (BTK) function is important to the development and expansion of chronic lymphocytic leukemia (CLL). Blood. 2014 Feb 20;123(8):1207–13. doi:10.1182/blood-2013-07-515361 PubMed PMID: 24311722; PubMed Central PMCID: PMC3931190.

193. Bradshaw JM. The Src, Syk, and Tec family kinases: distinct types of molecular switches. Cell Signal. 2010 Aug;22(8):1175–84. doi:10.1016/j.cellsig.2010.03.001 PubMed PMID: 20206686.

194. Vihinen M, Nilsson L, Smith CI. Tec homology (TH) adjacent to the PH domain. FEBS Lett. 1994 Aug 22;350(2–3):263–5. doi:10.1016/0014-5793(94)00783-7 PubMed PMID: 8070576.

195. Tzeng SR, Pai MT, Lung FD, Wu CW, Roller PP, Lei B, et al. Stability and peptide binding specificity of Btk SH2 domain: molecular basis for X-linked agammaglobulinemia. Protein Sci. 2000 Dec;9(12):2377–85. doi:10.1110/ps.9.12.2377 PubMed PMID: 11206059; PubMed Central PMCID: PMC2144513.

196. Baraldi E, Djinovic Carugo K, Hyvönen M, Surdo PL, Riley AM, Potter BV, et al. Structure of the PH domain from Bruton's tyrosine kinase in complex with inositol 1,3,4,5-tetrakisphosphate. Structure. 1999 Apr 15;7(4):449–60. doi:10.1016/s0969-2126(99)80057-4 PubMed PMID: 10196129.

197. Parmar S, Patel K, Pinilla-Ibarz J. Ibrutinib (imbruvica): a novel targeted therapy for chronic lymphocytic leukemia. P T. 2014 Jul;39(7):483–519. PubMed PMID: 25083126; PubMed Central PMCID: PMC4103574.

198. Rozkiewicz D, Hermanowicz JM, Kwiatkowska I, Krupa A, Pawlak D. Bruton's Tyrosine Kinase Inhibitors (BTKIs): Review of Preclinical Studies and Evaluation of Clinical Trials. Molecules. 2023 Mar 6;28(5):2400. doi:10.3390/molecules28052400

199. Hallek M. On the architecture of translational research designed to control chronic lymphocytic leukemia. Hematology Am Soc Hematol Educ Program. 2018 Nov 30;2018(1):1–8. doi:10.1182/asheducation-2018.1.1 PubMed PMID: 30504285; PubMed Central PMCID: PMC6245981.

200. Hallek M, Eichhorst BF. Chemotherapy combination treatment regimens with fludarabine in chronic lymphocytic leukemia. Hematol J. 2004;5 Suppl 1:S20-30. doi:10.1038/sj.thj.6200388 PubMed PMID: 15079150.

201. Tam CS, O'Brien S, Wierda W, Kantarjian H, Wen S, Do KA, et al. Long-term results of the fludarabine, cyclophosphamide, and rituximab regimen as initial therapy of chronic lymphocytic leukemia. Blood. 2008 Aug 15;112(4):975–80. doi:10.1182/blood-2008-02-140582 PubMed PMID: 18411418; PubMed Central PMCID: PMC3952498.

202. Robak T, Dmoszynska A, Solal-Céligny P, Warzocha K, Loscertales J, Catalano J, et al. Rituximab plus fludarabine and cyclophosphamide prolongs progression-free survival compared with fludarabine and cyclophosphamide alone in previously treated chronic lymphocytic leukemia. J Clin Oncol. 2010 Apr 1;28(10):1756–65. doi:10.1200/JCO.2009.26.4556 PubMed PMID: 20194844.

203. Burger JA, Keating MJ, Wierda WG, Hartmann E, Hoellenriegel J, Rosin NY, et al. Safety and activity of ibrutinib plus rituximab for patients with high-risk chronic lymphocytic leukaemia: a single-arm, phase 2 study. Lancet Oncol. 2014 Sep;15(10):1090–9. doi:10.1016/S1470-2045(14)70335-3 PubMed PMID: 25150798; PubMed Central PMCID: PMC4174348.

204. Woyach JA, Blachly JS, Rogers KA, Bhat SA, Jianfar M, Lozanski G, et al. Acalabrutinib plus Obinutuzumab in Treatment-Naïve and Relapsed/Refractory Chronic Lymphocytic Leukemia. Cancer Discov. 2020 Mar;10(3):394–405. doi:10.1158/2159-8290.CD-19-1130 PubMed PMID: 31915195; PubMed Central PMCID: PMC8176161.

205. Seymour JF, Ma S, Brander DM, Choi MY, Barrientos J, Davids MS, et al. Venetoclax plus rituximab in relapsed or refractory chronic lymphocytic leukaemia: a phase 1b study. Lancet Oncol. 2017 Feb;18(2):230–40. doi:10.1016/S1470-2045(17)30012-8 PubMed PMID: 28089635; PubMed Central PMCID: PMC5316338.

206. Hallek M. Chronic Lymphocytic Leukemia: 2025 Update on the Epidemiology, Pathogenesis, Diagnosis, and Therapy. American J Hematol. 2025 Mar;100(3):450–80. doi:10.1002/ajh.27546

207. Ahn IE, Tian X, Wiestner A. Ibrutinib for Chronic Lymphocytic Leukemia with TP53 Alterations. N Engl J Med. 2020 Jul 30;383(5):498–500. doi:10.1056/NEJMc2005943 PubMed PMID: 32726539; PubMed Central PMCID: PMC7456330.

208. Dreger P, Schetelig J, Andersen N, Corradini P, van Gelder M, Gribben J, et al. Managing high-risk CLL during transition to a new treatment era: stem cell transplantation or novel agents? Blood. 2014 Dec 18;124(26):3841–9. doi:10.1182/blood-2014-07-586826 PubMed PMID: 25301705; PubMed Central PMCID: PMC4276025.

209. Extermann M, Overcash J, Lyman GH, Parr J, Balducci L. Comorbidity and functional status are independent in older cancer patients. J Clin Oncol. 1998 Apr;16(4):1582–7. doi:10.1200/JCO.1998.16.4.1582 PubMed PMID: 9552069.

210. Gauthier J, Hirayama AV, Purushe J, Hay KA, Lymp J, Li DH, et al. Feasibility and efficacy of CD19-targeted CAR T cells with concurrent ibrutinib for CLL after ibrutinib failure. Blood. 2020 May 7;135(19):1650–60. doi:10.1182/blood.2019002936 PubMed PMID: 32076701; PubMed Central PMCID: PMC7205814.

211. Morabito F, Gentile M, Monti P, Recchia AG, Menichini P, Skafi M, et al. TP53 dysfunction in chronic lymphocytic leukemia: clinical relevance in the era of B-cell receptors and BCL-2 inhibitors. Expert Opinion on Investigational Drugs. 2020 Aug 2;29(8):869–80. doi:10.1080/13543784.2020.1783239

212. Bykov VJN, Eriksson SE, Bianchi J, Wiman KG. Targeting mutant p53 for efficient cancer therapy. Nat Rev Cancer. 2018 Feb;18(2):89–102. doi:10.1038/nrc.2017.109

213. Bykov VJN, Issaeva N, Shilov A, Hultcrantz M, Pugacheva E, Chumakov P, et al. Restoration of the tumor suppressor function to mutant p53 by a low-molecular-weight compound. Nat Med. 2002 Mar;8(3):282–8. doi:10.1038/nm0302-282 PubMed PMID: 11875500.

214. Bykov VJN, Issaeva N, Selivanova G, Wiman KG. Mutant p53-dependent growth suppression distinguishes PRIMA-1 from known anticancer drugs: a statistical analysis of information in the National Cancer Institute database. Carcinogenesis. 2002 Dec;23(12):2011–8. doi:10.1093/carcin/23.12.2011 PubMed PMID: 12507923.

215. Bykov VJN, Zache N, Stridh H, Westman J, Bergman J, Selivanova G, et al. PRIMA-1(MET) synergizes with cisplatin to induce tumor cell apoptosis. Oncogene. 2005 May 12;24(21):3484–91. doi:10.1038/sj.onc.1208419 PubMed PMID: 15735745.

216. Lambert JMR, Gorzov P, Veprintsev DB, Söderqvist M, Segerbäck D, Bergman J, et al. PRIMA-1 reactivates mutant p53 by covalent binding to the core domain. Cancer Cell. 2009 May 5;15(5):376–88. doi:10.1016/j.ccr.2009.03.003 PubMed PMID: 19411067.

217. Wassman CD, Baronio R, Demir Ö, Wallentine BD, Chen CK, Hall LV, et al. Computational identification of a transiently open L1/S3 pocket for reactivation of mutant p53. Nat Commun. 2013;4:1407. doi:10.1038/ncomms2361 PubMed PMID: 23360998; PubMed Central PMCID: PMC3562459.

218. Peng X, Zhang MQZ, Conserva F, Hosny G, Selivanova G, Bykov VJN, et al. APR-246/PRIMA-1MET inhibits thioredoxin reductase 1 and converts the enzyme to a dedicated NADPH oxidase. Cell Death Dis. 2013 Oct 24;4(10):e881. doi:10.1038/cddis.2013.417 PubMed PMID: 24157875; PubMed Central PMCID: PMC3920950.

219. Mohell N, Alfredsson J, Fransson Å, Uustalu M, Byström S, Gullbo J, et al. APR-246 overcomes resistance to cisplatin and doxorubicin in ovarian cancer cells. Cell Death Dis. 2015 Jun 18;6(6):e1794. doi:10.1038/cddis.2015.143 PubMed PMID: 26086967; PubMed Central PMCID: PMC4669826.

220. Menichini P, Monti P, Speciale A, Cutrona G, Matis S, Fais F, et al. Antitumor Effects of PRIMA-1 and PRIMA-1Met (APR246) in Hematological Malignancies: Still a Mutant P53-Dependent Affair? Cells. 2021 Jan 7;10(1):98. doi:10.3390/cells10010098 PubMed PMID: 33430525; PubMed Central PMCID: PMC7827888.

221. Tessoulin B, Descamps G, Moreau P, Maïga S, Lodé L, Godon C, et al. PRIMA-1Met induces myeloma cell death independent of p53 by impairing the GSH/ROS balance. Blood. 2014 Sep 4;124(10):1626–36. doi:10.1182/blood-2014-01-548800

222. Clemons NJ, Liu DS, Duong CP, Phillips WA. Inhibiting system xC- and glutathione biosynthesis - a potential Achilles' heel in mutant-p53 cancers. Mol Cell Oncol. 2017;4(5):e1344757. doi:10.1080/23723556.2017.1344757 PubMed PMID: 29057306; PubMed Central PMCID: PMC5644480.

223. Jaskova Z, Pavlova S, Malcikova J, Brychtova Y, Trbusek M. PRIMA-1MET cytotoxic effect correlates with p53 protein reduction in TP53-mutated chronic lymphocytic leukemia cells. Leuk Res. 2020 Feb;89:106288. doi:10.1016/j.leukres.2019.106288 PubMed PMID: 31924585.

224. Baeuerle PA, Baltimore D. NF-kappa B: ten years after. Cell. 1996 Oct 4;87(1):13–20. doi:10.1016/s0092-8674(00)81318-5 PubMed PMID: 8858144.

225. Thompson JE, Phillips RJ, Erdjument-Bromage H, Tempst P, Ghosh S. I kappa B-beta regulates the persistent response in a biphasic activation of NF-kappa B. Cell. 1995 Feb 24;80(4):573–82. doi:10.1016/0092-8674(95)90511-1 PubMed PMID: 7867065.

226. Wahl C, Liptay S, Adler G, Schmid RM. Sulfasalazine: a potent and specific inhibitor of nuclear factor kappa B. J Clin Invest. 1998 Mar 1;101(5):1163–74. doi:10.1172/JCI992 PubMed PMID: 9486988; PubMed Central PMCID: PMC508669.

227. Mansouri L, Papakonstantinou N, Ntoufa S, Stamatopoulos K, Rosenquist R. NF-κB activation in chronic lymphocytic leukemia: A point of convergence of external triggers and intrinsic lesions. Seminars in Cancer Biology. 2016 Aug;39:40–8. doi:10.1016/j.semcancer.2016.07.005

228. Hertlein E, Beckwith KA, Lozanski G, Chen TL, Towns WH, Johnson AJ, et al. Characterization of a new chronic lymphocytic leukemia cell line for mechanistic in vitro and in vivo studies relevant to disease. PLoS One. 2013;8(10):e76607. doi:10.1371/journal.pone.0076607 PubMed PMID: 24130782; PubMed Central PMCID: PMC3793922.

229. Stacchini A, Aragno M, Vallario A, Alfarano A, Circosta P, Gottardi D, et al. MEC1 and MEC2: two new cell lines derived from B-chronic lymphocytic leukaemia in prolymphocytoid transformation. Leuk Res. 1999 Feb;23(2):127–36. doi:10.1016/s0145-2126(98)00154-4 PubMed PMID: 10071128.

230. Mosmann T. Rapid colorimetric assay for cellular growth and survival: Application to proliferation and cytotoxicity assays. Journal of Immunological Methods. 1983 Dec;65(1–2):55–63. doi:10.1016/0022-1759(83)90303-4

231. Magrini R, Russo D, Ottaggio L, Fronza G, Inga A, Menichini P. PRIMA-1 synergizes with adriamycin to induce cell death in non-small cell lung cancer cells. J Cell Biochem. 2008 Aug 15;104(6):2363–73. doi:10.1002/jcb.21794 PubMed PMID: 18442053.

232. Koopman G, Reutelingsperger CP, Kuijten GA, Keehnen RM, Pals ST, van Oers MH. Annexin V for flow cytometric detection of phosphatidylserine expression on B cells undergoing apoptosis. Blood. 1994 Sep 1;84(5):1415–20. PubMed PMID: 8068938.

233. Vermes I, Haanen C, Steffens-Nakken H, Reutelingsperger C. A novel assay for apoptosis. Flow cytometric detection of phosphatidylserine expression on early apoptotic cells using fluorescein labelled Annexin V. J Immunol Methods. 1995 Jul 17;184(1):39–51. doi:10.1016/0022-1759(95)00072-i PubMed PMID: 7622868.

234. Berenbaum MC. What is synergy? Pharmacol Rev. 1989 Jun;41(2):93–141. PubMed PMID: 2692037.

235. Berenbaum MC. Criteria for analyzing interactions between biologically active agents. Adv Cancer Res. 1981;35:269–335. doi:10.1016/s0065-230x(08)60912-4 PubMed PMID: 7041539.

236. Fariss MW, Reed DJ. High-performance liquid chromatography of thiols and disulfides: dinitrophenol derivatives. Methods Enzymol. 1987;143:101–9. doi:10.1016/0076-6879(87)43018-8 PubMed PMID: 3657520.

237. Cossarizza A, Ferraresi R, Troiano L, Roat E, Gibellini L, Bertoncelli L, et al. Simultaneous analysis of reactive oxygen species and reduced glutathione content in living cells by polychromatic flow cytometry. Nat Protoc. 2009;4(12):1790–7. doi:10.1038/nprot.2009.189 PubMed PMID: 20010930.

238. Ravera S, Bertola N, Puddu A, Bruno S, Maggi D, Panfoli I. Crosstalk between the Rod Outer Segments and Retinal Pigmented Epithelium in the Generation of Oxidative Stress in an In Vitro Model. Cells. 2023 Aug 30;12(17):2173. doi:10.3390/cells12172173 PubMed PMID: 37681906; PubMed Central PMCID: PMC10487269.

239. Pasino M, Speciale A, Ravera S, Cutrona G, Massara R, Bertola N, et al. Targeting the p53/xCT/GSH Axis with PRIMA-1Met Combined with Sulfasalazine Shows Therapeutic Potential in Chronic Lymphocytic Leukemia.

Int J Mol Sci. 2025 Jun 10;26(12):5559. doi:10.3390/ijms26125559 PubMed PMID: 40565026; PubMed Central PMCID: PMC12193190.

240. Colla R, Izzotti A, De Ciucis C, Fenoglio D, Ravera S, Speciale A, et al. Glutathione-mediated antioxidant response and aerobic metabolism: two crucial factors involved in determining the multi-drug resistance of high-risk neuroblastoma. Oncotarget. 2016 Oct 25;7(43):70715–37. doi:10.18632/oncotarget.12209 PubMed PMID: 27683112; PubMed Central PMCID: PMC5342585.

241. Gout PW, Buckley AR, Simms CR, Bruchovsky N. Sulfasalazine, a potent suppressor of lymphoma growth by inhibition of the x(c)- cystine transporter: a new action for an old drug. Leukemia. 2001 Oct;15(10):1633–40. doi:10.1038/sj.leu.2402238 PubMed PMID: 11587223.

242. Fujihara KM, Corrales Benitez M, Cabalag CS, Zhang BZ, Ko HS, Liu DS, et al. SLC7A11 Is a Superior Determinant of APR-246 (Eprenetapopt) Response than TP53 Mutation Status. Mol Cancer Ther. 2021 Oct;20(10):1858–67. doi:10.1158/1535-7163.MCT-21-0067 PubMed PMID: 34315763.

243. Synnott NC, Madden SF, Bykov VJN, Crown J, Wiman KG, Duffy MJ. The Mutant p53-Targeting Compound APR-246 Induces ROS-Modulating Genes in Breast Cancer Cells. Transl Oncol. 2018 Dec;11(6):1343–9. doi:10.1016/j.tranon.2018.08.009 PubMed PMID: 30196236; PubMed Central PMCID: PMC6132178.

244. Birsen R, Larrue C, Decroocq J, Johnson N, Guiraud N, Gotanegre M, et al. APR-246 induces early cell death by ferroptosis in acute myeloid leukemia. Haematologica. 2022 Feb 1;107(2):403–16. doi:10.3324/haematol.2020.259531 PubMed PMID: 33406814; PubMed Central PMCID: PMC8804578.

245. Shih AY, Erb H, Sun X, Toda S, Kalivas PW, Murphy TH. Cystine/glutamate exchange modulates glutathione supply for neuroprotection from oxidative stress and cell proliferation. J Neurosci. 2006 Oct 11;26(41):10514–23. doi:10.1523/JNEUROSCI.3178-06.2006 PubMed PMID: 17035536; PubMed Central PMCID: PMC6674710.

246. Aquilano K, Baldelli S, Ciriolo MR. Glutathione: new roles in redox signaling for an old antioxidant. Front Pharmacol. 2014;5:196. doi:10.3389/fphar.2014.00196 PubMed PMID: 25206336; PubMed Central PMCID: PMC4144092.

247. Pecchillo Cimmino T, Ammendola R, Cattaneo F, Esposito G. NOX Dependent ROS Generation and Cell Metabolism. Int J Mol Sci. 2023 Jan 20;24(3):2086. doi:10.3390/ijms24032086 PubMed PMID: 36768405; PubMed Central PMCID: PMC9916913.

248. Gupta R, Yan XJ, Barrientos J, Kolitz JE, Allen SL, Rai K, et al. Mechanistic Insights into CpG DNA and IL-15 Synergy in Promoting B Cell Chronic Lymphocytic Leukemia Clonal Expansion. J Immunol. 2018 Sep 1;201(5):1570–

85. doi:10.4049/jimmunol.1800591 PubMed PMID: 30068596; PubMed Central PMCID: PMC6103916.

249. Tuval A, Strandgren C, Heldin A, Palomar-Siles M, Wiman KG. Pharmacological reactivation of p53 in the era of precision anticancer medicine. Nat Rev Clin Oncol. 2024 Feb;21(2):106–20. doi:10.1038/s41571-023-00842-2 PubMed PMID: 38102383.

250. Peuget S, Zhou X, Selivanova G. Translating p53-based therapies for cancer into the clinic. Nat Rev Cancer. 2024 Mar;24(3):192–215. doi:10.1038/s41568-023-00658-3 PubMed PMID: 38287107.

251. Pozzo F, Dal Bo M, Peragine N, Bomben R, Zucchetto A, Rossi F, et al. Detection of TP53 dysfunction in chronic lymphocytic leukemia by an in vitro functional assay based on TP53 activation by the non-genotoxic drug Nutlin-3: a proposal for clinical application. J Hematol Oncol. 2013 Nov 5;6:83. doi:10.1186/1756-8722-6-83 PubMed PMID: 24283248; PubMed Central PMCID: PMC4222122.

252. Liu Y, Gu W. The complexity of p53-mediated metabolic regulation in tumor suppression. Semin Cancer Biol. 2022 Oct;85:4–32. doi:10.1016/j.semcancer.2021.03.010 PubMed PMID: 33785447; PubMed Central PMCID: PMC8473587.

253. Ali D, Mohammad DK, Mujahed H, Jonson-Videsäter K, Nore B, Paul C, et al. Anti-leukaemic effects induced by APR-246 are dependent on induction of oxidative stress and the NFE2L2/HMOX1 axis that can be targeted by PI3K and mTOR inhibitors in acute myeloid leukaemia cells. Br J Haematol. 2016 Jul;174(1):117–26. doi:10.1111/bjh.14036 PubMed PMID: 26991755.